

VALIDATION OF SLEEVE WELD INTEGRITY
AND WORKMANSHIP LEVEL DEVELOPMENT

FINAL REPORT

July 2006

Submitted to:

The United States Department of Transportation
Research and Special Projects Administration
Pipeline Safety R&D
T.D. Williamson Inc.
Williamson Industries Inc.
Enbridge Pipelines Inc.
TransCanada PipeLines Limited

Submitted by:

BMT FLEET TECHNOLOGY LIMITED
311 Legget Drive
Kanata, ON
K2K 1Z8

BMT Contact: Robert B. Lazor, P. Eng.
Tel: 780-465-0077
Fax: 780-465-0085
Email: rlazor@fleetech.com

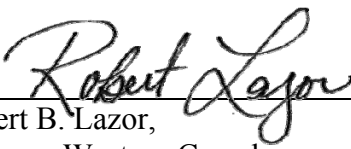


BMT FTL DOCUMENT QUALITY CONTROL DATA SHEET

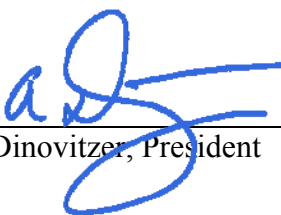
REPORT: Validation of Sleeve Weld Integrity and Workmanship
Level Development

DATE: July 2006


PREPARED BY:


Robert B. Lazor,
Manager Western Canada

**REVIEWED AND
APPROVED BY:**


Aaron Dinovitzer, President

**REPORT
PRODUCTION BY:**


Document Editor

PROJECT TEAM MEMBERS:

Robert Lazor
Darren Begg
James Luffman
Brock Bolton
Vlado Semiga

EXECUTIVE SUMMARY

This project was initiated to support a methodology for conducting an engineering assessment to determine the tolerable dimensions of flaw indications at full encirclement repair sleeve welds. The work described herein has been undertaken to validate the stresses estimated in finite element analysis (FEA) models against actual in-service loading conditions experienced at reinforcing sleeves. This project was intended to prove the feasibility of the concept and to provide details that could be incorporated into a future guidance note on sleeve installation procedures. The following general tasks were undertaken:

- ✕ Collection of full-scale structural behavior data during the sleeve installation process and during line operation;
- ✕ Calibration of a sleeve weld finite element model against field data; and
- ✕ Demonstration of the model as a design tool.

The current project has resulted in a better understanding of pressure retaining full encirclement repair sleeves often used as permanent repairs on pipelines to reinforce areas with defects, such as cracks or corrosion. In particular, this project has been undertaken to validate the stresses estimated in the finite element analysis (FEA) models against actual in-service loading conditions experienced at reinforcing sleeves.

The work completed in this project has focused on the collection of full-scale experimental data describing pipe and sleeve strains. This data was collected in the field and laboratory as follows:

- Strains induced by sleeve welding;
- Strains induced by pressurization of the sleeved pipe; and
- Strains induced by pressurization of the sleeved pipe and the annulus between the pipe and sleeve.

Finite element models of the field and laboratory sleeved pipe segments were developed and subjected to the same applied loading conditions as the full-scale sleeved pipe segments. The results of the full-scale data collection (strains) were compared with those estimated based upon the finite element models to demonstrate the ability of the models to predict the behaviour of the sleeved pipe segments. Comparisons were made to illustrate:

- ✕ relative strain levels,
- ✕ the accuracy of the strain predictions,
- ✕ local strain transfer functions (i.e. strain response per unit change in pressure),
- ✕ deformation trends,
- ✕ the differences in behaviours of tight and loose fitting sleeves, and
- ✕ the effects of pressurizing the annulus between the pipe wall and sleeve.

The results can be used to support the development of tools for sleeve design and for conducting engineering assessments to determine the tolerable dimensions of flaw indications at full encirclement repair sleeves.

ACKNOWLEDGEMENTS

The authors would like to acknowledge the support received from the following sponsors for their financial assistance and for the supply of materials and manpower towards completion of this project:

- ✕ The United States Department of Transportation, Research and Special Projects Administration, Pipeline Safety R&D
- ✕ T.D. Williamson Inc.
- ✕ Williamson Industries Inc.
- ✕ Enbridge Pipelines Inc.
- ✕ TransCanada PipeLines Limited

TABLE OF CONTENTS

1.	INTRODUCTION	1
2.	FIELD TRIALS	2
2.1	Instrumentation	4
2.1.1	KP 762 7	
2.1.2	KP 768 8	
2.2	Strain Readings on Pipe during Welding	8
2.3	Comparison of Strain Readings for Individual Passes	10
2.3.1	Gauge 1 10	
2.5	Summary of Field Results	17
3.	LAB TRIALS	18
3.1	Test Vessel Configuration	18
3.2	Assembly of Test Vessel	18
3.2.1	Reinforcing Sleeves	19
3.2.2	Vent Connections	22
3.3	Strain Gauge Locations and Installation	23
3.3.1	Pipe ID Gauges - Gauge 1 and Gauge 2	23
3.3.2	Pipe OD Gauges - Gauge 3 and Gauge 4	23
3.3.3	Sleeve OD Gauges - Gauges 5, 6, 7, and 8	23
3.3.4	Sleeve OD Gauges - Gauge 9 and Gauge 10	24
3.3.5	Sleeve OD Gauges - Gauge 11 and Gauge 12	24
3.3.6	Pipe/Sleeve Annulus Gauges 13, 14, 16, and 17	24
3.3.7	Pipe OD Gauges 15 and 18	25
3.4	Test Assembly	26
3.5	Strain Gauge Results	32
3.5.1	Strains after Completing Sleeve Fillet Welds	33
3.5.2	Strains Resulting from Welding Sleeves	35
3.5.3	Response to Pressure Fluctuations	36
3.5.4	Sleeve OD Strains	39
3.5.5	Axial Strains Between Sleeves	41
3.5.6	Summary of Strain Readings	41
4.	SLEEVE WELD FEA MODEL	43
4.1	Model Description	43
4.2	Modeling Data	44
4.2.1	Material Property Data	44
4.2.2	Model Geometry	45
4.2.3	Applied Loading Sequence and Boundary Conditions	47
4.3	Model Results Summary	48
5.	DISCUSSION	52
5.1	Field Results on Enbridge Odessa Line 3	52
5.2	FE Model and Lab Trial Comparisons	54
5.3	Circumferential Fillet Weld Root Details	59



6.	CONCLUDING REMARKS.....	65
6.1	Project Summary.....	65
6.2	Conclusions.....	65
6.3	Recommendations.....	66

APPENDICES

APPENDIX A: LOCATIONS OF GAUGES, FIELD TRIALS

APPENDIX B: STRAIN GAUGE RESULTS, FIELD TRIALS

APPENDIX C: STRAIN GAUGE DETAILS, LAB TRIALS

APPENDIX D: STRAIN GAUGE RESULTS, LAB TRIALS

LIST OF FIGURES

Figure 2.1: View of South Side of Sleeve at KP 762.....	2
Figure 2.2: General View (Looking East) of Excavation at KP 768	3
Figure 2.3: Dimensions on Sleeve Longitudinal Seams Prior to Welding [mm]	3
Figure 2.4: Typical Gauge Numbering and Placement (KP 768 Shown).....	5
Figure 2.5: Photo of Shield Positioned over Gauge 1.....	6
Figure 2.6: Strain Gauges after Welding. Top photo shows the damage to the cloth tape after welding, and the lower photographs show the gauge with protection removed.....	6
Figure 2.7: Strains Measured Near 3:00 O'clock Position during Completion of Circumferential Weld Pass 4 on Sleeve 2 (KP 768).	9
Figure 2.8: Strains Recorded Near 10:30 O'clock Position during Completion of Circumferential Weld Pass 4 on Sleeve 2 (KP 768).	9
Figure 2.9: Hoop Strains Measured at the Center of the Sleeves	10
Figure 2.10: Axial Gauge 4 Strains at the Sleeve 12:00 O'clock Position for Sleeve 1 (KP 762) and Sleeve 2 (KP 768).	11
Figure 2.11: Axial Gauge 5 Strains at the Pipe 12:00 O'clock Position for Sleeve 1 (KP 762) and Sleeve 2 (KP 768).	11
Figure 2.12: Strains for Axial Gauges 6 and 7 on the Pipe 10:30 O'clock Position for Sleeve 1 (KP 762) and Sleeve 2 (KP 768).	12
Figure 2.13: Strains for Rosette Gauge Pairs at the 9:30 O'clock Positions for Sleeve 1 (KP 762) and Sleeve 2 (KP 768).	13
Figure 2.14: Summary of Final Strains on Sleeves at KP 762 and KP 768.....	14
Figure 2.15: Odessa Discharge Pressure over the Period from 28-30 Sept 2004	15
Figure 3.1: General Configuration of Test Vessel	18
Figure 3.2: End View of Test Vessel Configuration.....	19
Figure 3.3: General View of Longitudinal Seam Root Gap on Side 1	20
Figure 3.4: General View of Longitudinal Seam Root Gap on Side 2	20
Figure 3.5: View of Root Gap between Pipe and End of Sleeve on Side 1	21
Figure 3.6: View of Fit-up Between Pipe and End of Sleeve on Side 2.....	21
Figure 3.7: View of 1.6 mm Root Gap between Pipe and End of Sleeve B	22
Figure 3.8: Sleeve Vent Details	22
Figure 3.9: Location of Gauges 1 and 2 on Pipe ID Opposite Fillet Welds	23
Figure 3.10: Sketch Showing Locations of Gauges on Sleeve OD	24
Figure 3.11: Gauge 13 was Located within a Machined Groove on Sleeve A. The second groove shown above was positioned over Gauge 14.	25
Figure 3.12: Gauge 16 was Located on Sleeve B ID in a Machined Groove	25
Figure 3.13: View of Completed Welds on Sleeve B	26
Figure 3.14: Fillet Weld Dimensions.....	27
Figure 3.15: Sketch of Active Gauges during Completion of Sleeve Welding	33
Figure 3.16: Assumed Deformed Shape of the Pipe and Sleeve after Welding	33
Figure 3.17: Sketch of Final Gauge Placement	35
Figure 3.18: Strains after Completion of Circumferential Fillet Welds (B2 Readings)	36
Figure 3.19: Locations of Hoop and Axial Gauges	36
Figure 3.20: Pipe and Sleeve Strains Remote from Fillet Welds (Pressure Only)	38

Figure 3.21: Strain Readings for OD Sleeve Gauges (Pressure Only); Sleeve A, No Gap; Sleeve B (1.6 mm Gap)	40
Figure 3.22: Axial Strains between Sleeves (Pressure Only)	41
Figure 3.23: Schematic of Strains Resulting from Welding Sleeves to the Pipe.....	42
Figure 3.24: Hoop and Axial Strains on Pipe and Sleeve (Pressure Only).....	42
Figure 4.1: Schematic of Sleeve on Pipe Model.....	43
Figure 4.2: True Stress – True Strain Pipe Material Model.....	45
Figure 4.3: Dimensions of Pipe and Sleeves	45
Figure 4.4: End Cap Detail	46
Figure 4.5: Sleeve and Weld Designations.....	47
Figure 4.6: Axial Strain Results for Sleeve A, No Gap; B4: 250 psi to Pipe Only, B7: 500 psi to Pipe Only, and B9: 500 psi to Pipe and Annulus between Sleeve and Pipe	49
Figure 4.7: Axial Strain Results for Sleeve B, 1.6 mm Gap; B4: 250 psi to Pipe Only, B7: 500 psi to Pipe Only, and B9: 500 psi to Pipe and Annulus between Sleeve and Pipe....	50
Figure 4.8: Comparison of 250 psi Strains against 500 psi Strains	51
Figure 5.1: Summary of Final Strains on Sleeves at KP 762 and KP 768.....	52
Figure 5.2: Sketch Showing $\Delta\epsilon / \Delta P$ Transfer Functions from Field Trials (Bold numbers indicate strain gauge numbers)	53
Figure 5.3: Lab Trial and Predicted Strains; Pipe Strain Gauges 3, 4, 14, 15, and 18.	55
Figure 5.4: Comparison of Strains Calculated by FE Model to Strains Measured in Lab.....	56
Figure 5.5: Lab Trial and Predicted Strains; Sleeve A, No Gap, Gauges 5, 6, 9, 11, and 13	57
Figure 5.6: Lab Trial and Predicted Strains; Sleeve B, 1.6 mm Gap.....	58
Figure 5.7: Example of Fillet Weld Root Crack	59
Figure 5.8: Axial Strain Results for Sleeve A, No Gap; B7: 500 psi to Pipe Only, and B9: 500 psi to Pipe and Annulus between Sleeve and Pipe	60
Figure 5.9: Axial Strain Results for Sleeve B, 1.6 mm Gap; B7: 500 psi to Pipe Only, and B9: 500 psi to Pipe and Annulus between Sleeve and Pipe	61
Figure 5.10: Sleeve A (Ungapped) Radial Displacement, Load Condition B7 (500 psi Pressurized Pipe Only)	62
Figure 5.11: Sleeve A (Ungapped) Radial Displacement, Load Condition B9 (500 psi Pressurized Pipe and Sleeve Annuli).....	62
Figure 5.12: Sleeve B (Gapped) Radial Displacement, Load Condition B7 (500 psi Pressurized Pipe Only).....	63
Figure 5.13: Sleeve B (Gapped) Radial Displacement, Load Condition B9 (500 psi Pressurized Pipe and Sleeve Annuli)	63
Figure 5.14: Comparison of Sleeves with 500 psi to Pipe.....	64
Figure 5.15: Comparison of Sleeves with 500 psi to Pipe and Annulus between Sleeve and Pipe	64

LIST OF TABLES

Table 2.1: Station and Sleeve Locations.....	2
Table 2.2: Summary of Strain Gauge Positions.....	4
Table 2.3: KP 762 Strain Changes on Sleeve	16
Table 2.4: KP 768 Strain Changes.....	17
Table 3.1: Welding Details for Circumferential Fillet Weld on Outside of Pipe (Away from Gauges), Sleeve A.....	28
Table 3.2: Welding Details for Circumferential Fillet Weld on Inside of Pipe (Near Gauges), Sleeve A	29
Table 3.3: Welding Details for Circumferential Fillet Weld on Outside of Pipe (away from gauges), Sleeve B.....	30
Table 3.4: Welding Details for Circumferential Fillet Weld on Inside of Pipe (near gauges), Sleeve B	31
Table 3.5: File Descriptions	32
Table 3.6: Gauge Data Reporting Summary.....	32
Table 3.7: Hoop and Axial Strain Readings (Pressure Only)	37
Table 4.1: Engineering Stress – Strain Properties Used in FEA Models.....	44
Table 4.2: Material Thicknesses	46
Table 4.3: Weld Dimensions.....	47
Table 4.4: Applied Pressure Summary	47
Table 5.1: Field Trials Strain Changes	53
Table 5.2: Pressure Transfer Functions from FE Models	59

1. INTRODUCTION

Full encirclement repair sleeves with fillet-welded ends are often used as permanent repairs on pipelines to reinforce areas with defects, such as cracks or corrosion. Once installed, the welds must be examined to ensure that there are no defects that could lead to in-service failures, such as the ones that have occurred as a result of both excessive and inadequate fillet weld size and sleeve longitudinal seam ruptures.

This project was initiated to support a methodology for conducting an engineering assessment to determine the tolerable dimensions of flaw indications at full encirclement repair sleeve welds. The work described herein has been undertaken to validate the stresses estimated in finite element analysis (FEA) models against actual in-service loading conditions experienced at reinforcing sleeves. This project was intended to prove the feasibility of the concept and to provide details that could be incorporated into a future guidance note on sleeve installation procedures. The following general tasks were undertaken:

- ✦ Collection of full-scale structural behavior data during the sleeve installation process and during line operation;
- ✦ Calibration of a sleeve weld finite element model against field data; and
- ✦ Demonstration of the model as a design tool.

The work described herein addresses components required to develop a fitness-for-service methodology for fillet welds and longitudinal seam welds on pipelines. The results will provide pipeline companies and others with guidance to complete assessments of the design details for welded connections such as fillet welds on reinforcement sleeves and STOPPLE®¹ fittings. With the continued emphasis on maintaining the existing pipeline infrastructure, in-service welding and system modifications will continue to be a necessary consideration for all pipeline systems. API RP 579 specifically states that the analysis of flaws in sleeved reinforced cylinders (i.e. fillet weld toe flaws) required a specific stress analysis of the sleeved cylinder configuration. Due to the complexity of the geometry and loading this cannot be accomplished realistically without the use of a validated FE model.

One of the main technical barriers to overcome is the process of modeling the stresses resulting from the installation of repair sleeves or Stopple tees onto an in-service pipeline. This can be examined through FEA to determine the sensitivity to the perceived variables to the range of expected changes such as dimensions and tolerances, and later confirmed through the field installation process and strain measurements. The instrumentation can record the strains during installation and also for subsequent operation of the line to confirm the loading due to operating pressures on the pipeline.

The outcome of the overall process described above will provide industry with the current state-of-the-art in pipeline repair methods and assessment techniques, thus providing pipeline operators with the necessary information to safely complete maintenance operations on their lines with due consideration for pipeline safety, both for short- and long-term evaluations.

¹ STOPPLE is a registered trademark of T.D. Williamson, Inc., Tulsa, OK.

2. FIELD TRIALS

The two sites that were available for field work were located just downstream (east) of the Odessa Line 3 station on the Enbridge Pipelines Inc. system in south-central Saskatchewan. The station and sleeve locations are as listed in Table 2.1, and the field instrumentation was completed between September 27-30, 2004. The excavations were located within 0.45 km and 5.65 km of the station upstream boundary.

Table 2.1: Station and Sleeve Locations

Description	Kilometer Post	Milepost
Upstream Boundary of Odessa Station	761.971	473.47
Sleeve 1 – 28/29 September 2004	762.4199	473.7457
Sleeve 2 – 29/30 September 2004	767.6204	476.9772

The general view of the sleeve at KP 762.4199 (KP 762) and the excavation at KP 767.6204 (KP 768) are shown in Figures 2.1 and 2.2, respectively. The sleeves had been positioned on the pipe and two passes had been completed on the sleeve long seams to hold them in position. The pipe long seam at KP 762 was at the 3:00 o'clock position and the sleeve long seam was located just above the weld long seam (see Figure 2.1). The pipe long seam at KP 768 was located near the 12:00 o'clock position and the sleeve long seams were near 3:00 and 9:00 o'clock. The weld seams had not been removed prior to sleeve installation, resulting in a gap of as much as 3 mm at the 12:00 o'clock position of the sleeve at KP 768. The pipe seam at KP 762 was on the opposite side of the pipe from where any measurements were taken.



Figure 2.1: View of South Side of Sleeve at KP 762



Figure 2.2: General View (Looking East) of Excavation at KP 768

The sleeve longitudinal seams incorporated 38 mm wide, 1.98 mm thick (14 gauge) backing strips to avoid welding the long seams directly to the pipe. The root spacing was approximately 5 mm and the spacing across the weld bevels at the sleeve OD surfaces are summarized in Figure 2.3.

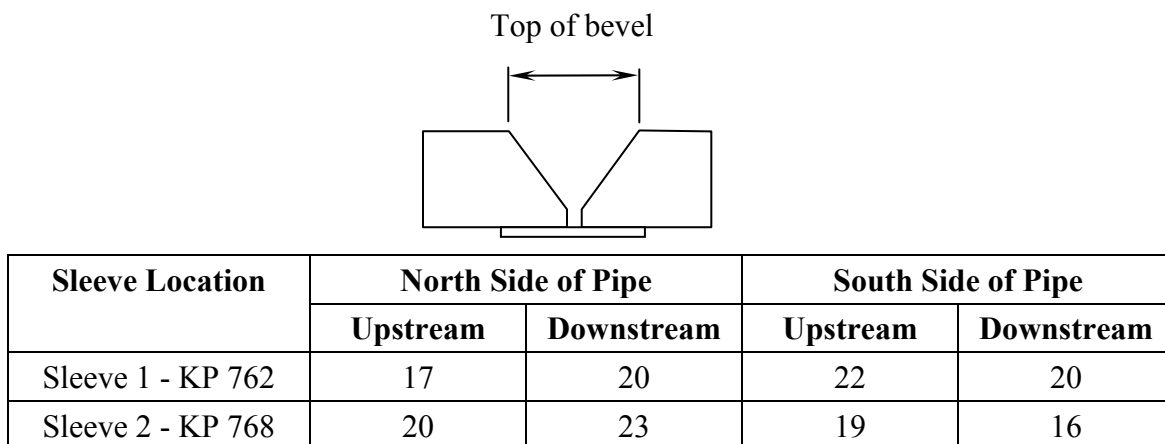


Figure 2.3: Dimensions on Sleeve Longitudinal Seams Prior to Welding [mm]

2.1 Instrumentation

Weldable strain gauges were attached to the north side of the pipe and on the upstream (west) ends of the sleeves at the locations listed in Table 2.2. The weldable strain gauges selected for this project were Micro-Measurements LWK-06-W250B-350 and LWK-06-W250D-350 gauges. The W250B gauges are single element, while the W250D are a 90° rosette gauge pattern with two gauges. All gauges are supplied with 250-mm long, Teflon-coated pre-attached leads, and gauges were connected to the instrumentation to provide lead wire temperature compensation. Figure 2.4 gives a general view of the completed installation. Sketches detailing the exact placement of the gauges with respect to the sleeve edges are shown in Appendix A.

Table 2.2: Summary of Strain Gauge Positions

Gauge	Direction	Comments
1	Hoop	Center of sleeve longitudinal weld, 40 mm from edge of sleeve
2	Axial	Near corner of sleeve longitudinal weld and end of sleeve
3	Hoop	Near corner of sleeve longitudinal weld and end of sleeve
4	Axial	On sleeve at 12:00 O'clock, 50 mm from edge of sleeve
5	Axial	On pipe at 12:00 O'clock, 65 mm from edge of sleeve
6	Axial	On pipe at 10:30 O'clock, 60 mm from edge of sleeve
7	Axial	On pipe at 10:30 O'clock, approx. 90 mm from edge of sleeve
8	Hoop	On pipe at 10:30 O'clock, approx. 800 mm from edge of sleeve
9	Hoop	On pipe at 9:15 O'clock, 50 or 60 mm from edge of sleeve
10	Axial	On pipe at 9:15 O'clock

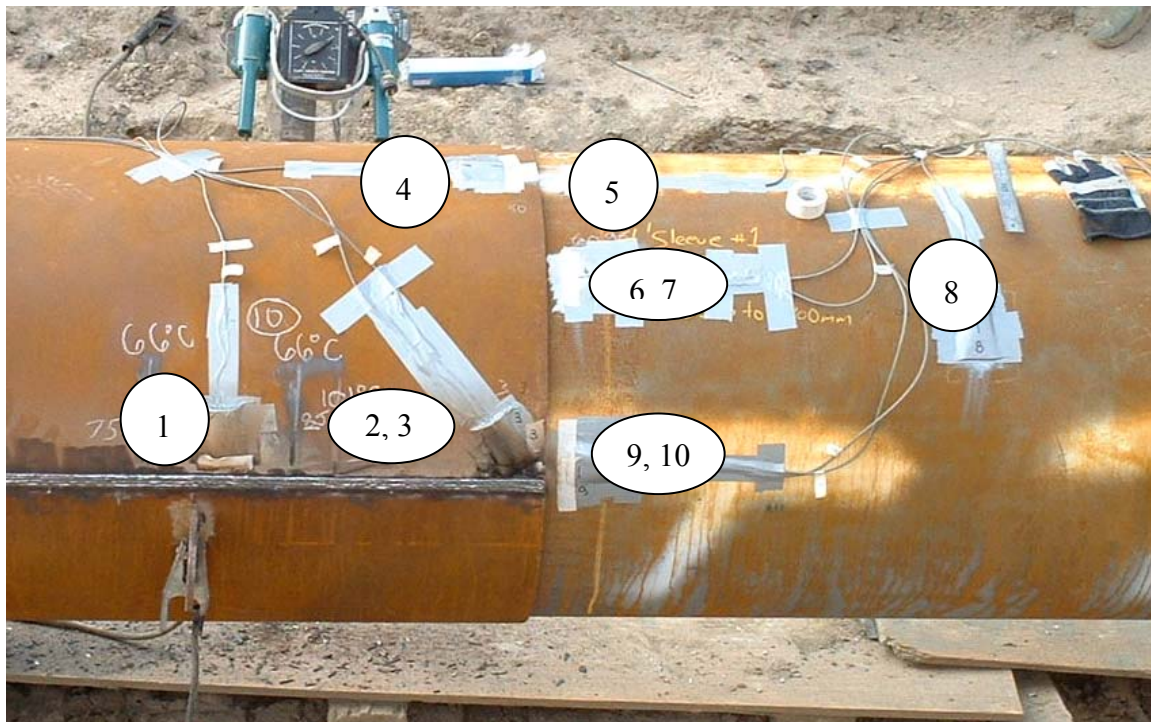


Figure 2.4: Typical Gauge Numbering and Placement (KP 768 Shown)

The primary protection for the gauges was provided using 100 mm long metal shields that were prepared from 45 mm diameter electrical conduit. The conduit was flattened to reduce the curvature, and made almost flat at the ends closest to welding to minimize the obstruction to the welders. The shields and wires were attached to the pipe using duct tape, ensuring they were completely protected from welding sparks and mechanical damage to the wires. An example of a shield positioned over Gauge 1 is shown in Figure 2.5. Additional duct tape was added to prevent sparks from rolling under the protectors. It was found during welding that the duct tape became damaged, with the glue softening and some charring to the edges of the tape closest to the weld, exposing the space under the shields. Cloth tape applied to the edges nearest the weld was found to provide better protection, and this was used in all cases where the duct tape became damaged.

The effectiveness of the protection is shown in Figure 2.6 for the sleeve at KP 768, with the figure showing the protectors in place and photos of the gauges after removal of the protectors. The lower photos show that there was only some minor smoke staining noted, as shown beside Gauge 2. Visual examination of all other gauges confirmed that they had been well protected.



Figure 2.5: Photo of Shield Positioned over Gauge 1

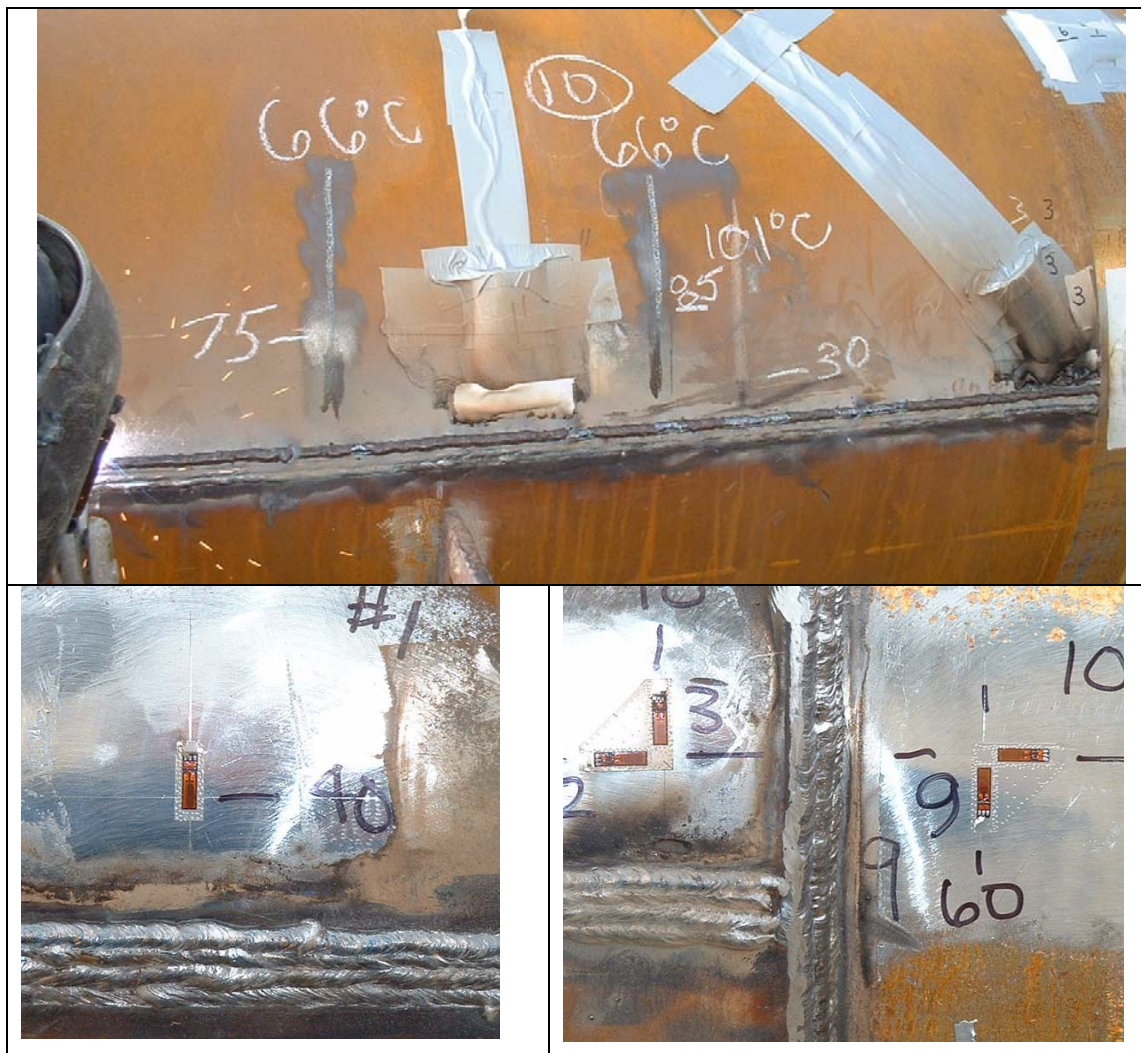


Figure 2.6: Strain Gauges after Welding. Top photo shows the damage to the cloth tape after welding, and the lower photographs show the gauge with protection removed.

Figure 2.6 also shows several vertical white lines made using both 66°C and 101°C Tempelstiks, which were used to provide an indication of the maximum temperatures resulting from completion of the final weld pass on the longitudinal weld. A maximum temperature of 66°C was observed at 75 mm and 85 mm from the longitudinal seam, and the maximum temperature of 101°C was observed at 30 mm from the edge of the weld preparation. Using a linear interpolation between the positions and the peak temperatures, Gauge 1 in this instance would have seen a maximum temperature of 94°C at the center of its gauge length.

2.1.1 KP 762

The instrumentation and welding of the sleeve at KP 762 was completed on 28-29 September 2004. Gauges 1, 2, 3, and 4 were installed on the top half of the sleeve pair in the morning and welding of the longitudinal seams started at 1330 pm. The pipe temperature was 18°C at the start of welding. Nine passes were used to complete the horizontal butt weld on the north side of the pipe (and similarly on the south side), using 4 mm and 4.8 mm diameter E7018 electrodes. Welding of the longitudinal seam was completed at 1446h, and readings were taken at 1457h when there was no noticeable difference in the sleeve temperature.

The remaining gauges were then installed on the pipe in preparation for welding the circumferential fillet welds. Gauge installation was completed and readings taken at 1700h.

The following day, all 10 gauges were connected and readings were taken at 0835h. The east fillet weld was completed at 1150h; no strain readings were taken during this time as this weld would not be expected to cause strain changes on the far end of the sleeve. The west circumferential fillet (with instrumentation) was started at 1215h and completed at 1405h, for a total time of 1 hour 50 min, as summarized below:

1215	Started west (upstream) circumferential fillet weld
1240	1st bead completed and buffed
1300	2nd pass completed
1322	3rd pass completed
1342	4th pass completed
1405	5th pass completed

The strain reading for Gauge 8, the hoop gauge 800 mm from the edge of the sleeve did not show any significant change over the day, indicating that Line 3 was still not operating. Contact with the pipeline maintenance (PLM) foreman gave us the indication that the line would still be down for an indefinite period of time, so final readings were taken at 1540h and we moved to the next site to install gauges and hopefully ‘capture’ readings with a significant change in pressure, i.e., when the line was restarted.

2.1.2 KP 768

The instrumentation and welding of the sleeve at KP 762 was completed on 29-30 September 2004. Gauge 8 (pipe hoop gauge) was connected and the first reading was taken on 29 September at 1618h, and then the remaining strain gauges were connected. Readings at 1644h indicated that the strain on Gauge 8 had increased by 136 $\mu\epsilon$, which suggested that there had been a change in operation on Line 3; this would be confirmed later during review of the line pressure readings over this period. All wires were connected by 1711h, final readings for the day were completed, and then the wires were removed for the night.

The gauges were connected by 0830h on 30 September and welding of the longitudinal seams started at 0850h. Eleven passes were used to complete the horizontal butt weld on the north side of the pipe (and similarly on the south side), using 3.2 mm, 4 mm, and 4.8 mm diameter E7018 electrodes. The longitudinal weld seams were completed at 1009h. The circumferential fillet weld on the east side of the sleeve was welded between 1030h and 1230h, a total of 2 hours. Welding of the west circumferential fillet started at 1320h and was similarly completed exactly 2 hours later at 1520h, as summarized below:

1320	Started west (upstream) circumferential fillet weld
1344	1st bead completed and buffed
1107	2nd pass completed
1430	3rd pass completed
1459	4th pass completed
1520	5th pass completed

2.2 Strain Readings on Pipe during Welding

The strains measured during the field trials (see complete listing in Appendix B) are used in the following discussions to describe the strains in selected locations around the sleeve and the pipe surface.

The strains were recorded during welding of the longitudinal seams and during welding of the circumferential fillet welds on the west ends of the sleeves. Typically, the strains were observed to vary significantly as the welding arc approached and moved away from the gauge locations. The typical case for an axial gauge transverse to the welding direction was that the strain would go negative as the arc approached and then go in a positive direction as the arc moved away. The increased negative readings (compression) indicate that heating of the pipe during welding is constrained by the cooler surrounding material, and then the removal of heat upon cooling causes contraction in the weld region and an increase in tensile strain. The opposite would be observed for the gauges installed in the hoop direction, i.e., Gauges 3 and 9, where the strains would become tensile as the arc approached and then decrease as the arc passed on and the weld cooled. An example of this behavior was recorded during completion of Pass 4 on the sleeve at KP 768 (Sleeve 2), as shown in Figures 2.7 and 2.8.

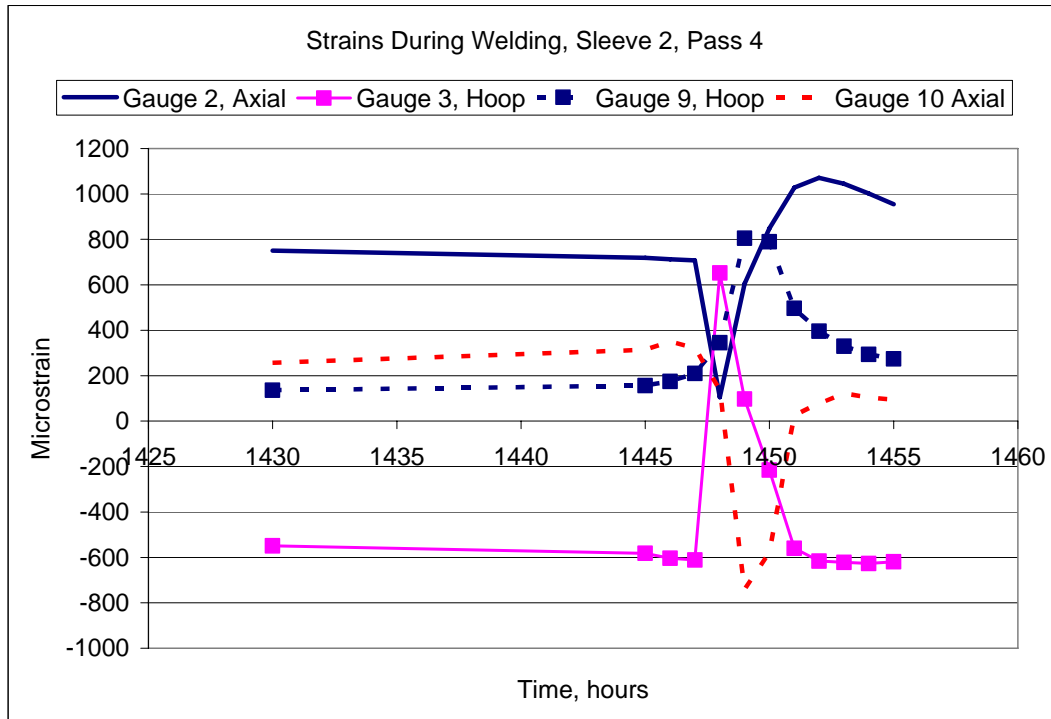


Figure 2.7: Strains Measured Near 3:00 O'clock Position during Completion of Circumferential Weld Pass 4 on Sleeve 2 (KP 768).

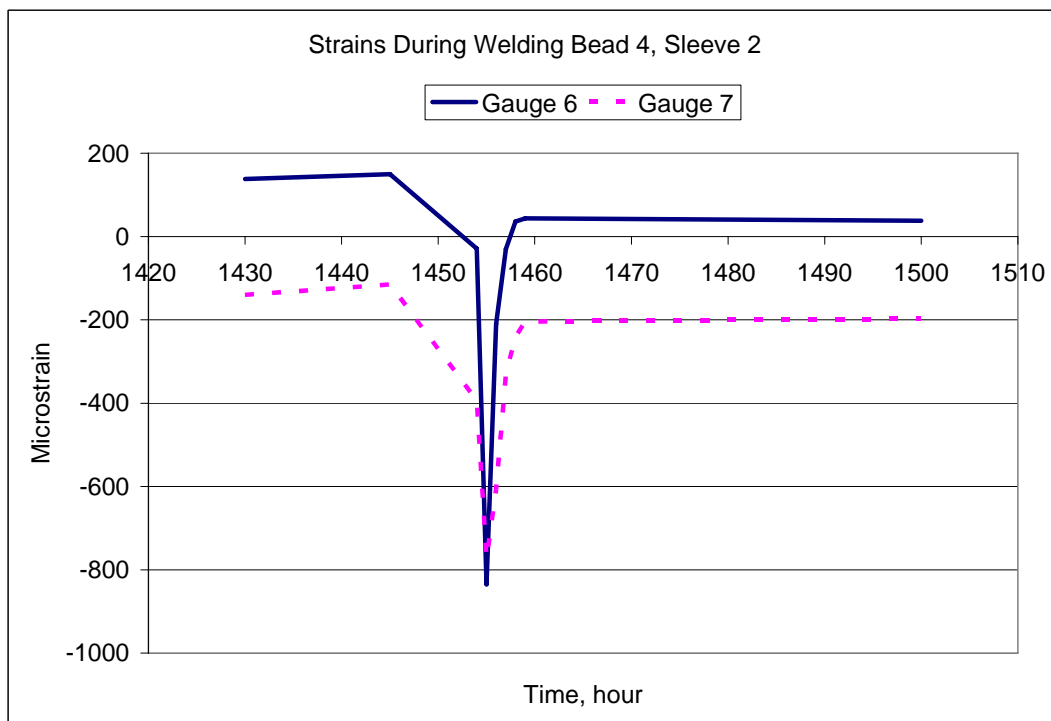


Figure 2.8: Strains Recorded Near 10:30 O'clock Position during Completion of Circumferential Weld Pass 4 on Sleeve 2 (KP 768).

2.3 Comparison of Strain Readings for Individual Passes

The strains for each weld should be similar as the gauges were similarly located at KP 762 and KP 768 with only minor changes in position for some of the gauges on the pipe.

2.3.1 Gauge 1

The comparison of Gauge 1 strain readings indicates similar trends for both sleeves. The initial horizontal weld passes produce a tensile strain across the weld, followed by compressive strains, and then tensile as the weld is completed. The compressive values for Sleeve 1 (KP 762) occurred following the 3rd pass (of 9), while the peak compressive value for Sleeve 2 (KP 768) occurred after the 5th pass (of 11). The remaining weld passes increase the magnitude of the tensile strains, and as the welds cool the strains are reduced by just over 300 $\mu\epsilon$ for both sleeves. The hoop strains at the midpoints of the sleeves are not affected by subsequent welding at the sleeve ends.

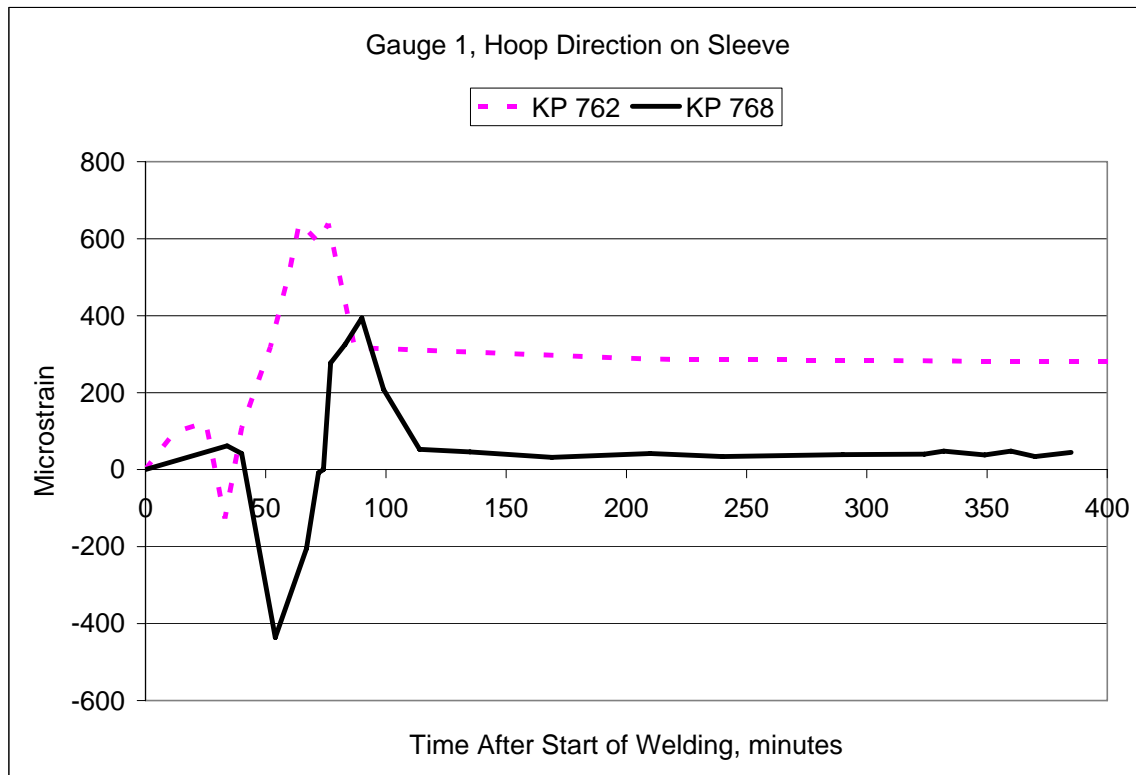


Figure 2.9: Hoop Strains Measured at the Center of the Sleeves

Axial Gauges 4 and 5 at the 12:00 O'clock position (Figures 2.10 and 2.11, respectively) show that the sleeve strains are tensile during and after welding the circumferential fillet welds, while the strains on the pipe vary considerably with the end result being little net change in strain or a compressive strain. In Figures 2.10 to 2.13 the horizontal axes represent the strain reading event, as the important details are the development of strain and the bead sequence, and not the actual timing of the strain development due to welding.

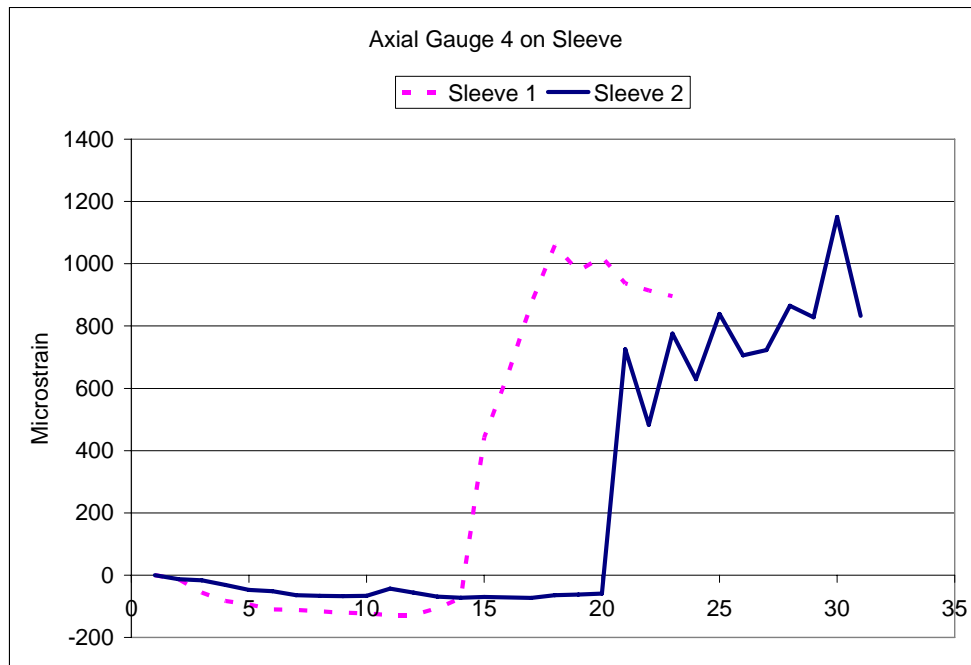


Figure 2.10: Axial Gauge 4 Strains at the Sleeve 12:00 O'clock Position for Sleeve 1 (KP 762) and Sleeve 2 (KP 768).

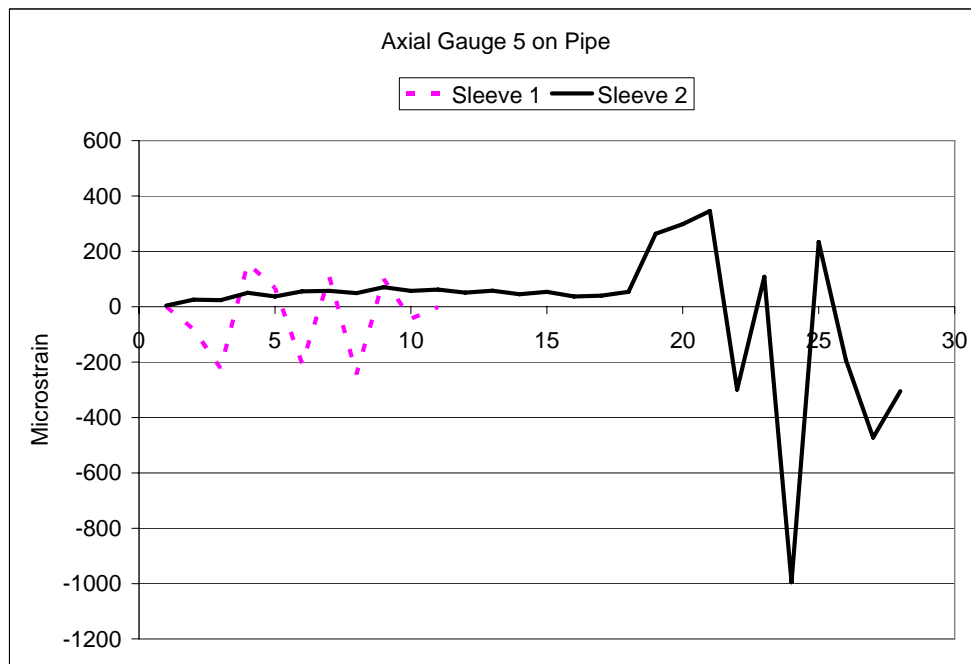


Figure 2.11: Axial Gauge 5 Strains at the Pipe 12:00 O'clock Position for Sleeve 1 (KP 762) and Sleeve 2 (KP 768).

In comparing the axial gauges at the 10:30 O'clock positions (Figure 2.12), it is noted that the Sleeve 1 (KP 762) readings are more tensile than the Sleeve 2 (KP 768) strains. This difference is considered to be attributable mainly to the pipe temperature, with KP 762 being warmer than KP 768. The line was not operating during welding at KP 762, and the pipe temperature became as high as 32°C at 12:00 O'clock and 24°C along Gauges 6 and 7. The pipe temperature at KP 762 reduced further upon continued cooling to its initial temperature of 18°C. The line was in continuous operation during welding at KP 768, and the pipe maintained a steady temperature of 12°C. The pipe temperature did not change during the period of the readings at each location once it had cooled down to the ambient conditions.

The negative strain readings for Sleeve 2 (KP 768) measured during welding show that heating of the pipe during welding produces compressive strains that become positive as the weld area and pipe cool.

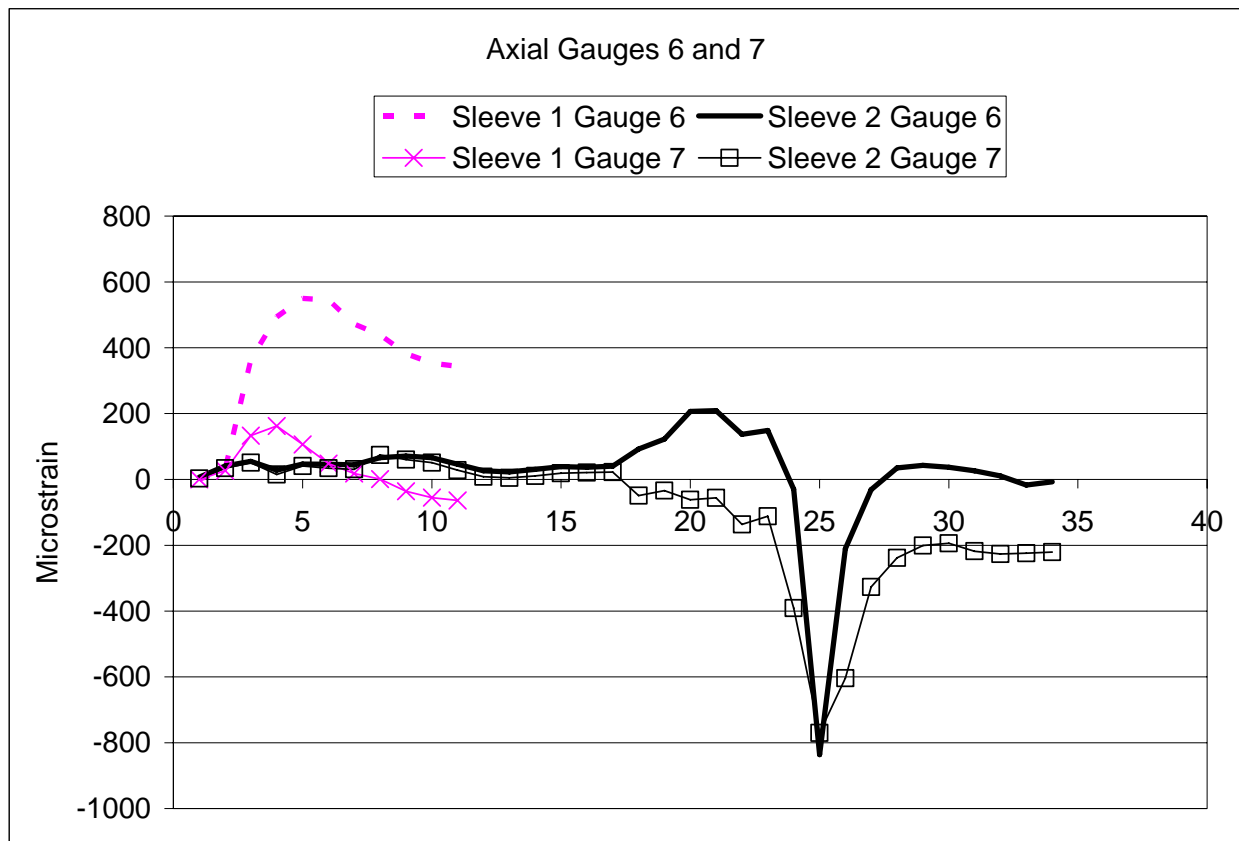


Figure 2.12: Strains for Axial Gauges 6 and 7 on the Pipe 10:30 O'clock Position for Sleeve 1 (KP 762) and Sleeve 2 (KP 768).

A comparison of the strains from Gauges 2, 3, 9, and 10 (Figure 2.13) shows that the magnitudes of the strains and the manner in which the strains changed due to welding were similar for both sleeves. Axial Gauge 2 on the sleeve results in the highest tensile strains after the welds cool, and hoop Gauge 3 has the greatest compressive strains. The axial and hoop gauges on the pipe, Gauge 9 and Gauge 10, have a final tensile strain after the fillet welds have cooled.

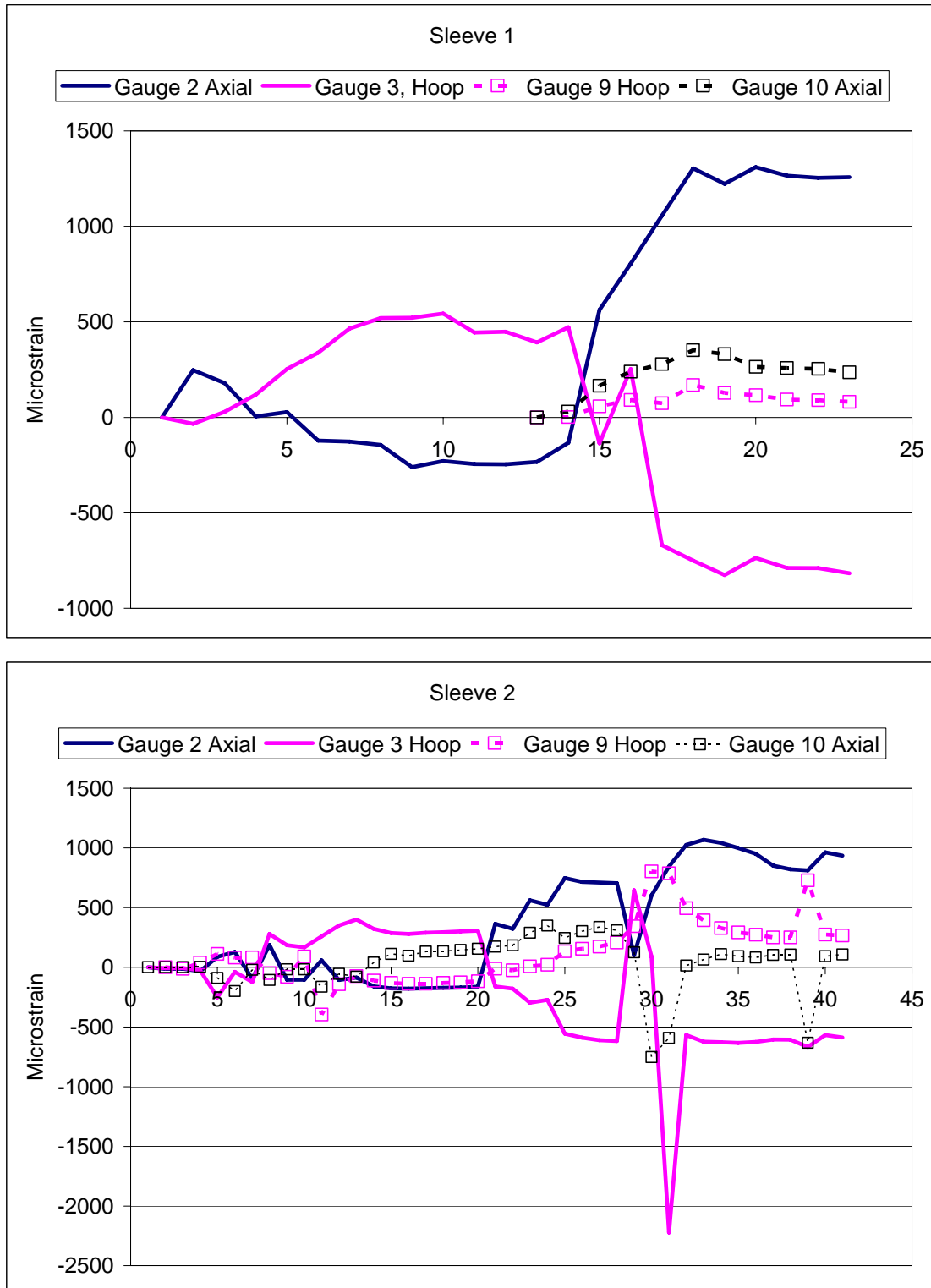


Figure 2.13: Strains for Rosette Gauge Pairs at the 9:30 O'clock Positions for Sleeve 1 (KP 762) and Sleeve 2 (KP 768).

The final strains around the sleeves show consistent behaviors at the two locations upon completion of the circumferential fillet welds. Along the length of the sleeve longitudinal welds the hoop strains near the center of the sleeves were tensile and compressive near the ends of the long seams. The axial strains on the sleeves near the fillet welded ends were tensile, while the axial strains on the pipe could be either tensile or compressive. The pipe strains appeared to depend on the local welding heat input and pipe temperature in the vicinity of the gauges, and in general are lower than the strains observed on the sleeves. The general sense of this behavior is shown in Figure 2.14 in which the letters indicate the final strains as either tensile (T) or compressive (C), with the longer dimension of each box indicating the direction of strain measurement. Note that the final strain reading at 12:00 O'clock on the pipe at KP 762 was approximately zero.



Figure 2.14: Summary of Final Strains on Sleeves at KP 762 and KP 768

2.4 Line Operation during Welding

The Odessa station pressures for the week of 27 September 2004 were obtained from Enbridge Pipelines Inc. The pressures for the period of time over which sleeve welding and data recording was completed are shown in Figure 2.15. The maximum operating pressure out of Odessa station based on a 0.72 design factor and nominal 7.14 mm WT is as follows:

$$\text{MOP} = \frac{0.72 \times \text{SMYS} \times \text{WT}}{\text{OD}/2} = \frac{0.72 \times 359000 \times 7.14}{864 / 2} = 4272 \text{ kPa (620 psi)}$$

Due to low throughputs, Odessa pumps were not operating and the low station discharge indicates that the station was bypassed, with flow being controlled by the upstream station at Regina. Nonetheless, there are a number of points to note in relation to large changes in pressure, with the most noticeable being a drop in pressure at 12:40 am on 29 September, followed by a steady decrease until just after 4:00pm on 29 September when the line was restarted and the pressure steadied at about 200 psi at 6:00 pm. Another significant change with a rapid change in pressure of approximately 200 psi occurred around 9:50 am on 30 September.

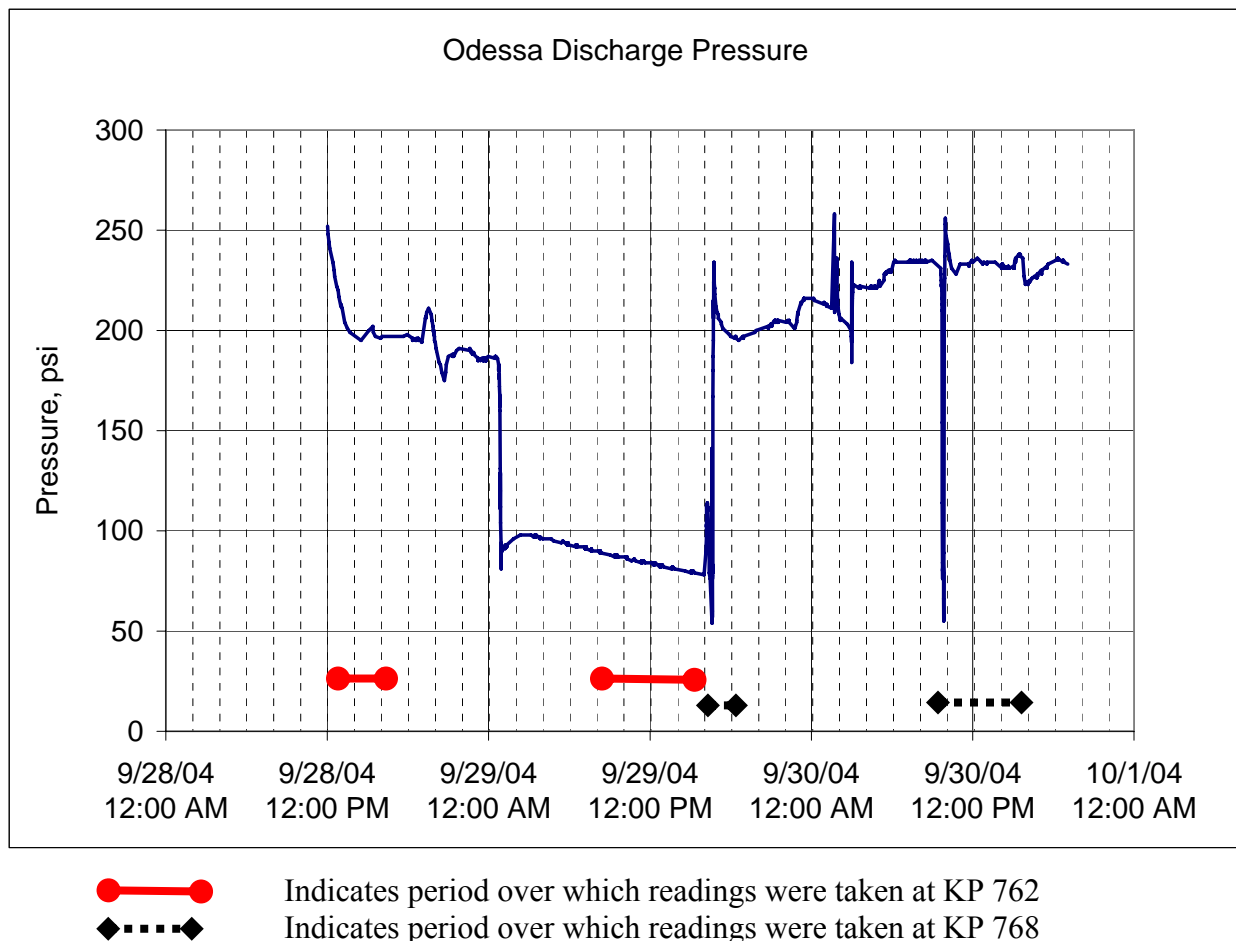


Figure 2.15: Odessa Discharge Pressure over the Period from 28-30 Sept 2004

The pressure changes in the pipeline are important in terms of the resultant strain changes in the sleeves. On the graph of discharge pressure are the times indicated when strain gauges were connected to the line, as shown by the red lines along the bottom of Figure 2.15. The two higher lines represent the KP 762 readings and the two lower lines indicate when the gauges were connected at KP 768. At KP 762 the line pressure was just below 200 psi during completion of the sleeve longitudinal welds on 28 September, at which time Gauges 1, 2, 3, and 4 were connected. The following day all 10 gauges were connected in the morning and readings were taken until 1540. During this time the circumferential welds were completed and there was a gradual decrease in line pressure from 90 to 80 psi.

The change in pressure between the 28th and 29th, from 200 to 90 psi, can be used to examine how the sleeve reacts to changes in line pressure. The results summarized in Table 2.3 show that the 110 psi reduction in pressure results in a decrease in hoop strain of 36 $\mu\epsilon$ at the center of the sleeve and 55 $\mu\epsilon$ decrease near the end of the sleeve to that the $\Delta \epsilon / \Delta P$ values are 0.33 $\mu\epsilon/\text{psi}$ and 0.5 $\mu\epsilon/\text{psi}$. With the reduction in pressure the axial strains, Gauges 2 and 4, show an increase in pressure of 13 and 22 $\mu\epsilon$, roughly one-third of the hoop strain changes in the hoop direction.

Table 2.3: KP 762 Strain Changes on Sleeve

Date	Time	Pressure, psi	Strain Gauge Readings, microstrain			
			1	2	3	4
28 September	1700 h	200	287	-246	448	-128
29 September	0835 h	90	251	-233	393	-106
Differences		-110	-36	13	-55	22
$\Delta \epsilon / \Delta P$, $\mu\epsilon/\text{psi}$			0.33	-0.12	0.5	-0.2

After moving to KP 768 on 29 September, Gauge 8 was connected and then the remaining wires were attached to the other gauges and readings were taken to confirm that all gauges were working properly. During this time it can be seen from Figure 2.15 that the line had been restarted, and the pressures were approximately 195 psi at 1830 h. There was considerable fluctuation in the pressure as the remaining gauges were being attached, so the only readings that can be correlated to pressure changes are the Gauge 8 readings. Gauge 8 was installed and zeroed when the line was at 80 psi, and the hoop strain increased to 156 $\mu\epsilon$ when the pressure was at 195 psi. This gives a value of 0.8 $\mu\epsilon/\text{psi}$ which is higher than the corresponding hoop strain changes on the sleeve at KP 762. This change is consistent with what one could expect as the combined sleeve and pipe thickness should give lower strain changes for the same increase in line pressure.

There was one other pressure change event on 30 September between approximately 0945 h and 1000 h that can be used to calibrate the pressure and strain changes. Figure 2.15 shows an abrupt pressure drop and then returns to its previous pressure after 20 minutes. During this period the longitudinal sleeve welds were being completed and readings were taken at intervals as short as two minutes apart.

This was somewhat fortuitous in that the strain changes were recorded as this event occurred. Field and pipeline times were not correlated exactly so there would be likely some discrepancies in the calculations that follow.

Table 2.4: KP 768 Strain Changes

Date	Time	Pressure, psi	Strain Gauge Readings, microstrain				
			5	6	7	8	10
30 September	0944 h	235	57	44	31	122	-17
30 September	0947 h	55	49	66	74	-104	-164
Differences		-180	-8	22	43	-226	-147
$\Delta \epsilon / \Delta P$, $\mu\epsilon/\text{psi}$			0.04	-0.12	-.24	1.26	0.82
30 September	0947 h	55	49	66	74	-104	-164
30 September	1009 h	235	62	46	28	165	40
Differences		180	13	-20	-46	269	204
$\Delta \epsilon / \Delta P$, $\mu\epsilon/\text{psi}$			0.07	-0.11	-0.26	1.5	1.13

The theoretical change in hoop strain with pressure on the pipe, i.e., Gauge 8, can be calculated according to the following formula:

$$\Delta \sigma = \Delta \epsilon \times E$$

Where $\Delta \sigma$ = change in hoop stress [psi];

$\Delta \epsilon$ = change in strain [in./in.]; and

E = Young's modulus, 30×10^6 psi.

Substituting Barlow's formula for hoop stress, calculated using the p (line pressure), pipe radius (r = 17 in.), and wall thickness (t = 0.281 in.), and rearranging gives the following:

$$\frac{\Delta \epsilon}{\Delta p} = \frac{r}{t \times E} = \frac{17}{0.281 \times 30 \times 10^6} \approx 2 \mu\epsilon/\text{psi}$$

A theoretical change in pressure of 10 psi should result in a strain change of 20 $\mu\epsilon$. The results in Table 3.4 show that the observed change was slightly lower at 1.5 $\mu\epsilon/\text{psi}$.

2.5 Summary of Field Results

The results obtained at the Enbridge Pipelines Inc. excavations east of Odessa, SK provided strains related to welding the sleeve longitudinal welds and the circumferential fillet welds. Some of the gauges recorded changes due only to pressure and will be used to compare to the laboratory and calculated values of strain changes as influenced by line pressure.

3. LAB TRIALS

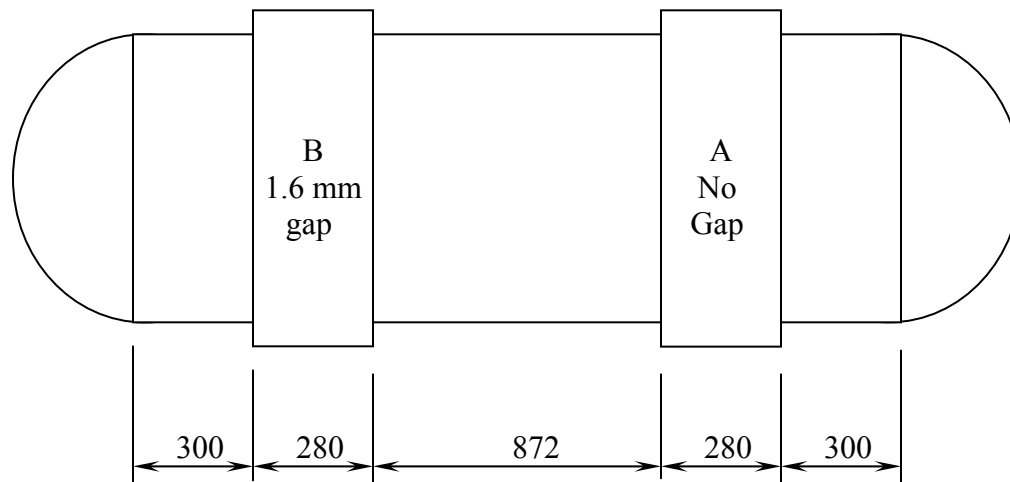
The lab trials were undertaken to investigate the individual effects of each of the sleeve configuration changes on the resultant strains on the sleeve and in the fillet weld areas. The strain changes in a fillet welded reinforcing sleeve due to pressure changes in the pipe were to be obtained for the following cases:

- No pressure in annulus, no gap between sleeve and pipe;
- No pressure in annulus, 1.6 mm gap between sleeve and pipe;
- Pressure in annulus, no gap between sleeve and pipe; and
- Pressure in annulus, 1.6 mm gap between sleeve and pipe.

3.1 Test Vessel Configuration

The overall configuration consists of a 2032 mm length of NPS 12, 6.4 mm WT, Grade X52 seamless pipe with two 9.75 mm thick end caps, onto which are positioned two 16 mm thick sleeves, as shown in Figure 3.1. The pipe had been manufactured in 1998 to the Category II toughness requirements of CSA Standard Z245.1, Steel Line Pipe, and the matching end caps had been produced to the requirements of CSA Standard Z245.11, Steel Fittings.

The sleeves were supplied by TD Williamson.



All dimensions in mm. Not to scale.

Figure 3.1: General Configuration of Test Vessel

3.2 Assembly of Test Vessel

The strain gauges were installed along a line (Gauge Line) located 45 degrees from the 12:00 O'clock position of the pipe. The sleeve longitudinal seam welds would be located 90 degrees from the Gauge Line, as shown in Figure 3.2. The Vent Line, positioned along the 12:00 O'clock position of the pipe, would be used to pressurize the pipe, annulus, or both.

This configuration was chosen to aid mainly with gauge installation along the side of the pipe assembly.

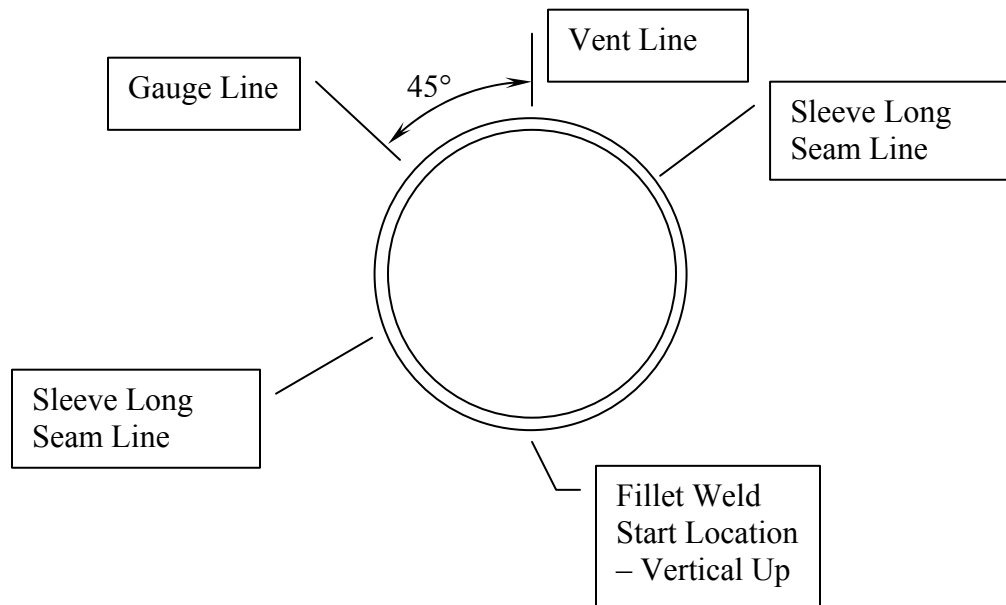


Figure 3.2: End View of Test Vessel Configuration

3.2.1 Reinforcing Sleeves

The split reinforcing sleeves provided by TDW, and manufactured by Williamson Industries, were positioned on the pipe to check the fit and to determine if the root gap on the longitudinal seam welds would need to be adjusted at any position. The sleeves fit very well along the length with a uniform root gap on Side 1 (Figure 3.3) and only a slight variation in the root gap on Side 2 (Figure 3.4). The sleeves also were in good contact with the pipe around the ends where the sleeves would eventually be fillet welded to the pipe (Figures 3.5 and 3.6). The two halves of each sleeve pair were the same length and the circumferential edges were aligned at the longitudinal seams. Due to the quality of the sleeve preparation/geometry and its fit to the pipe surface there was no need to use chain clamps to align the weld edges or to bring the sleeve and pipe surfaces into contact before welding.

The second sleeve was positioned over the pipe using 1.6 mm thick spacers beneath the longitudinal weld seams and tack welds around the circumference (Figure 3.7). The shims were removed once the sleeve was tacked. This resulted in a slightly wider gap on the sleeve longitudinal welds and subsequently required additional weld passes to complete the longitudinal seams, compared to the Sleeve A (no gap).



Figure 3.3: General View of Longitudinal Seam Root Gap on Side 1



Figure 3.4: General View of Longitudinal Seam Root Gap on Side 2



Figure 3.5: View of Root Gap between Pipe and End of Sleeve on Side 1



Figure 3.6: View of Fit-up Between Pipe and End of Sleeve on Side 2



Figure 3.7: View of 1.6 mm Root Gap between Pipe and End of Sleeve B

3.2.2 Vent Connections

The first step in assembly of the vessel was to locate and weld vent connections in the pipe at the middle of each of the sleeve locations. This was followed by locating and welding vent connections at the mid-length position of each sleeve and $\frac{1}{4}$ around the circumference, so that they would be directly over the vents on the pipe. The configuration of the two aligned vent connections is shown in Figure 3.8. This sketch had been prepared to confirm that an NPS 1 thredolet would fit within a larger NPS 2 thredolet and still allow connections to pipe nipples. (It is noted that the manufacturer's catalogue showed only weldolet dimensions, and these were used to prepare the sketches. It was considered that thredolets would have the same relative dimensions as the weldolets and that the pipe nipples would fit within each other.) Due to local availability, NPS $\frac{3}{4}$ and NPS 2 thredolets were used.

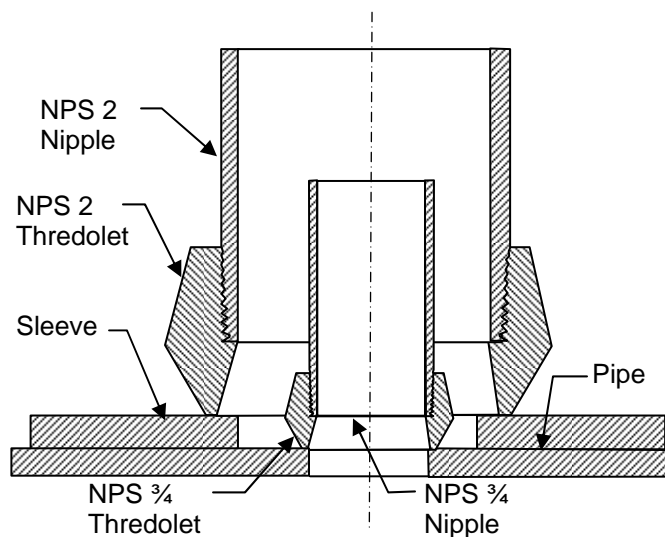


Figure 3.8: Sleeve Vent Details

The first pressure sequence would require applying pressure only to the pipe, in which case the NPS $\frac{3}{4}$ pipe nipple was capped. To apply pressure to both the pipe and annulus between the pipe and the reinforcing sleeves, the NPS $\frac{3}{4}$ nipple was removed and the pressure was applied to the test assembly through the NPS 2 nipple.

3.3 Strain Gauge Locations and Installation

The sections that follow provide details on the position and orientation of the strain gauges used to monitor the test vessel during the investigation. In all instances, the dimensions provided to locate the position of the strain gauge reference the centre of the strain gauge 2, 5, or 6.4 mm gauge lengths. The 6.4 mm gauge length strain gauges (Gauges 13, 14, 16. and 17) were weldable gauges mounted on shims, and were spot welded to the pipe or sleeve surface near welds since they could better tolerate the heat of welding. The 2 mm gauges (Gauges 15 and 18) were located on the pipe near the fillet weld toes, and the 5mm gauge length gauges were used at all other locations (Gauges 1 to 12); all of these gauges were bonded to the pipe/sleeve surface. Details of the gauge types are summarized in Table C1, Appendix C.

3.3.1 Pipe ID Gauges - Gauge 1 and Gauge 2

With the pipe ID being accessible during fabrication of the test assembly, gauges were installed on the pipe ID beneath the fillet welds at the outside ends of each sleeve. The strains on the ID surface of the pipe were to be measured to determine what effect a gap would have on the resultant inner surface strains following completion of the circumferential fillet welds. The gauges were placed approximately 300 mm from each pipe end, and were located such that the gauges were centered 4 mm from the edges of the sleeves, as shown in Figure 3.9. The wires were connected through the sleeve vents and were used only to determine the ID strains during welding as the wires could not remain in place during pressurization.

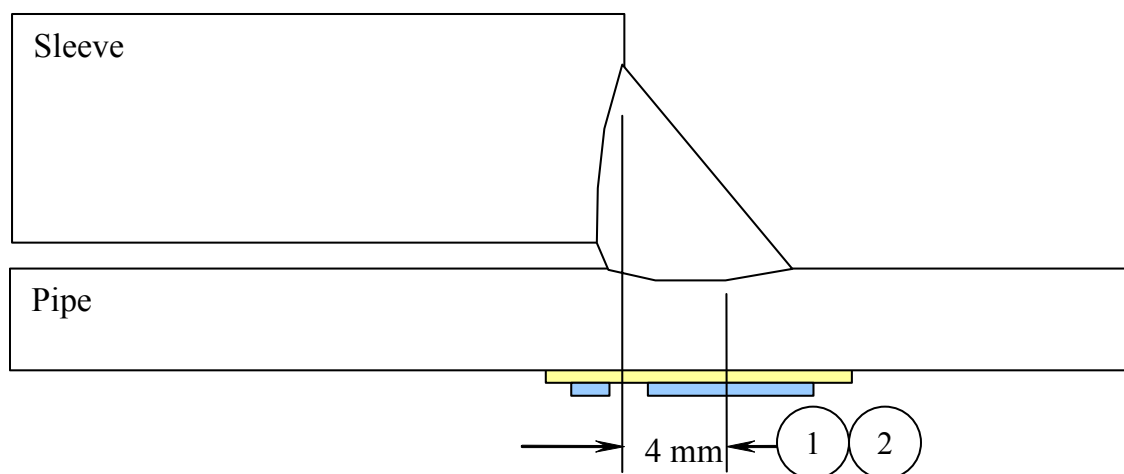


Figure 3.9: Location of Gauges 1 and 2 on Pipe ID Opposite Fillet Welds

3.3.2 Pipe OD Gauges - Gauge 3 and Gauge 4

The gauges were placed on the pipe OD at the mid-length position of the test assembly, with Gauge 3 measuring the hoop strain and Gauge 4 measuring the longitudinal strain on the pipe.

3.3.3 Sleeve OD Gauges - Gauges 5, 6, 7, and 8

The gauges were placed on the sleeve OD at the mid-length position, with Gauges 5 and 6 measuring the hoop and axial strains, respectively, on Sleeve A, and Gauges 7 and 8 measuring the hoop and axial strains, respectively, on Sleeve B.

3.3.4 Sleeve OD Gauges - Gauge 9 and Gauge 10

The gauges were placed on the sleeve OD, 50 mm from the edge of the sleeve to measure the axial strains. Gauge 9 was placed on Sleeve A, and Gauge 10 was on Sleeve B.

3.3.5 Sleeve OD Gauges - Gauge 11 and Gauge 12

The gauges were placed on the sleeve; 10 mm from the edge of the sleeve after the fillet welds had been completed. Both were positioned along the pipe axis, Gauge 11 was placed on Sleeve A and Gauge 12 was on Sleeve B.

The relative positions of Gauges 9, 10, 11, and 12 are shown in Figure 3.10.

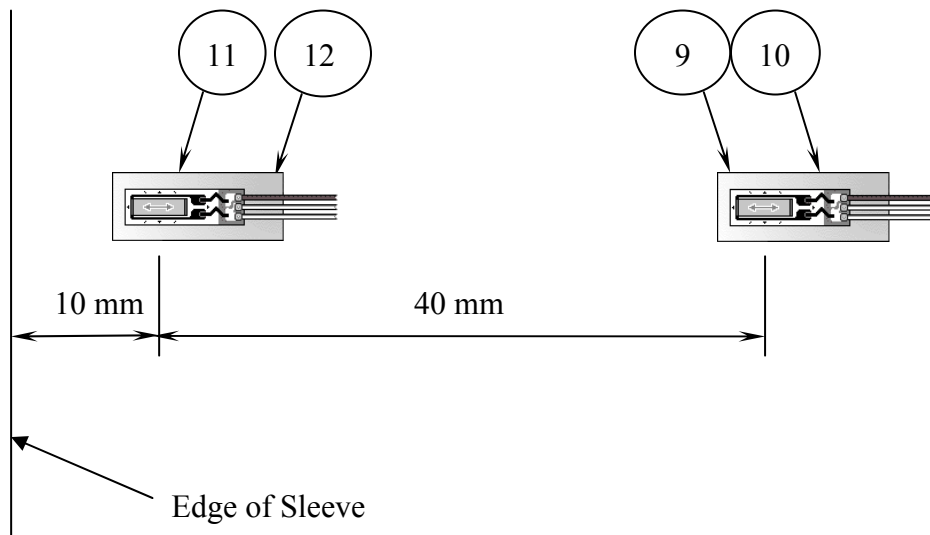


Figure 3.10: Sketch Showing Locations of Gauges on Sleeve OD

3.3.6 Pipe/Sleeve Annulus Gauges 13, 14, 16, and 17

These gauges were used to measure the strains in the annular space between the pipe and sleeve near the fillet welded ends. All four of these gauges were positioned 20 mm from the edge of the sleeve. Gauges 14 and 17 were installed on the pipe OD surface, while Gauges 13 and 16 were installed on the ID surfaces of the sleeve. The gauge pairs were located 20 mm apart, i.e. 10 mm above and below the Gauge Line, so that the wires would not interfere with the opposite gauges, particularly at the solder connections. As Sleeve A had no gap between the sleeve and the pipe, it was necessary to machine shallow grooves near the sleeve ends to accommodate the gauges and the lead wires that would come out through the vent connections, as shown in Figure 3.11. The grooves were 2 mm deep, 10 mm wide, and either 75 mm or 80 mm long. The shorter grooves were used for relief on Gauges 14 and 17 that were mounted on the pipe. The groove in Figure 3.11 above Gauge 13 will end up over Gauge 14 on the pipe OD surface.

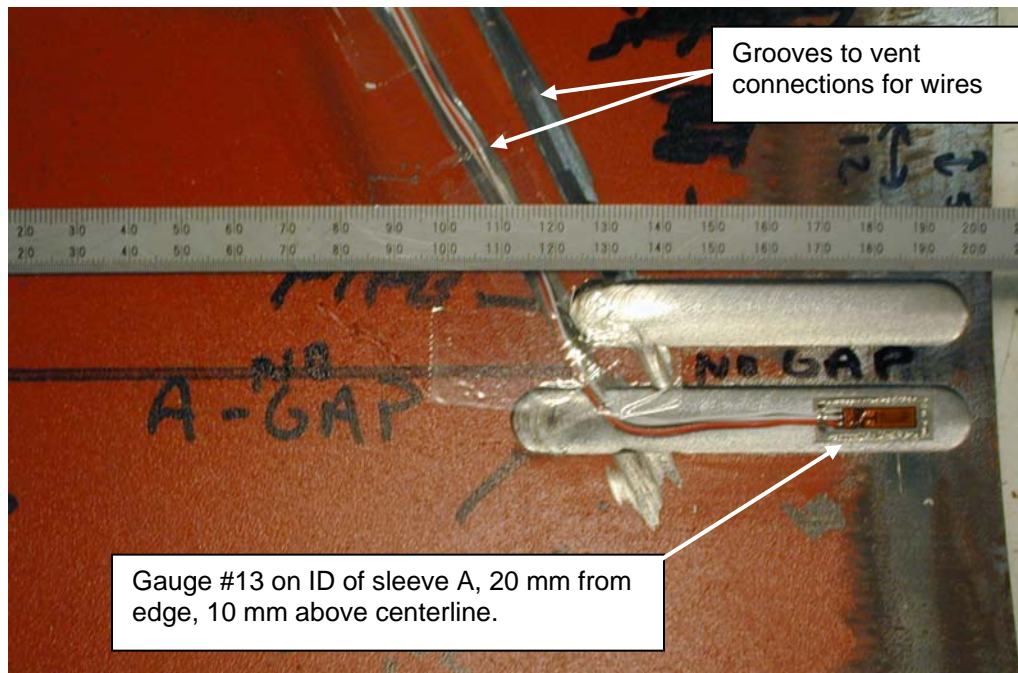


Figure 3.11: Gauge 13 was Located within a Machined Groove on Sleeve A. The second groove shown above was positioned over Gauge 14.

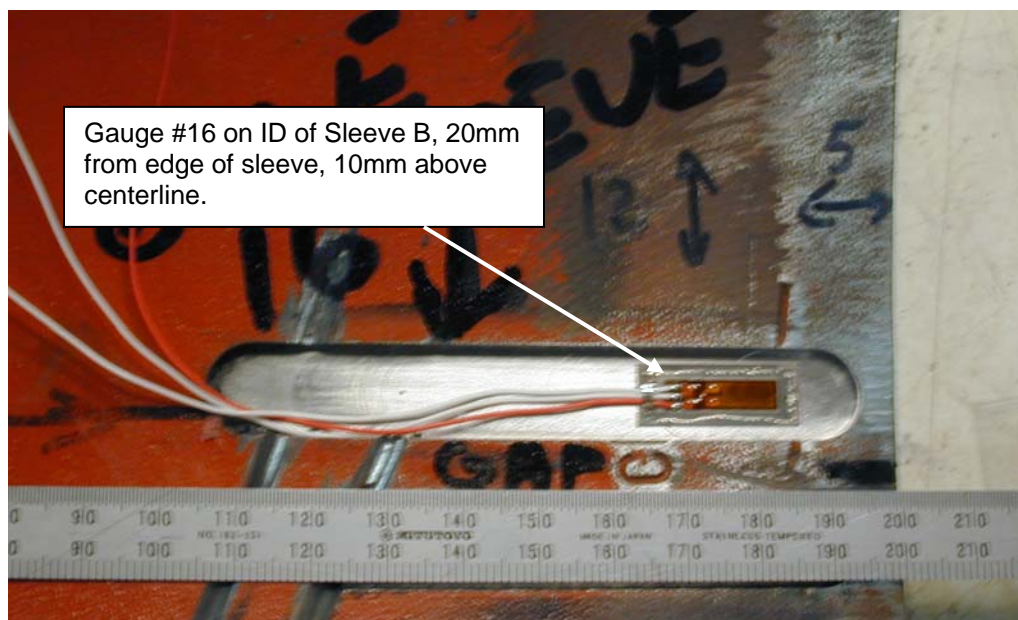


Figure 3.12: Gauge 16 was Located on Sleeve B ID in a Machined Groove

3.3.7 Pipe OD Gauges 15 and 18

These gauges were placed 5 mm from the circumferential fillet weld toes on the pipe OD surface, with Gauge 15 located adjacent to Sleeve A and Gauge 18 located near Sleeve B.

3.4 Test Assembly

The welds used to fabricate the test assembly were all completed using the pulsed GMAW process using a Miller Axxess 450 power source operating in the Accupulse Mode (combination constant current / constant voltage waveform). The consumable was a 0.9 mm Thyssen K-Nova (ER70S-G) wire at a wire feed speed of 5080 mm/min. using a 15% CO₂-Ar shielding gas at 35 CFM.

The welding parameters and sequence for all passes of the circumferential fillet welds are listed in Tables 3.1 to 3.4.

The thredolets were attached to the pipe and sleeve, followed by welding of the end caps, the sleeve longitudinal welds, and finally the circumferential fillet welds on the sleeves. The fillet weld sequence was as follows:

1. Fillet weld on the end of Sleeve A closest to the end cap.
2. Fillet weld on the end of Sleeve A towards the middle of the pipe assembly.
3. Fillet weld on the end of Sleeve B closest to the end cap.
4. Fillet weld on the end of Sleeve B towards the middle of the pipe assembly.

Figure 3.13 shows an overall view of Sleeve B (1.6 mm gap) after completing all of the welds.



Figure 3.13: View of Completed Welds on Sleeve B

The measured dimensions of all fillet welds are summarized in Figure 3.14. The nominal weld size of 9 mm with equal legs was generally obtained for the welds. Note that measurements along the gauge line, as well as at 45 degree increments on both sides of the gauge line were taken, for a total of 5 weld measurements on each fillet weld. The average weld size is the weld shape, which will be used in the modelling process, discussed in Section 4.0.

The dimensions T, x, and V are all measured quantities, with the weld leg height, H, calculated by taking the difference between dimensions T and x.

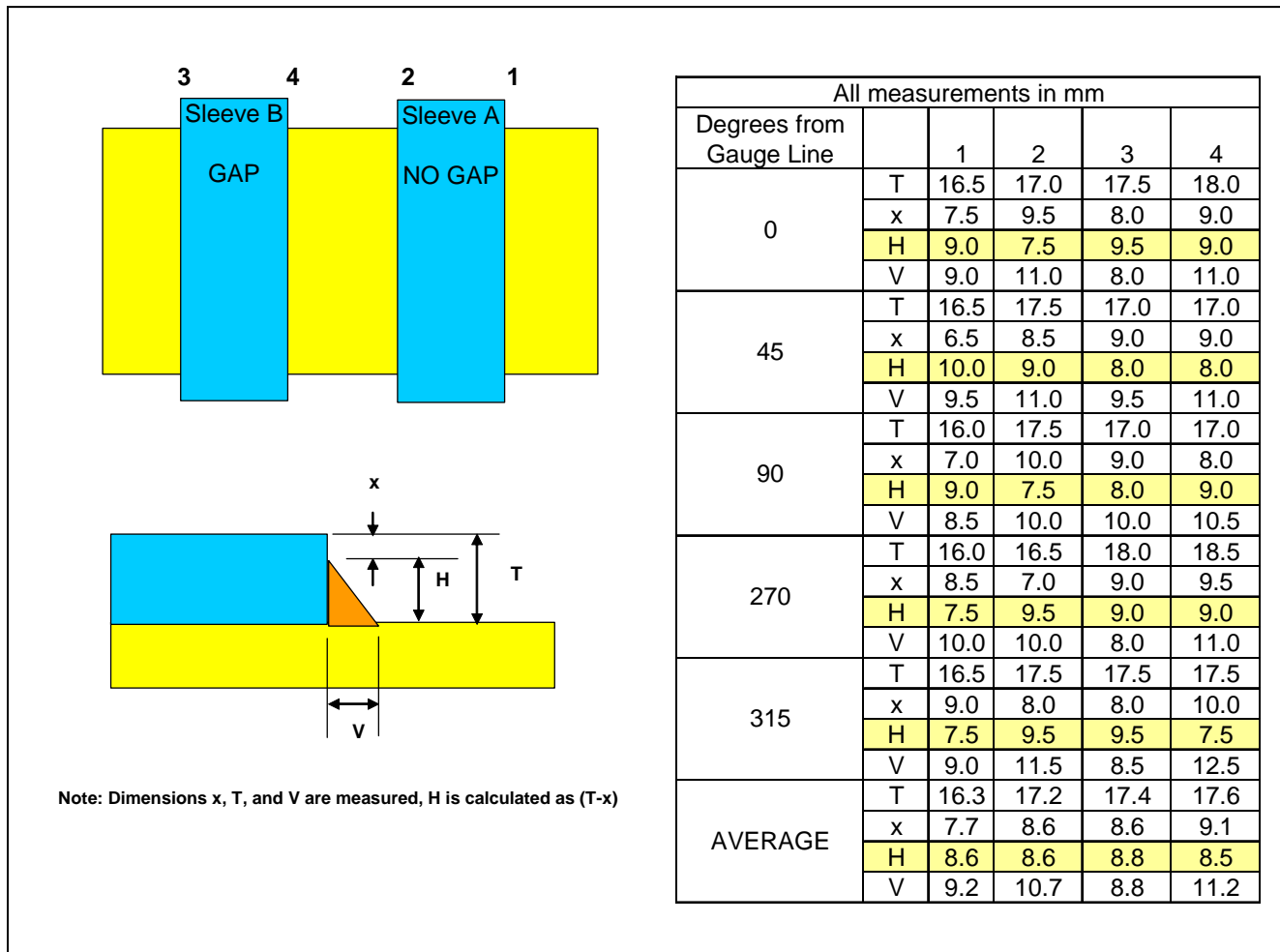


Figure 3.14: Fillet Weld Dimensions

Table 3.1: Welding Details for Circumferential Fillet Weld on Outside of Pipe (Away from Gauges), Sleeve A

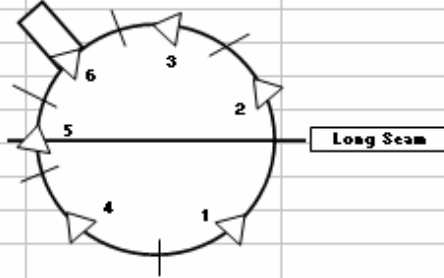
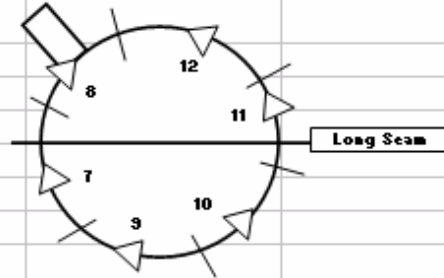
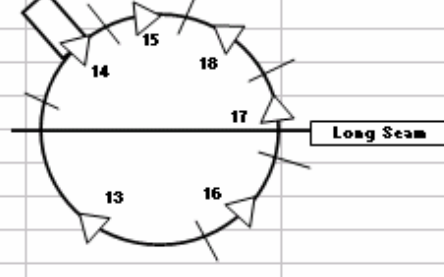
	Weld Segment	Amps (A)	Volts (V)	Length (mm)	Time (s)	Time (min)	Travel Speed (mm/min)	Heat Input (kJ/mm)	
First Pass	1	104	19.7	270	87	1.45	186.21	0.66	
	2	102	19.6	170	57	0.95	178.95	0.67	
	3	101	19.7	150	44	0.73	204.55	0.58	
	4	105	19.4	180	52	0.87	207.69	0.59	
	5	102	19.6	190	61	1.02	186.89	0.64	
	6	101	19.7	120	38	0.63	189.47	0.63	
Second Pass	7	114	19.4	200	59	0.98	203.39	0.65	
	8	104	19.7	150	43	0.72	209.30	0.59	
	9	106	19.6	190	36	0.60	316.67	0.39	
	10	101	19.6	210	39	0.65	323.08	0.37	
	11	108	19.5	210	49	0.82	257.14	0.49	
	12	109	19.5	150	24	0.40	375.00	0.34	
Third Pass	13	100	19.5	260	69	1.15	226.09	0.52	
	14	102	19.7	165	59	0.98	167.80	0.72	
	15	104	19.7	140	42	0.70	200.00	0.61	
	16	102	19.6	190	45	0.75	253.33	0.47	
	17	99	19.7	220	72	1.20	183.33	0.64	
	18	104	19.6	130	36	0.60	216.67	0.56	

Table 3.2: Welding Details for Circumferential Fillet Weld on Inside of Pipe (Near Gauges), Sleeve A

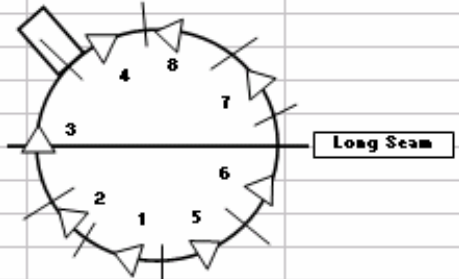
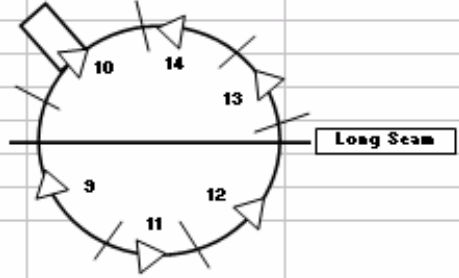
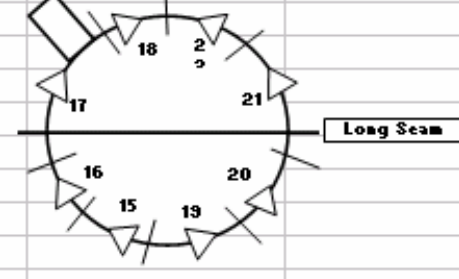
	Weld Segment	Amps (A)	Volts (V)	Length (mm)	Time (s)	Time (min)	Travel Speed (mm/min)	Heat Input (kJ/mm)	
First Pass	1	95	19.6	100	34	0.57	176.47	0.63	
	2	99	19.5	50	17	0.28	176.47	0.66	
	3	102	19.6	270	98	1.63	165.31	0.73	
	4	102	19.6	220	38	0.63	347.37	0.35	
	5	104	19.6	140	36	0.60	233.33	0.52	
	6	100	19.7	200	60	1.00	200.00	0.59	
Second Pass	7	99	19.6	120	45	0.75	160.00	0.73	
	8	95	19.7	120	31	0.52	232.26	0.48	
	9	101	19.6	330	72	1.20	275.00	0.43	
	10	109	19.6	140	32	0.53	262.50	0.49	
	11	100	19.6	170	31	0.52	329.03	0.36	
	12	101	19.5	220	41	0.68	321.95	0.37	
Third Pass	13	98	19.6	155	39	0.65	238.46	0.48	
	14	101	19.4	90	18	0.30	300.00	0.39	
	15	99	19.7	60	22	0.37	163.64	0.72	
	16	102	19.6	130	40	0.67	195.00	0.62	
	17	100	19.6	245	86	1.43	170.93	0.69	
	18	106	19.6	140	38	0.63	221.05	0.56	
	19	101	19.5	130	33	0.55	236.36	0.50	
	20	101	19.5	120	33	0.55	218.18	0.54	
	21	101	19.6	185	51	0.85	217.65	0.55	
	22	105	19.8	140	46	0.77	182.61	0.68	

Table 3.3: Welding Details for Circumferential Fillet Weld on Outside of Pipe (away from gauges), Sleeve B

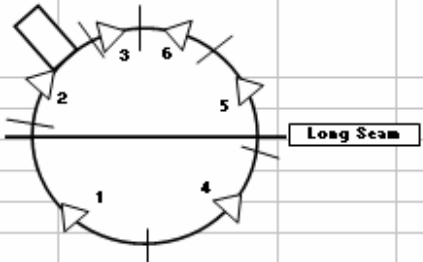
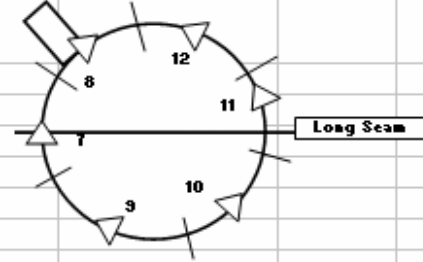
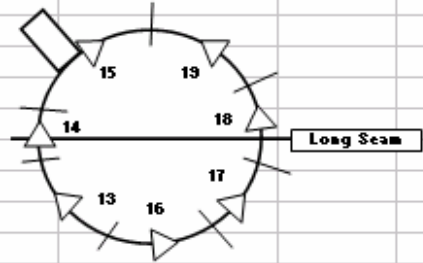
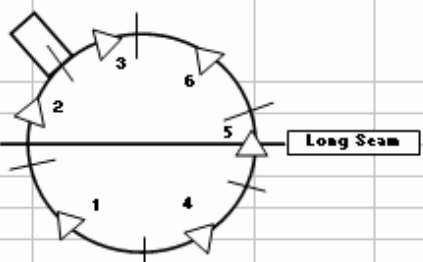
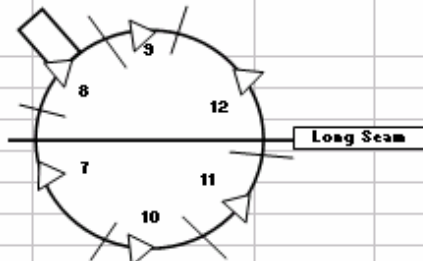
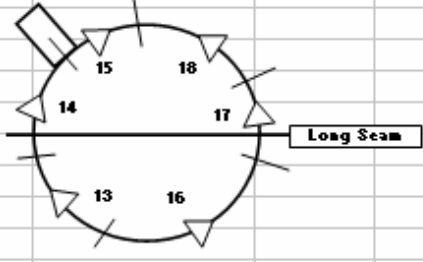
	Weld Segment	Amps	Volts	Length	Time		Travel Speed	Heat Input	
		(A)	(V)	(mm)	(s)	(min)	(mm/min)	(kJ/mm)	
First Pass	1	95	19.4	260	102	1.70	152.94	0.72	
	2	100	18.5	195	72	1.20	162.50	0.68	
	3	98	19.2	110	37	0.62	178.38	0.63	
	4	108	19.3	240	62	1.03	232.26	0.54	
	5	104	19.4	190	52	0.87	219.23	0.55	
	6	103	19.5	120	32	0.53	225.00	0.54	
Second Pass	7	99	19.2	210	60	1.00	210.00	0.54	
	8	105	19.5	135	29	0.48	279.31	0.44	
	9	99	19.4	190	51	0.85	223.53	0.52	
	10	104	19.5	120	23	0.38	313.04	0.39	
	11	106	19.4	200	44	0.73	272.73	0.45	
	12	105	19.5	235	54	0.90	261.11	0.47	
Third Pass	13	100	19.7	190	66	1.10	172.73	0.68	
	14	102	19.7	180	79	1.32	136.71	0.88	
	15	101	19.8	150	58	0.97	155.17	0.77	
	16	93	19.6	130	38	0.63	205.26	0.53	
	17	102	19.7	190	42	0.70	271.43	0.44	
	18	109	19.8	90	55	0.92	98.18	1.32	
	19	106	19.8	80	23	0.38	208.70	0.60	

Table 3.4: Welding Details for Circumferential Fillet Weld on Inside of Pipe (near gauges), Sleeve B

	Weld Segment	Amps	Volts	Length	Time		Travel Speed	Heat Input	
		(A)	(V)	(mm)	(s)	(min)	(mm/min)	(kJ/mm)	
First Pass	1	99	19.7	190	63	1.05	180.95	0.65	
	2	102	19.7	220	79	1.32	167.09	0.72	
	3	104	19.6	180	57	0.95	189.47	0.65	
	4	99	19.8	200	74	1.23	162.16	0.73	
	5	98	19.7	160	66	1.10	145.45	0.80	
	6	102	19.7	160	61	1.02	157.38	0.77	
Second Pass	7	102	19.7	240	59	0.98	244.07	0.49	
	8	109	19.5	120	33	0.55	218.18	0.58	
	9	98	19.6	170	40	0.67	255.00	0.45	
	10	96	19.7	150	34	0.57	264.71	0.43	
	11	101	19.6	190	4	0.07	2850.00	0.04	
	12	105	19.7	245	57	0.95	257.89	0.48	
Third Pass	13	104	19.7	170	50	0.83	204.00	0.60	
	14	104	19.7	210	68	1.13	185.29	0.66	
	15	100	19.8	145	40	0.67	217.50	0.55	
	16	99	19.6	220	81	1.35	162.96	0.71	
	17	102	19.6	220	85	1.42	155.29	0.77	
	18	98	19.9	150	48	0.80	187.50	0.62	

3.5 Strain Gauge Results

The strains were recorded before and after welding of the sleeves to the pipe and before, during, and after pressurization. The readings were stored in files listed from B1 to B10, as described in Table 3.5. The significant strain readings are found in Files B2, B4, B7, and B9. These readings include the:

- B2 readings taken following completion of the circumferential fillet welds,
- B4 readings taken with the pipe pressurized to 250 psi,
- B7 readings taken with the pipe pressurized to 500 psi, and
- B9 readings taken with both the pipe and annulus pressurized to 500 psi.

The Gauge Summary in Table 3.6 shows which gauges were used for each of the files. Gauges 1 and 2 on the pipe ID were disconnected following welding as the wires could not be routed outside of the pressurized vessel. The other gauges were added after all welding had been completed. Only Gauge 17 did not provide strain readings, presumably as it had become shorted after fillet welding the sleeve ends.

Table 3.5: File Descriptions

File	Pressure	Description
B1	0	Zeros before welding
B2	0	After welding of both sleeves finished
B3	0	New zeros with 8 new gages
B4	250	250 psi test, pipe pressurized
B5	0	After 250 test back to 0
B6	0	0 reading before 500 psi test June 27
B7	500	1 st 500 psi test, pipe pressurized
B8	0	After 500 psi test back to 0 psi
B9	500	2 nd 500 psi test, pipe and annulus pressurized
B10	0	After 2 nd 500 psi test back to 0

Table 3.6: Gauge Data Reporting Summary

File	Pressure	Strain Gauge Numbers																	
		1	2	3	4	5	6	7	8	9	10	11	12	13	14	15	16	17	18
B1	0	●	●	●	●					●	●			●	●		●	(c)	
B2	0	●	●	●	●					●	●			●	●		●	(c)	
B3	0	(a)	(a)	●	●	●	●	●	●	●	●	●	●	●	●	●	●	(c)	●
B4	250	(a)	(a)	●	●	●	●	●	●	●	●	●	●	●	●	●	●	(c)	●
B5	0	(a)	(a)	●	●	●	●	●	●	●	●	●	●	●	●	●	●	(c)	●
B6	0	(a)	(a)	●	●	●	●	●	●	●	●	●	●	●	●	●	●	(c)	●
B7	500	(a)	(a)	●	●	●	●	●	●	●	●	●	●	●	●	●	●	(c)	●
B8	0	(a)	(a)	●	●	●	●	●	●	●	●	●	●	●	●	●	●	(c)	●
B9	500	(a)	(a)	●	●	●	●	●	●	●	●	●	●	(b)	(b)	●	(b)	(b)	●
B10	0	(a)	(a)	●	●	●	●	●	●	●	●	●	●	(b)	(b)	●	(b)	(b)	●

(a) Gauge 1 and Gauge 2 on the pipe ID were disconnected in order to pressurize the pipe.

(b) Gauges 13, 14, 15, and 16 were disconnected in order to pressurize the pipe and annulus.

(c) Gauge 17 did not provide strain readings.

3.5.1 Strains after Completing Sleeve Fillet Welds

The strains were recorded for the gauges shown in Figure 3.15 during completion of welding of the sleeves to the pipe. Of these gauges, Gauge 3 was the only one that had been installed to record strains in the hoop direction. As noted earlier, Gauge 17 was shorted out during welding of the sleeves to the pipe.

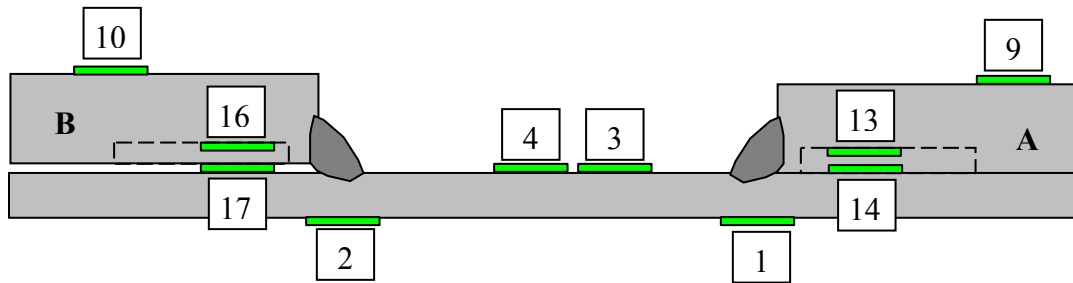
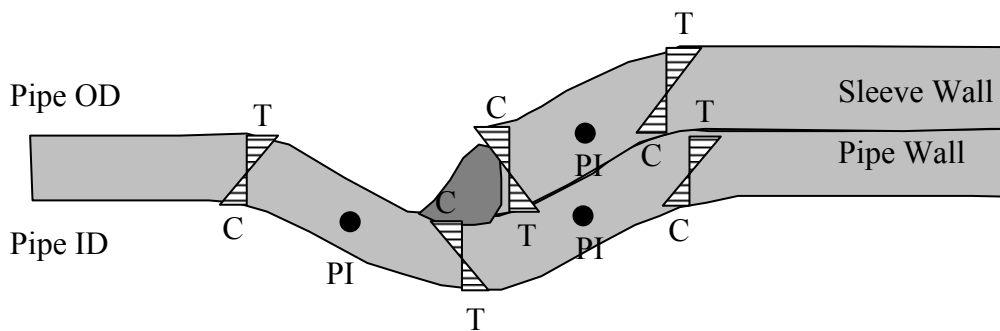


Figure 3.15: Sketch of Active Gauges during Completion of Sleeve Welding

In the description of the reading for each strain gauge a commentary is given regarding the observed and assumed strains based upon an assumed pipe and sleeve deformed shape as shown in Figure 3.16. The idealized stress or strain distributions shown in Figure 3.16 illustrate the sense of the local bending stress distributions. Since a membrane stress, of constant magnitude through the wall thickness, may be added to each local bending stress distribution, the idealized bending stress distributions illustrated may be used to identify the relative magnitude of local stresses and strains on either side of the pipe or sleeve wall thickness. For example, using a sign convention that assigns positive strains to tensile stresses and negative to compression, a location showing a strain distribution varying from “T” to “C” indicates that it is expected that the measured “T” side would be more positive (greater tension) than the “C” side.



- | | |
|----|---|
| C | = Compression (more negative strain at this side of the wall) |
| T | = Tension (more positive strain at this side of the wall) |
| PI | = Point of Inflection of Bending Moment Distribution (local maximum bending stress = 0) |

Figure 3.16: Assumed Deformed Shape of the Pipe and Sleeve after Welding

Gauges 1 and 2: These strains were recorded on the pipe ID, 4 mm from the edge of the sleeve so that they would be directly beneath the circumferential fillet welds. A strain of $-769\ \mu\epsilon$ resulted at Gauge 1 on the tight-fitting sleeve, which was approximately 4 times greater than the $-187\ \mu\epsilon$ beneath the weld at Gauge 2 on the sleeve with a 1.6 mm gap. This difference indicates that the gap between the sleeve and the pipe is significant in terms of the strains on the pipe at the ends of the fillet welds. When the sleeve and pipe are in contact before welding, the resultant shrinkage as the weld cools is transferred more completely to the pipe wall. With the 1.6 mm gap between the sleeve and pipe, the sleeve and pipe shrinkage appears to be independent of one another and the strain measured at Gauge 2 results only from the contraction of the pipe. The weld shrinkage forces with the gapped sleeve likely only reduce the gap between the sleeve and the pipe; this observation could not be confirmed through measurements on the test assembly, but is considered to be a logical explanation for the observed differences in strain.

Gauges 3 and 4: These two gauges were located at the midpoint of the test assembly approximately 435 mm from each of the sleeves, measuring the strains on the pipe away from the sleeve welds. As a result of completing the fillet welds on both sleeves, the hoop strain measured $388\ \mu\epsilon$ and the axial gauge measured $-57\ \mu\epsilon$. This suggests that the installation of the sleeves causes outward bulging away from the sleeve fillet welds.

Gauges 9 and 10: These gauges were located on the sleeve OD surfaces, 50 mm from the edge of the sleeve, and recorded axial strains. After welding the strains were $830\ \mu\epsilon$ and $713\ \mu\epsilon$ for Sleeve A (no gap) and Sleeve B (1.6 mm gap), respectively. These strains are presumably due to local bending associated with the response of the sleeve to the circumferential fillet weld shrinkage forces. The sense of the strains agrees with the assumed pipe deformed shape illustrated in Figure 3.16.

Gauges 13 and 16: These gauges were located on the sleeve ID surfaces, 20 mm from the edge of the sleeve, and recorded axial strains. The strain on Sleeve A was slightly compressive for Gauge 13, whereas Gauge 16 on the Sleeve B had a strain of $444\ \mu\epsilon$ after welding. While both of these strains are presumably due to the response of the sleeve to the weld shrinkage loads, the effect of the gap has been to move the point of inflection (see Figure 3.16) and as a result one of the strain gauges is located in the zone of positive bending while the other is in the negative bending moment zone.

Gauges 14 and 17: These gauges were located on the pipe OD surfaces, 20 mm from the edge of the sleeve, and recorded axial strains. Gauge 17 was not working after the sleeves had been welded to the pipe. A reading of -306 for Gauge 14 indicates that the area beneath the weld on Sleeve A was in compression following completion of the fillet weld.

The remaining eight (8) strain gauges were glued in position after the circumferential fillet welds had been completed. Figure 3.17 gives the approximate locations for the final gauge placement, showing that they were located in close proximity to the fillet welds on both sleeves.

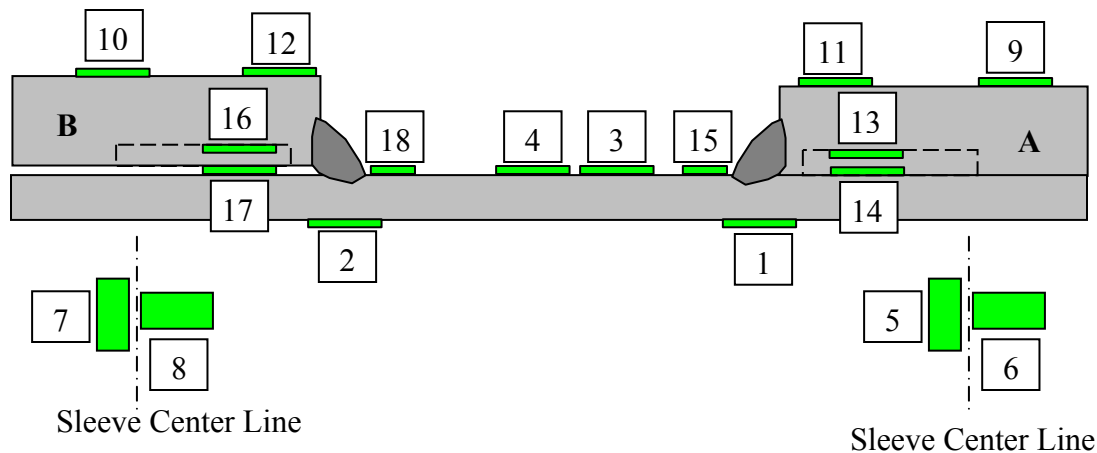


Figure 3.17: Sketch of Final Gauge Placement

3.5.2 Strains Resulting from Welding Sleeves

The strains following welding can be compared as in Figure 3.18 where the strains for gauges on Sleeve A and Sleeve B are plotted for comparison. In both cases, it is seen that the outer surface of the sleeve is in tension and the inner surface of the pipe is in compression. The differences between the maximum and minimum strains on each sleeve are $1699 \mu\epsilon$ for Sleeve A and $900 \mu\epsilon$ for Sleeve B. This difference between the two sleeves is due mainly to the higher compressive strain on the pipe ID surface of Sleeve A. The most significant observation from these readings is that the root of the fillet/sleeve interface of Sleeve B (1.6 mm gap) is in tension as opposed to the compressive strains in the same region of Sleeve A. This result shows that large weld root gaps can lead to high tensile strains across the root of the fillet weld due to thermal contraction of the weld.

In the subsequent discussions, the strains resulting from completion of the fillet welds will be subtracted from the strains attributable to pressure only. This correction will isolate the response of the pipe and sleeve due to pressure fluctuations from those introduced by welding of the sleeve.

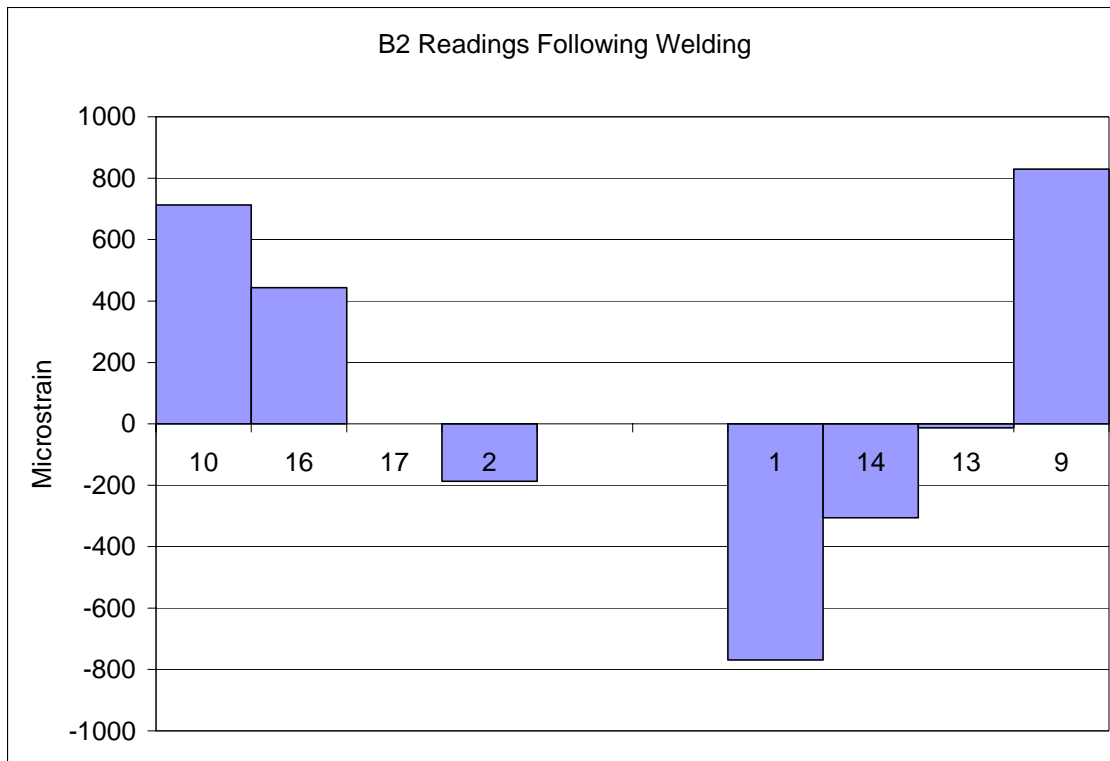


Figure 3.18: Strains after Completion of Circumferential Fillet Welds (B2 Readings)

3.5.3 Response to Pressure Fluctuations

Three pairs of gauges were used to record the strains remote from the fillet welds between the sleeves and the pipe; Gauges 3 and 4 were centered between the sleeves on the pipe, Gauges 5 and 6 were on Sleeve A, and Gauges 7 and 8 were on Sleeve B (see Figure 3.19). The strain readings for these gauges are summarized in Table 3.7 and plotted in Figure 3.20.

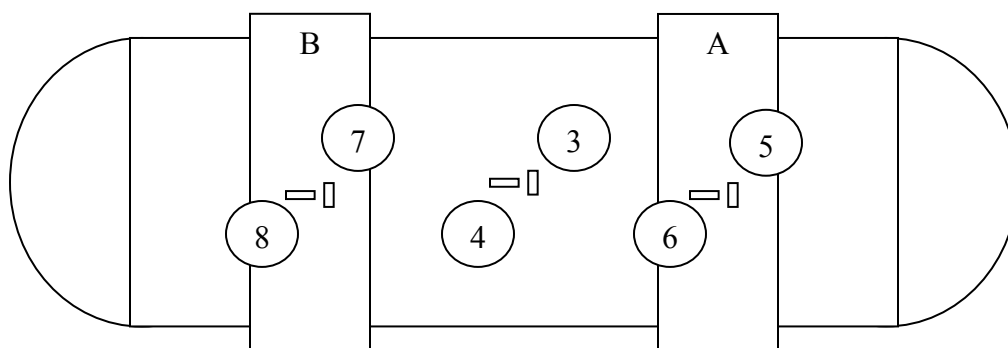


Figure 3.19: Locations of Hoop and Axial Gauges

Table 3.7: Hoop and Axial Strain Readings (Pressure Only)

File	Gauges					
	Hoop Strain ($\mu\epsilon$)			Axial Strain ($\mu\epsilon$)		
	3	5	7	4	6	8
B3	0	0	0	0	0	0
B4	117	-15	-40	26	2	12
B5	0	0	-1	-5	-3	-1
B6	-1	-2	9	8	4	1
B7	252	-34	-69	65	6	24
B8	1	-5	9	5	0	0
B9	249	49	42	69	40	28
B10	-4	-9	6	4	-4	-2

The B4 readings at 250 psi are approximately one-half of the value of the B7 readings at 500 psi, with both sets of readings taken with only the pipe pressurized. This is expected as the stress (and strain) increases linearly with pressure according to Barlow's formula, as follows:

$$\sigma = \frac{\text{Pressure} \times \text{Radius}}{\text{Thickness}}$$

The strain can be obtained by dividing the calculated stress by Young's modulus, 30×10^6 psi. The hoop strain on the NPS 12 (12.75 in. OD), 0.25 in. WT pipe at 250 psi is calculated as follows:

$$\sigma = \frac{Pr}{Et} = \frac{250 \times 6.375}{0.25 \times 30 \times 10^6} = 213 \mu\epsilon$$

The measured hoop strain was only $117 \mu\epsilon$, almost one-half of the strain calculated for an infinitely long cylinder pressurized to 250 psi, which suggests that the sleeves prevent the pipe from expanding as expected. Further comparison of the behavior of the test specimen will be completed based upon comparison to FE models.

The hoop strains on the sleeves with only the pipe pressurized indicate negative strains for both sleeves, and with the sleeves pressurized the strains are both positive values and approximately equal.

The axial strains are all positive on the pipe and the sleeve, and higher strains are observed with the higher pressures. With only the pipe pressurized the strains are greater with Sleeve B (1.6 mm gap) compared to no gap. The strains with the annulus pressurized are greater for Sleeve A compared to Sleeve B, which is opposite to the trend observed with only the pipe pressurized.

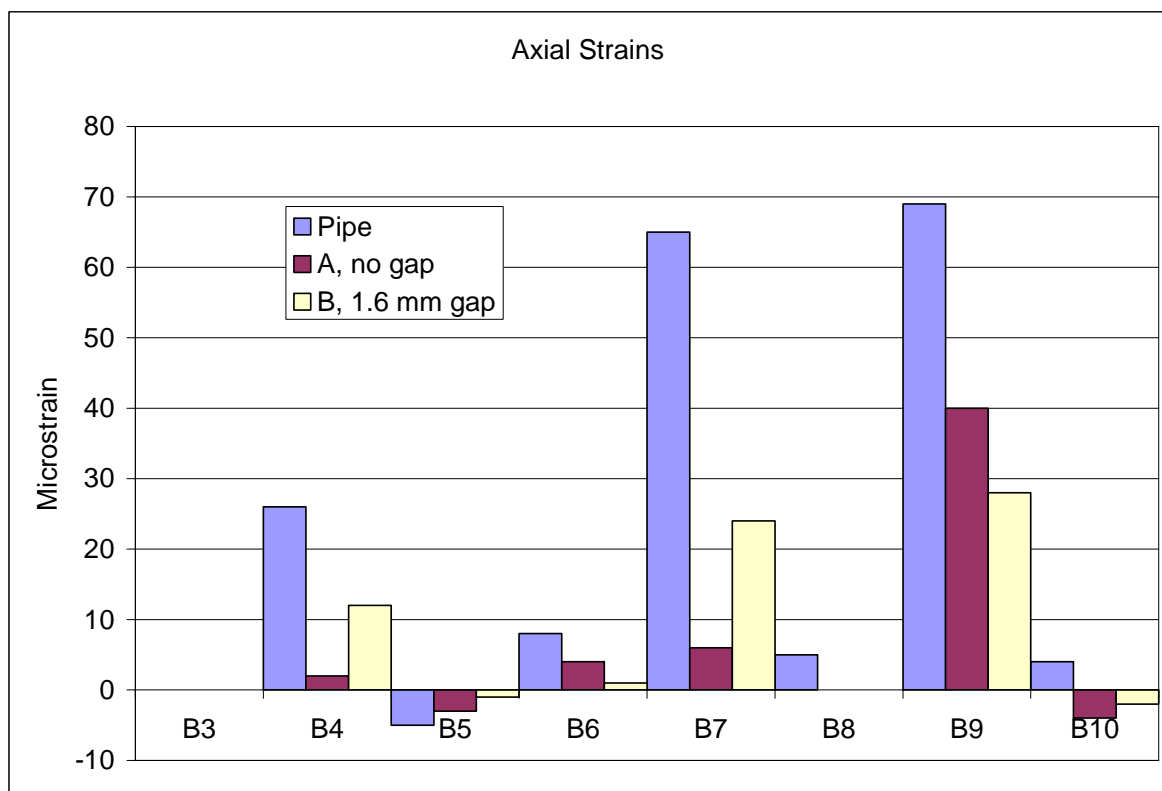
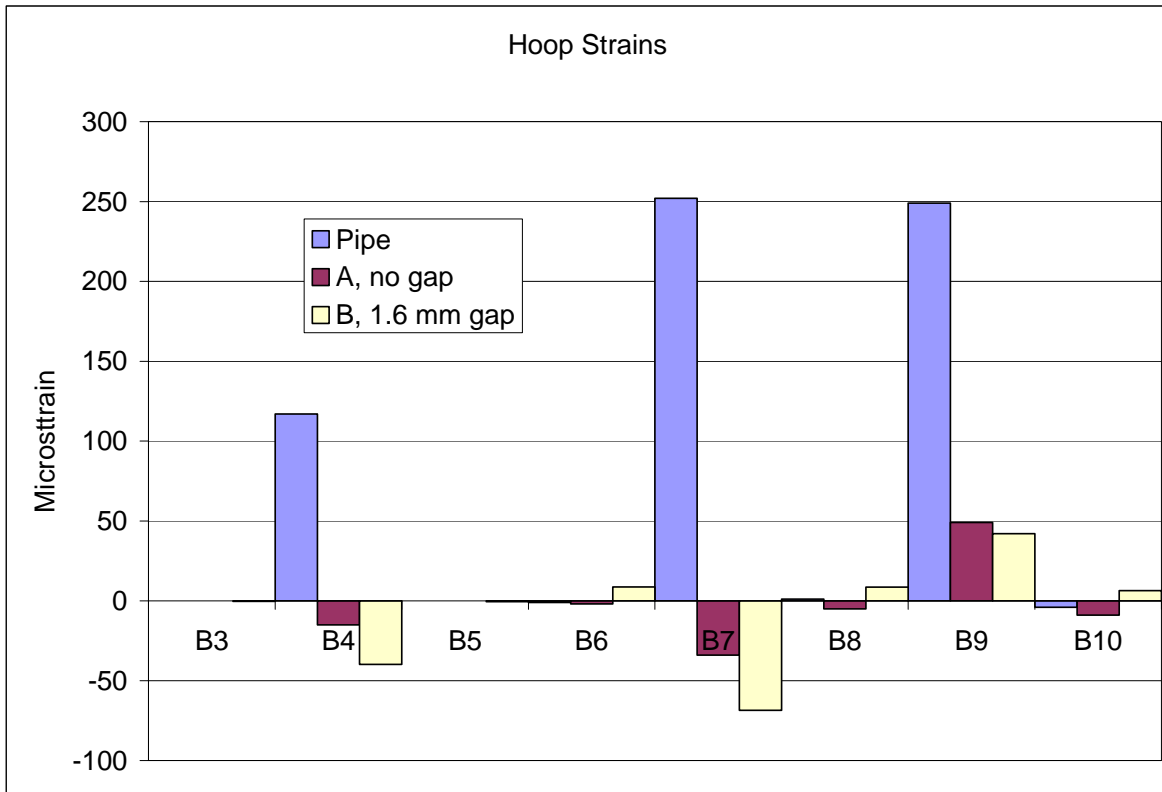


Figure 3.20: Pipe and Sleeve Strains Remote from Fillet Welds (Pressure Only)

3.5.4 Sleeve OD Strains

The strains on the sleeve OD were measured at 10 and 50 mm from the sleeve edges. Gauges 11 and 12, located 10 mm from the sleeve edge, and were glued on after the fillet welds had been completed. The strains in Figure 3.21 show that all of the strains were compressive on the outer surfaces of the sleeves. The highest compressive axial strains were measured near the edge of Sleeve A for Gauge 11.

A comparison of the strains for the two sleeves shows that there is considerable difference in strain near the end of Sleeve A compared to Sleeve B where the strains of Gauges 10 and 12 are essentially the same for the pressurized pipe results. The B9 and B10 readings for Gauge 10 are the same which suggests that this gauge was not functioning properly on the last two readings.

The compressive strains at the ends are opposite to the tensile axial strains shown in Figure 3.20 for both sleeves.

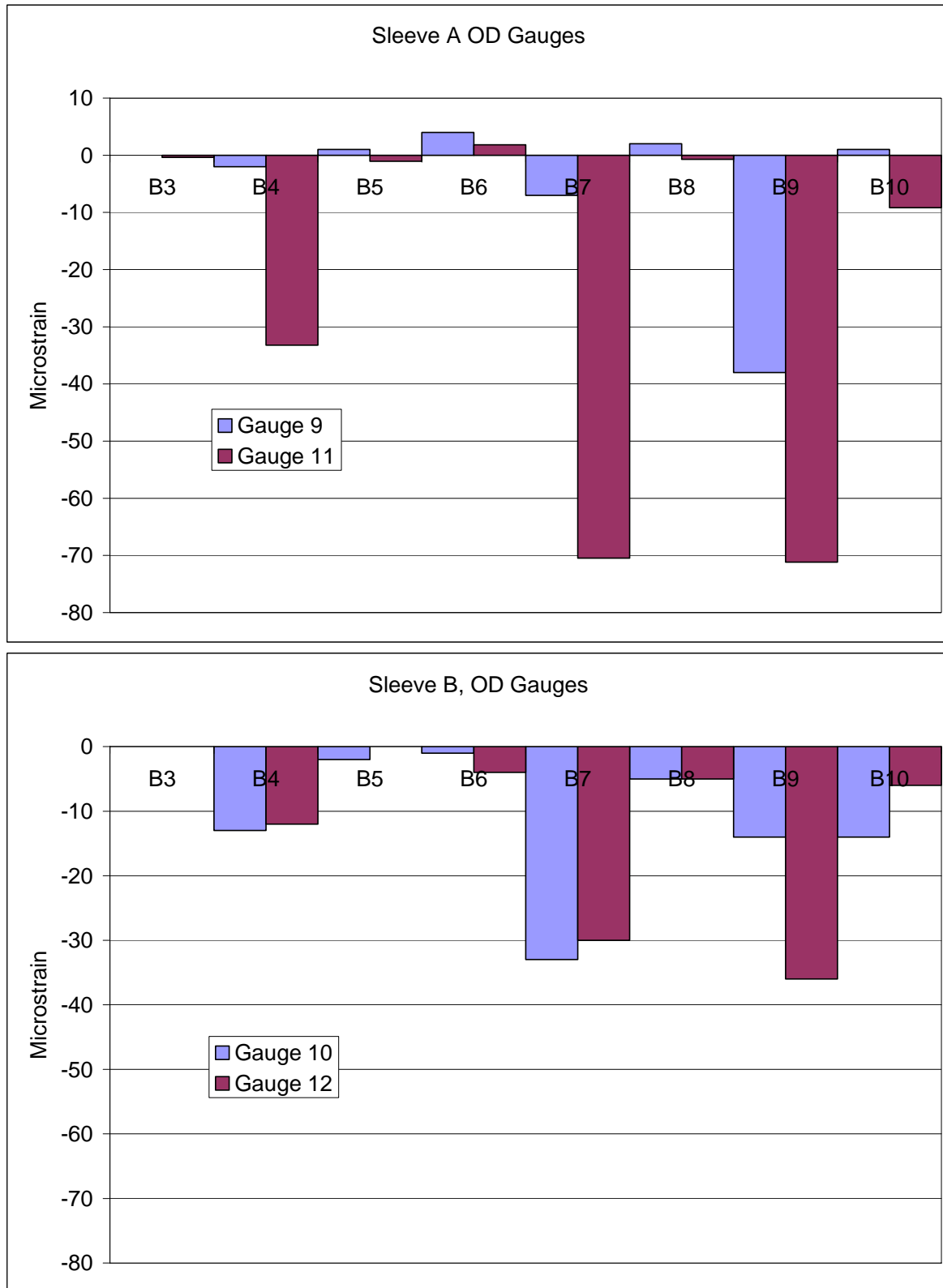


Figure 3.21: Strain Readings for OD Sleeve Gauges (Pressure Only); Sleeve A, No Gap; Sleeve B (1.6 mm Gap).

3.5.5 Axial Strains Between Sleeves

There are three strain gauges located between the two sleeves that measure axial strains on the pipe surface. Gauge 3 is located midway between the two sleeves and the other gauges are centered 5 mm from the weld toe.

The strains in Figure 3.22 show that the strains are tensile across this area and that the strains are higher near the weld toes. With just the pipe pressurized the strains measure just over 150 $\mu\epsilon$ near the weld toes compared to 60 $\mu\epsilon$ at the middle of the pipe. After pressurizing the annulus, the strains near the toe increased significantly by about 100 $\mu\epsilon$ up to 260 $\mu\epsilon$. The small difference in strain is likely due to weld bead and fit-up differences.

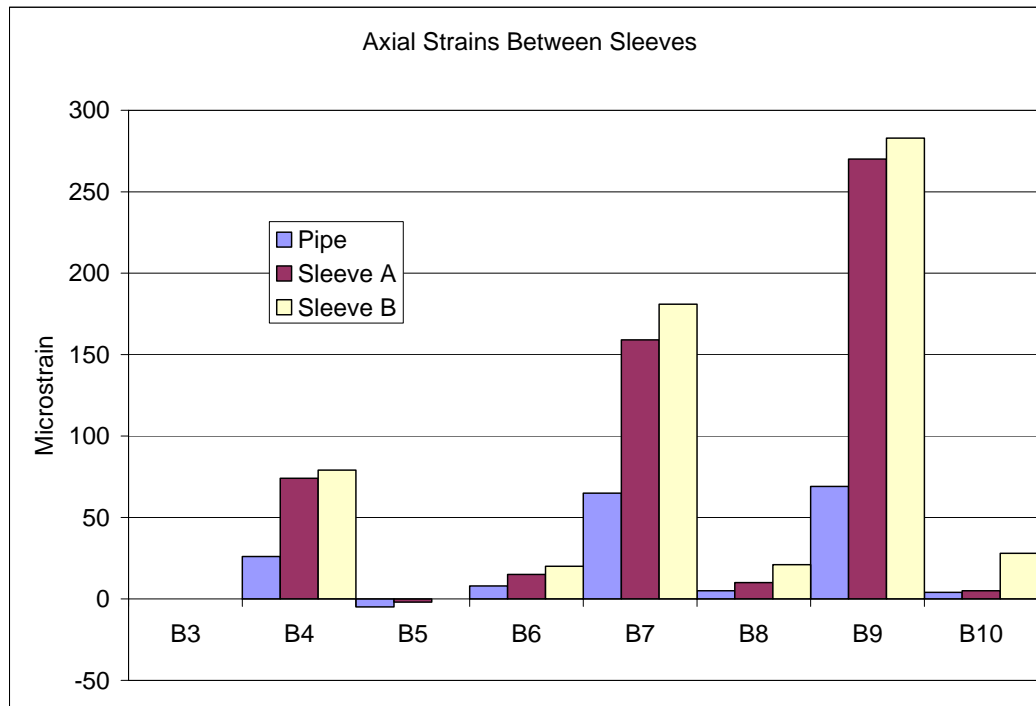


Figure 3.22: Axial Strains between Sleeves (Pressure Only)

3.5.6 Summary of Strain Readings

The results were presented by considering the strains due to welding the sleeves to the pipe and then examining the changes in strain due to the application of up to 500 psi pressure in the pipe and then 500 psi in the annulus between the sleeve and pipe.

The summary of strains resulting from welding the sleeves to the pipe is shown schematically in Figure 3.23. The strains on the outer surface are tensile and similar in magnitude, but the main difference is seen with the strains on the pipe ID surface and at the interfaces between the pipe and sleeve. Sleeve A with no root gap at the fillet weld shows that the strain at the weld root is near zero, whereas the root of Sleeve B with 1.6 mm gap is in tension across the weld root area. There are slight differences in weld bead size, with the fillet weld on Sleeve A having a slightly shorter vertical leg length, but it is not known if this slight difference in weld size could have resulted in the strain differences on the pipe ID and at the interface.

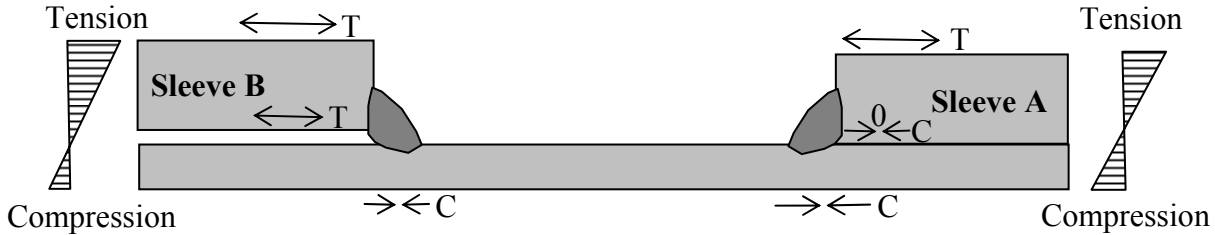


Figure 3.23: Schematic of Strains Resulting from Welding Sleeves to the Pipe

The hoop and axial strains in Figure 3.20 at 500 psi are replotted in Figure 3.24 with histograms in position on the pipe to show the relative magnitudes and the effect of pressurizing the annulus. Both examples show that the pipe attains the same hoop and axial strains in both instances, roughly $250 \mu\epsilon$ and $65 \mu\epsilon$, respectively. With only the pipe pressurized the hoop strains are negative and the axial strains are slightly positive. Once the annulus between the sleeve and pipe is pressurized the hoop and axial strains become positive in both sleeves. There are small differences in the magnitudes of the strains in this figure, but they are not considered to be significant. The important point to note from this comparison is that the strains increase as the space becomes pressurized. One exception is the axial strain on Sleeve B, which remained the same with and without pressure in the annulus.

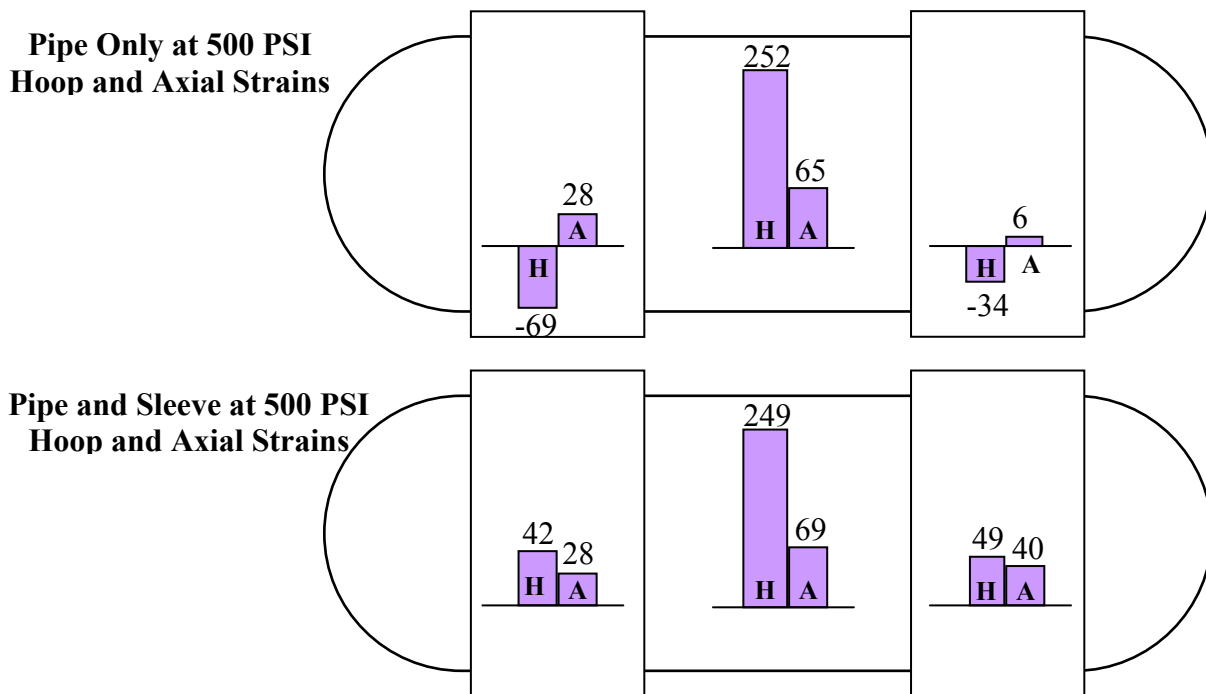


Figure 3.24: Hoop and Axial Strains on Pipe and Sleeve (Pressure Only)

4. SLEEVE WELD FEA MODEL

The two sleeves described in Section 4 were used to assemble the finite element model with the aim of being able to directly compare the measured strains with the calculated strains.

4.1 Model Description

Element plots of the model used in this report are shown in Figure 4.1. The model consisted of a pipe with end caps welded to the end, and two sleeves fillet welded to the pipe at equal distances from the pipe end. The sleeve on pipe model used in this report was created in ANSYS 10.0 using PLANE183 axisymmetric elements, exploiting the axisymmetric nature of the problem. As such, details such as the longitudinal sleeve weld, and various details used to pressurize the vessel were not modeled, as the cross section shown in Figure 4.1 was assumed to remain constant along the circumference. The model featured non-linear material models, but did not take into account non-linear geometry effects, since global strains were expected to remain within yield levels and deformations were expected to be small.

The entire model is shown in the upper portion of Figure 4.1, along with the global Cartesian coordinate axis. The X-direction represents the radial direction, the Y-direction represents the axial direction, and the Z-direction represents the hoop direction. The inset in the lower left of Figure 4.1 shows the sleeve with a gap between the sleeve and pipe along with fillet weld attaching the sleeve to the pipe. Similarly, the inset in the lower right of Figure 4.1 shows the sleeve without a gap between the sleeve and pipe along with fillet weld attaching the sleeve to the pipe. In both insets in Figure 4.1, the red elements represent the sleeve material, the light aqua the pipe material, and the purple elements represent the weld material. The edge lengths of the elements used in all welds modeled were approximately 0.375mm.

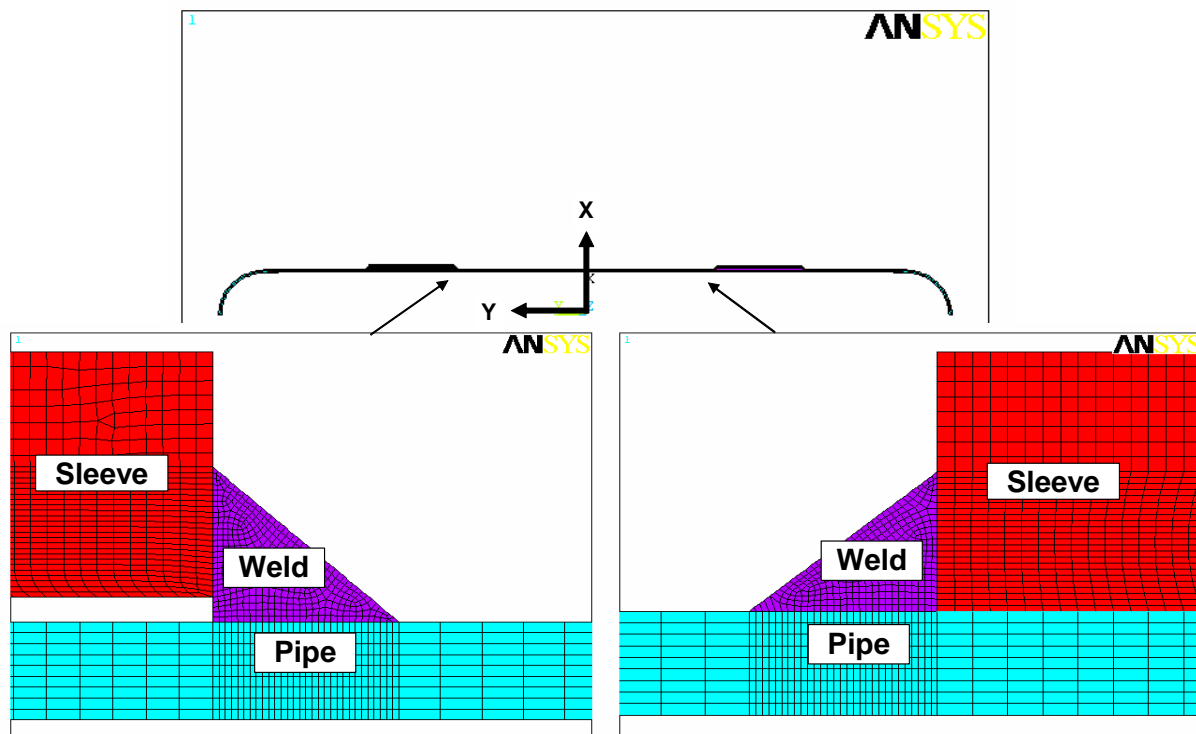


Figure 4.1: Schematic of Sleeve on Pipe Model

To model the contact between the sleeve and pipe when there was no gap between them, CONTA172 and TARGE169 elements were used at the interface between the pipe and the sleeve. The CONTA172 contact elements were placed on the inner diameter (ID) surface of the sleeve, while the TARGE169 target elements were placed on the outer diameter (OD) surface of the pipe. These contact and target elements were not used on the sleeve where there was a gap modeled, as it was assumed (and later verified) that the displacements of the OD of the pipe under pressure relative to the ID sleeve surface would be small enough to avoid contact between the two surfaces.

4.2 Modeling Data

4.2.1 Material Property Data

The weld, pipe, sleeve, and end caps, all had unique non-linear material models, as shown in Table 4.1. All materials used a Young's modulus of 207 GPa and a Poisson's ratio of 0.3. Figures 4.2 shows the true stress-strain curve for the pipe used for the FE models, which uses the total true stress versus logarithmic strain; the other materials had similar curves. The true strain (ϵ) is related to engineering strain (e) by the relation:

$$\epsilon = \ln(1 + e)$$

The true stress (σ) is defined, in terms of the engineering stress and strain, as:

$$\sigma = s(1 + e)$$

The results of the stress analysis presented later in the report are in terms of true stresses and strains; however, engineering and true stresses and strains are equal prior to the yield point.

Table 4.1: Engineering Stress – Strain Properties Used in FEA Models

Engineering Strain	Yield Strength, MPa		Tensile Strength, MPa	
	0.1 %	0.2 %	0.5 %	9.5 %
X52 pipe	207	n/a	359	455
Sleeve	207	n/a	373	530
End Caps	207	n/a	352	526
Weld Metal	n/a	414	555	607

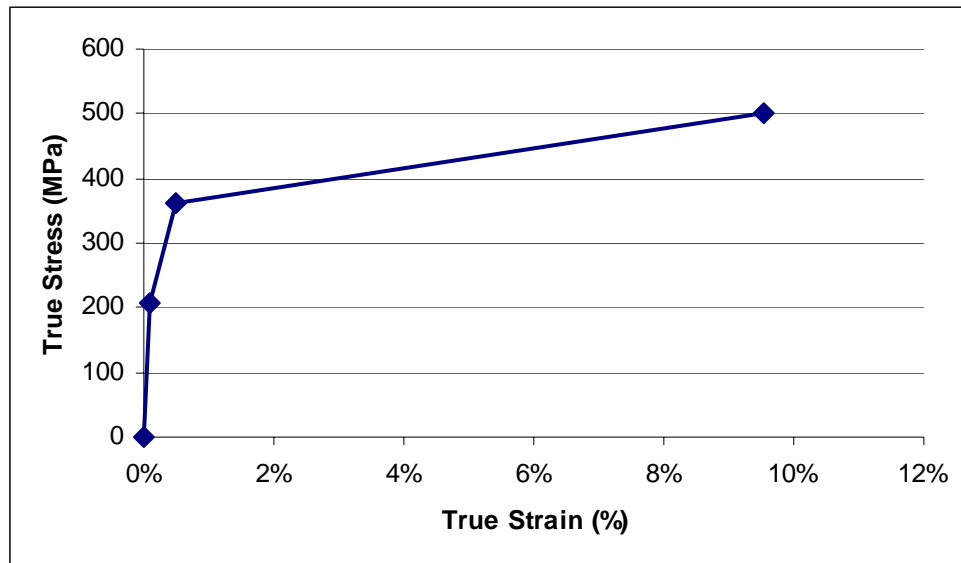


Figure 4.2: True Stress – True Strain Pipe Material Model

4.2.2 Model Geometry

Figure 4.3 shows the overall dimensions of the pipe and sleeves, with dimensions shown in millimeters (mm). Both sleeves were geometrically identical, and both were modeled to be 300mm from the end of the pipe, with a length of approximately 280mm. The total length of the pipe was modeled to be approximately 2032mm in length, with an OD of 323.85mm.

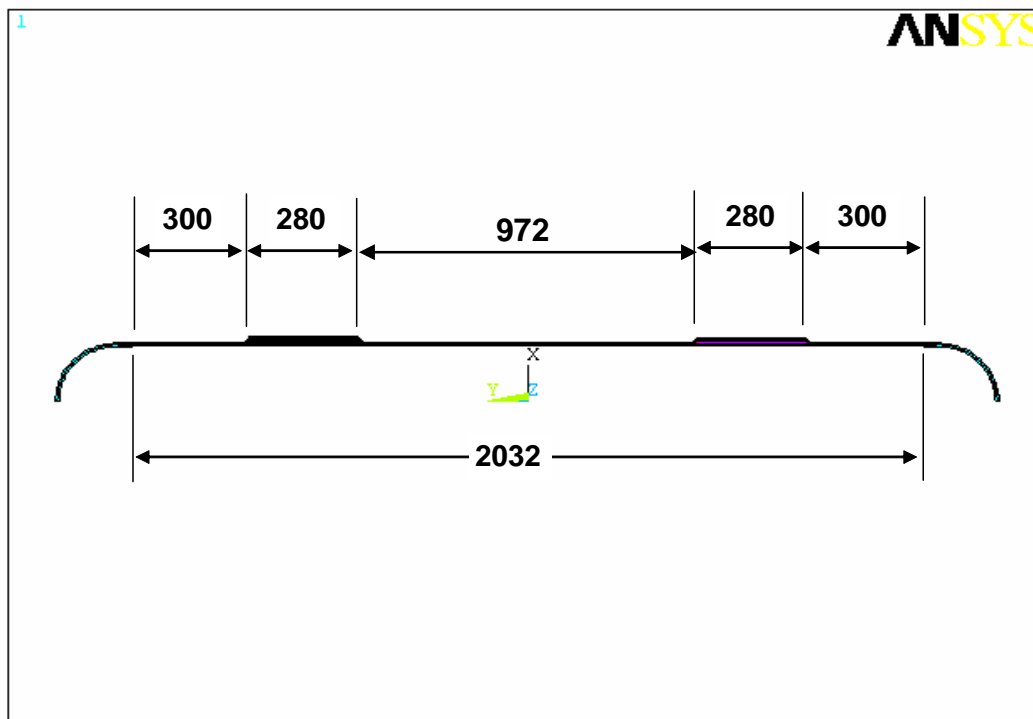


Figure 4.3: Dimensions of Pipe and Sleeves

Table 4.2 shows the thicknesses of the sleeve, pipe, and end caps. The thickness difference between the pipe and end caps was modeled by chamfering the inner surface of the end cap, as shown in the element plot of the end cap assembly in Figure 4.4. The dimensions shown in Figure 4.7 are in millimeters (mm). No weld was modeled between the pipe and end caps as it was not within the scope of this study. The flange of the end cap is modeled to be approximately 38mm in length, and is dimensioned in Figure 4.4.

Table 4.2: Material Thicknesses

Sleeves	16.0	mm
Pipe	6.4	mm
End Cap	9.75	mm

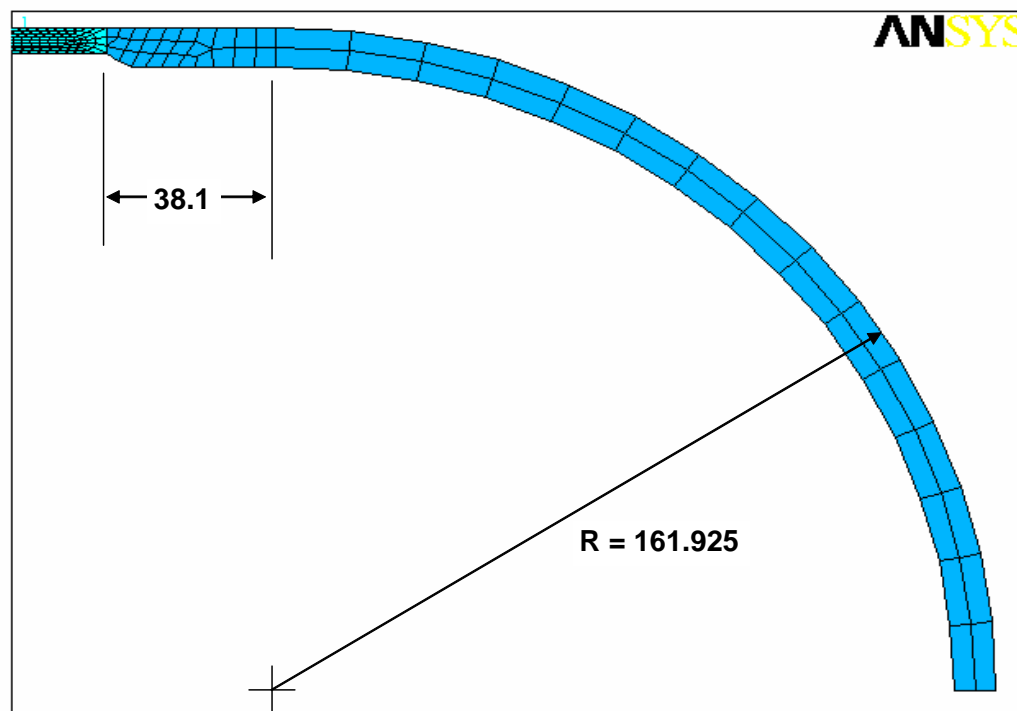


Figure 4.4: End Cap Detail

The dimensions of the welds modeled are shown in Table 4.3, with the labels for each weld defined in Figure 4.5. Horizontal weld leg length indicates the leg length of the fillet weld along the pipe, whereas the vertical weld leg length indicates the length of the fillet weld along the sleeve. The dimensions of the welds were derived by averaging measurements of the actual welds at 45 degree intervals on both sides of the gauge line on the top half of the pipe (see Figure 3.14).

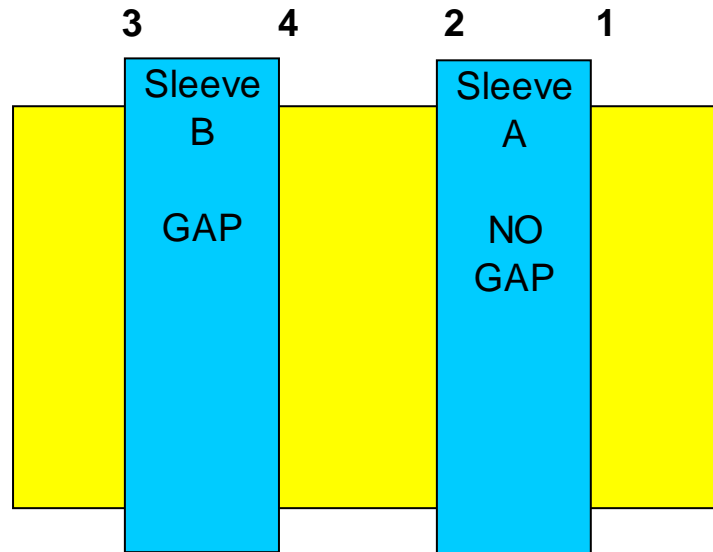


Figure 4.5: Sleeve and Weld Designations

Table 4.3: Weld Dimensions

Weld	1	2	3	4
Vertical Leg Length (mm)	8.6	8.6	8.8	8.5
Horizontal Leg Length (mm)	9.2	10.7	8.8	11.2

4.2.3 Applied Loading Sequence and Boundary Conditions

The loading in the model was defined to replicate the loading conditions in the lab trials as closely as possible. Table 4.4 outlines the applied pressures at each load step, the associated lab trial designation, and a brief description on their application.

Table 4.4: Applied Pressure Summary

Load Step	Lab Notation	Applied Pressure (psi)	Description
1	B4	250	Pressurize Pipe to 250 psi
2	B5,B6	0	Remove Pressure
3	B7	500	Pressurize Pipe to 500 psi
4	B8	0	Remove Pressure
5	B9	500	Pressurize Pipe and Sleeve Annuli to 500 psi
6	B10	0	Remove Pressure

4.3 Model Results Summary

The finite element sleeve models used the material properties and geometries from the laboratory trials and applied pressures of 250 and 500 psi to estimate the sleeved pipe behavior at each step in the loading process. The results described in this section will be further discussed in Section 6, comparing the strains between the lab and FE models.

The results from the modeling process can only be compared with the lab trial results after welding has been completed as the FE model does not take into account the residual stresses and strains as a result of the welding process. In this section, the summary of the modeling results will be presented to describe the general observations of the modeled geometries and conditions.

The axial strain results for both sleeves are plotted in Figures 4.6 and 4.7, showing the three loading conditions for each model. The first two models in each figure compare the case with only the pipe pressurized, B4 at 250 psi and B7 at 500 psi. The model results illustrating the axial strain distributions in Figures 4.6 and 4.7 appear exactly the same in the B4 and B7 loading conditions, but it is noted that the scale for B7 is twice that shown for B4. The last model axial strain distribution in each figure presents the results for the cases where both the annulus between the sleeve and the pipe is pressurized. Similar result plots were generated for the hoop strains, axial stresses, and hoop stresses, but for comparison with the measured strain values in the experimental work the discussions will focus on the strains.

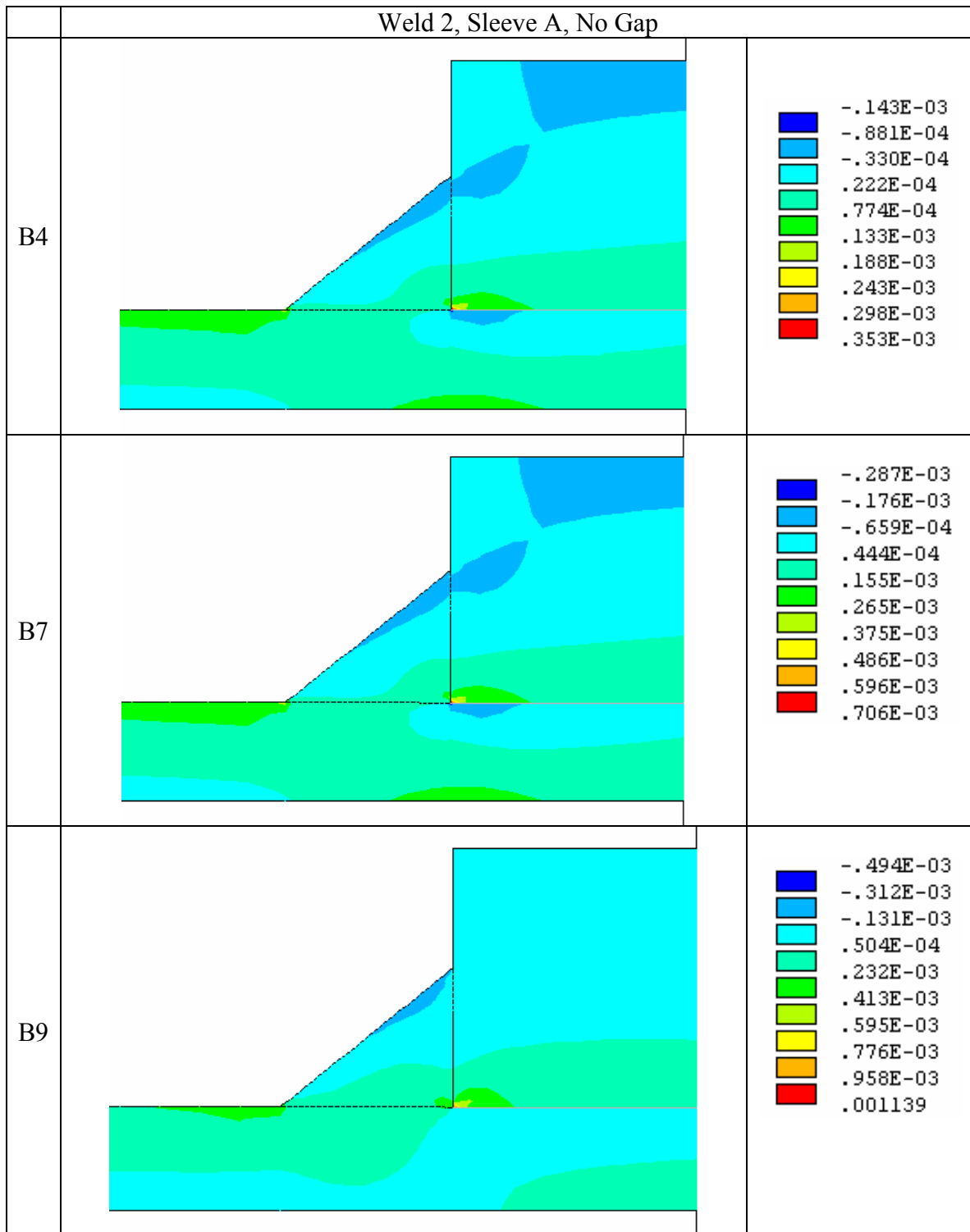


Figure 4.6: Axial Strain Results for Sleeve A, No Gap; B4: 250 psi to Pipe Only, B7: 500 psi to Pipe Only, and B9: 500 psi to Pipe and Annulus between Sleeve and Pipe

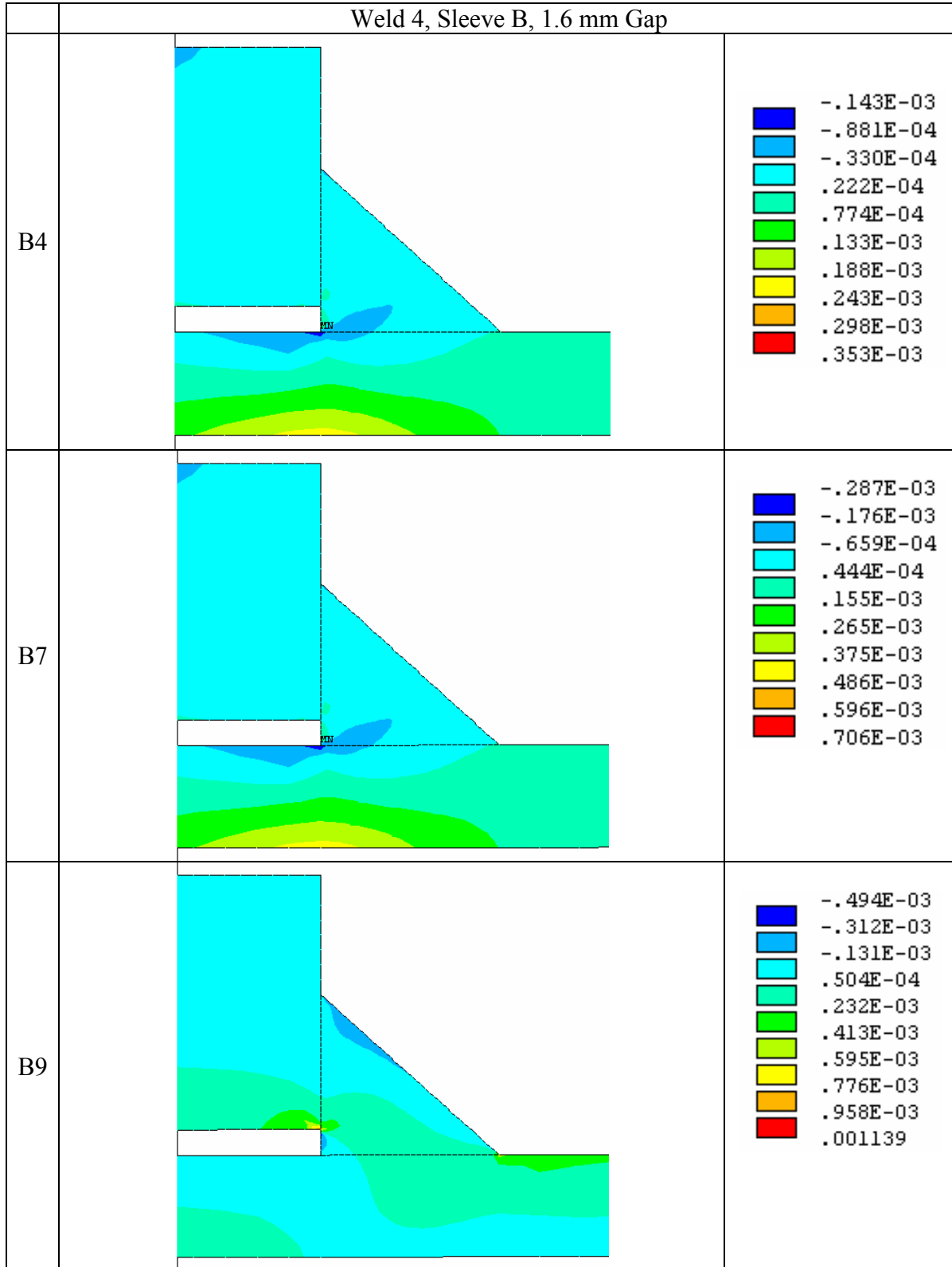


Figure 4.7: Axial Strain Results for Sleeve B, 1.6 mm Gap; B4: 250 psi to Pipe Only, B7: 500 psi to Pipe Only, and B9: 500 psi to Pipe and Annulus between Sleeve and Pipe

To demonstrate the trending in strains from 250 psi to 500 psi, the lab and model results are plotted for the 250 psi and 500 psi load cases against one another, as shown in Figure 4.8. The results show that both the model and the laboratory behaviors follow a linear elastic behavior since the strains at 500 psi pressure are twice those measured for the 250 psi pressure conditions. The two laboratory outlying points that do not follow this trend suggest that these points may include some significant experimental error.

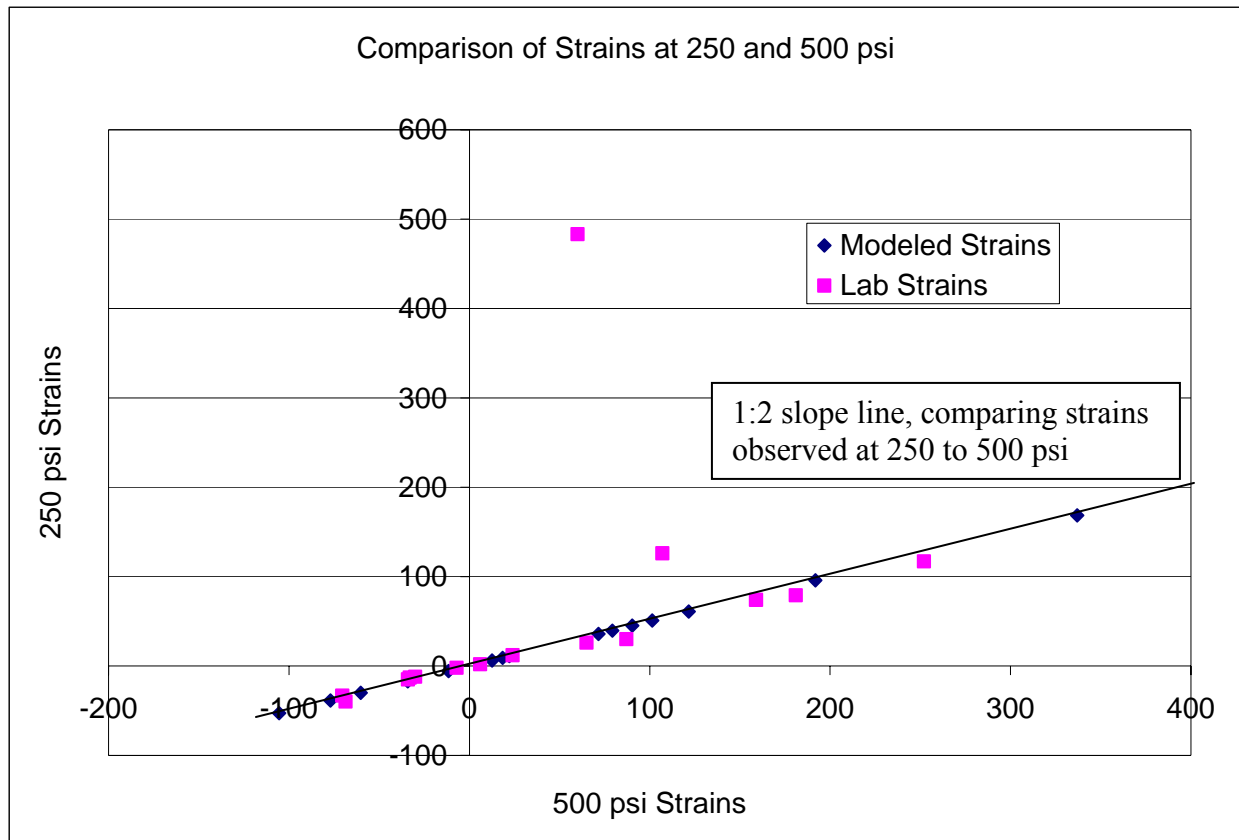


Figure 4.8: Comparison of 250 psi Strains against 500 psi Strains

5. DISCUSSION

The results from the field trials are summarized to obtain a general sense of the sleeve and pipe behaviour during pressurization, and similarly the lab trials and FE model results are summarized. The discussion will highlight the similarities and differences amongst the different cases with the objective of providing validation or criticism of the FE modeling process and results. This comparison will identify whether changes are warranted in the modeling process and to provide a description of the differences between pressurized and non-pressurized sleeves.

5.1 Field Results on Enbridge Odessa Line 3

The field results provided information related to the residual strains that results from the application of full encirclement reinforcing sleeves to the pipe and the response of the sleeve and pipe to changes in line pressure. Figure 5.1 (same as Figure 2.14) shows the general nature of the strains that were observed after welding had been completed.



Figure 5.1: Summary of Final Strains on Sleeves at KP 762 and KP 768

In both cases, the axial strains at the sleeve ends and hoop strains near the center of the sleeves are tensile. The axial strains on the pipe adjacent to the circumferential fillet welds were found to be both tensile and compressive. The variation at KP 762 towards the top of the pipe could be due to the higher temperatures of the pipe during fillet welding compared to KP 768 that had maintained a constant pipe temperature during welding. The additional heating would have allowed for greater expansion of the pipe and this subsequently resulted in higher tensile residual strains. The strain measurements due to sleeve installation do show that one can observe high axial strains across the sleeve fillet welds.

The changes in pressure on the mainline were able to be used to calculate how changes in mainline pressure would affect the measured strains on the installed sleeves. The $\Delta \epsilon / \Delta P$ results from Tables 2.3 and 2.4 are summarized in Table 5.1 and shown on a sleeve sketch in Figure 5.2.

Table 5.1: Field Trials Strain Changes

Strain Gauge			$\Delta \epsilon / \Delta P$, strain/psi
Number	Type	Placement	
1	Hoop	Center of Sleeve	0.33
2	Axial	End of Sleeve	-0.12
3	Hoop	End of Sleeve	0.5
4	Axial	End of Sleeve	-0.2
5	Axial	On Pipe	0.04, 0.07
6	Axial	On Pipe	-0.12, -0.11
7	Axial	On Pipe	-0.24, -0.26
8	Hoop	On Pipe	1.26, 1.5

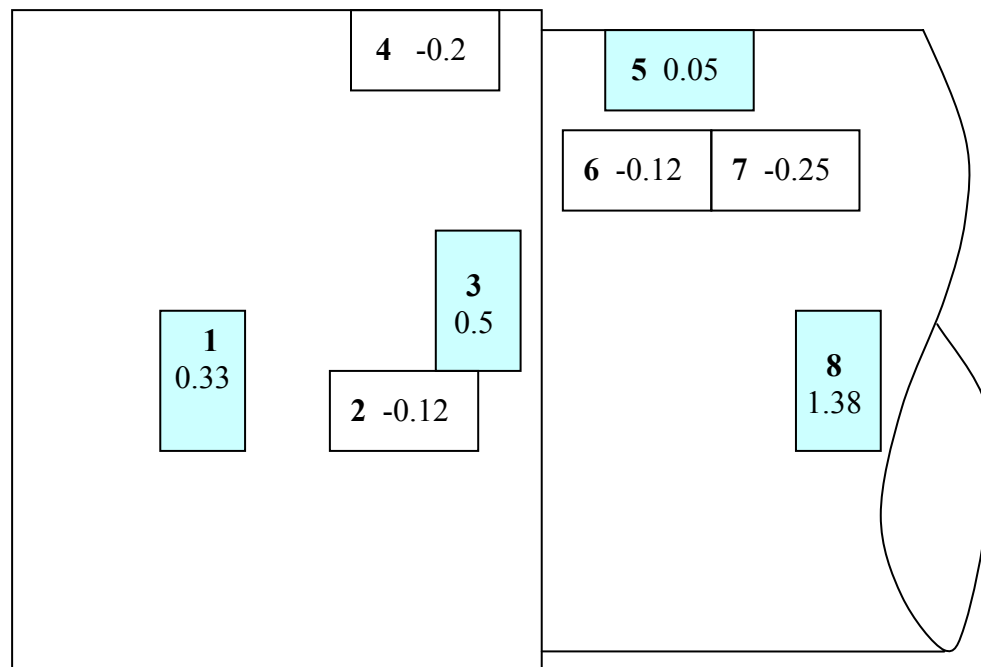


**Figure 5.2: Sketch Showing $\Delta \epsilon / \Delta P$ Transfer Functions from Field Trials
(Bold numbers indicate strain gauge numbers)**

The pressure transfer functions show only one inconsistency with Gauge 5 on the pipe at 12:00 O'clock which gives a positive transfer while the remainder of the axial gauges have negative transfer functions. The positive hoop strain results are as expected, with the greatest transfer observed for the hoop strain on the pipe removed from the sleeve with an average value of 1.38. Intermediate magnitude transfer functions are observed on the sleeve near the fillet weld, and the lowest value at the middle of the sleeve. The transfer function is higher near the fillet weld because it is likely that the weld has brought the pipe and sleeve surfaces closer together and the pressure changes are picked up sooner by the sleeve compared to near the sleeve center where there is possibly more gap between the sleeve and the pipe. This presumed behaviour is assumed based on the overall trend in the results observed from the field trials.

5.2 FE Model and Lab Trial Comparisons

The results from the modeling process can only be compared with the lab trial results where the strains have been normalized after welding is complete. The FE model does not take into account the residual stresses and strains as a result of the welding process. The FE model strains were averaged over the active gauge lengths of the strain gauges, which could be from 2 mm to 6.4 mm in length.

Of note, Gauge 17 did not function properly in the lab trials, and as such, is not used in this comparison of lab trial results and model results. Also, Gauges 1 and 2 were disconnected after welding had been completed in order to pressurize the pipe, thus no results are available for these locations.

Figures 5.3, 5.4, and 5.5, illustrate the predicted and actual strains for the strain gauge locations (see Figure 3.15 and 3.16 to identify strain gauge location and orientation):

- ✖ affixed to the pipe (Gauges 3, 4, 14, 15, and 18),
- ✖ -affixed to Sleeve A, no gap (Gauges 5, 6, 9, 11, and 13), and
- ✖ affixed to Sleeve B, 1.6 mm gap (Gauges 7, 8, 10, 12, and 16).

In these figures, the legends indicate the pressurization state (B4, B7, or B9) as defined in Table 3.5, and whether the value is from the lab trial (Lab) or the model (Model).

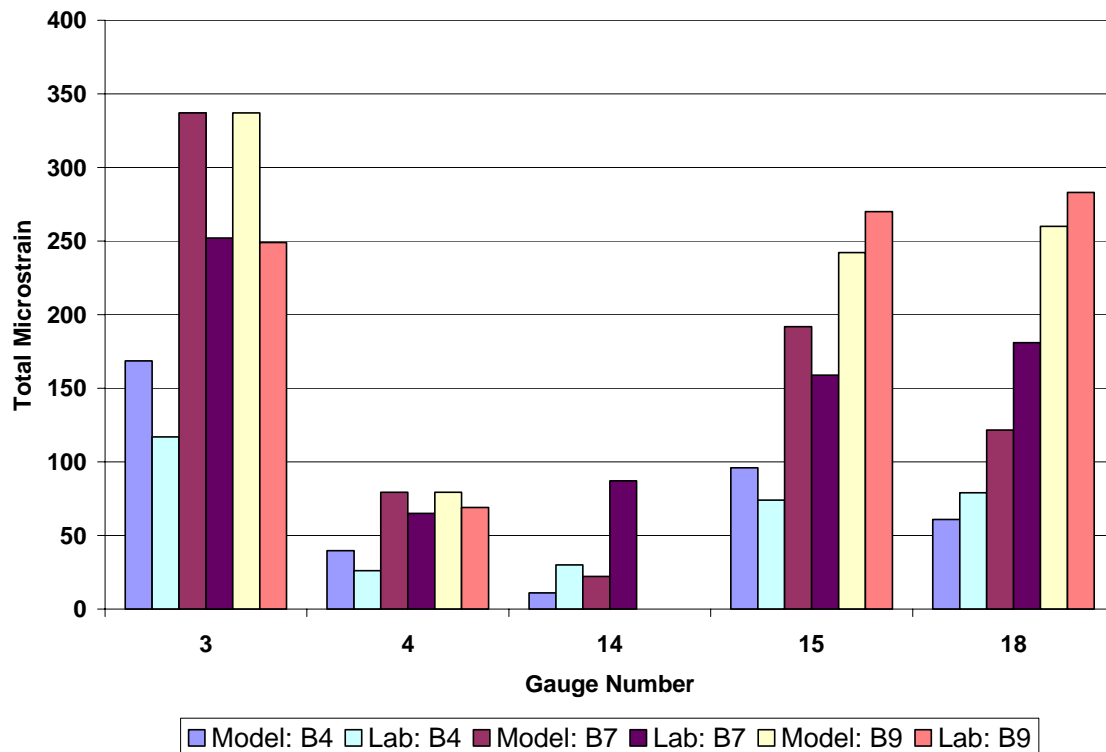


Figure 5.3: Lab Trial and Predicted Strains; Pipe Strain Gauges 3, 4, 14, 15, and 18.

In Figure 5.4, the strains calculated using the FE model are plotted against the strains measured in the lab for all load conditions. This included the 250 psi and 500 psi tests with pressure only in the pipe, and the test with 500 psi to the pipe and annulus between the pipe and sleeve, and includes the results for the sleeve with no gap and the sleeve with the 1.6 mm gap. The results show a good correlation in that most of the observations lie within a 10 microstrain error band. One significant exception to this is the value at a lab strain of 490 $\mu\epsilon$ which was demonstrated to be a suspicious value based upon the comparison illustrates in Figure 4.11.

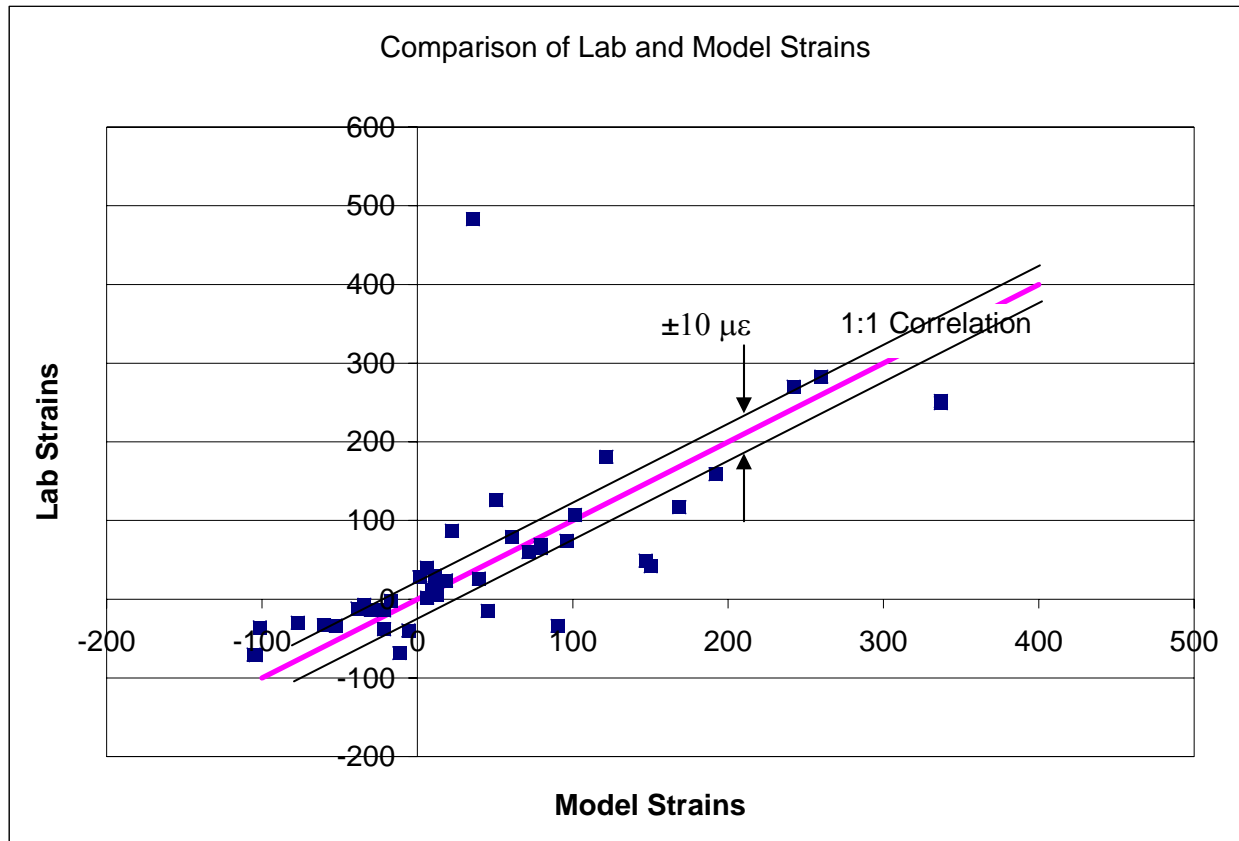


Figure 5.4: Comparison of Strains Calculated by FE Model to Strains Measured in Lab

The hoop and axial strains on the pipe, Gauges 3 and 4 are slightly higher for the FE model compared to the lab results, while for the majority of the remaining readings the lab results show slightly higher strains than those calculated from the FE model. The model appears to provide a good overall prediction of the magnitudes of the strains at the different locations, considering that the precise location of the gauges and structural geometries were not identical for the FE models and the test specimens.

The comparisons in Figure 5.5 for the strains on Sleeve A, no gap, shows that Gauge 5 produced strains in the lab trials opposite to those expected from the FE model when only the pipe was pressurized, but the correlation is the same for Gauge 5 when the annulus is pressurized. The other gauges on Sleeve A show consistent behavior trends between the lab and FE model. The results for Gauges 9, 11, and 13 show that the strains on the outer surface of the sleeve are compressive, with the higher compressive strains near the end of the sleeve, and the strain on the sleeve ID is tensile with a similar magnitude as the compressive strain near the edge of the sleeve.

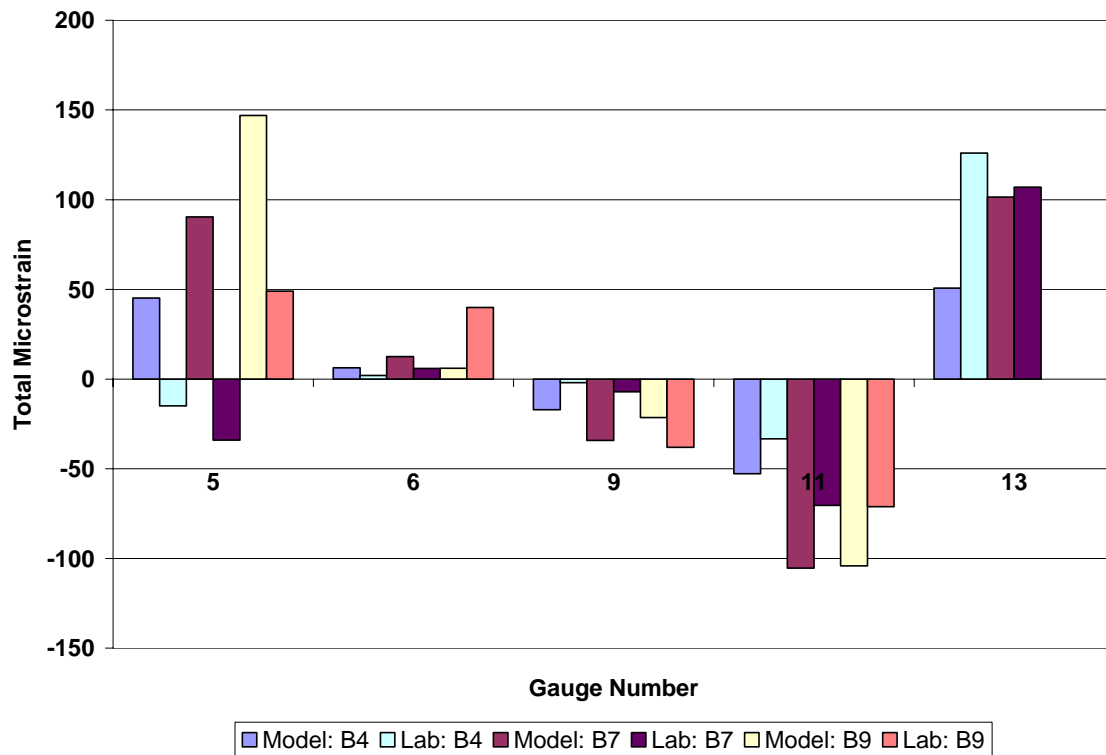


Figure 5.5: Lab Trial and Predicted Strains; Sleeve A, No Gap, Gauges 5, 6, 9, 11, and 13

The comparison of the lab and FE results in Figure 5.6 for the strains on Sleeve B, 1.6 mm gap, show that the FE model and lab results predict the same sense of strains for Gauge 5 at the center of the sleeve. With Sleeve A the pipe pressurized case predicted opposite strains between the FE model and lab trials when only the pipe was pressurized, but they were in the same direction when both the pipe and annulus were pressurized. The remaining strains between the FE model and lab results in Figure 5.6 are mainly in close agreement with each other, except for Gauge 16 for the 250 psi test to the pipe where the lab results were over 10 times greater than the predicted values. This could indicate an intermittent instrumentation problem as the next load case at 500 psi gave comparable strains between lab and calculated values. The last point to make regarding the strain results on Sleeve B is that the same general behavior is observed as for Sleeve A in that the outer surface of the sleeve is in compression and the sleeve ID surface is in tension as the pressure is increased.

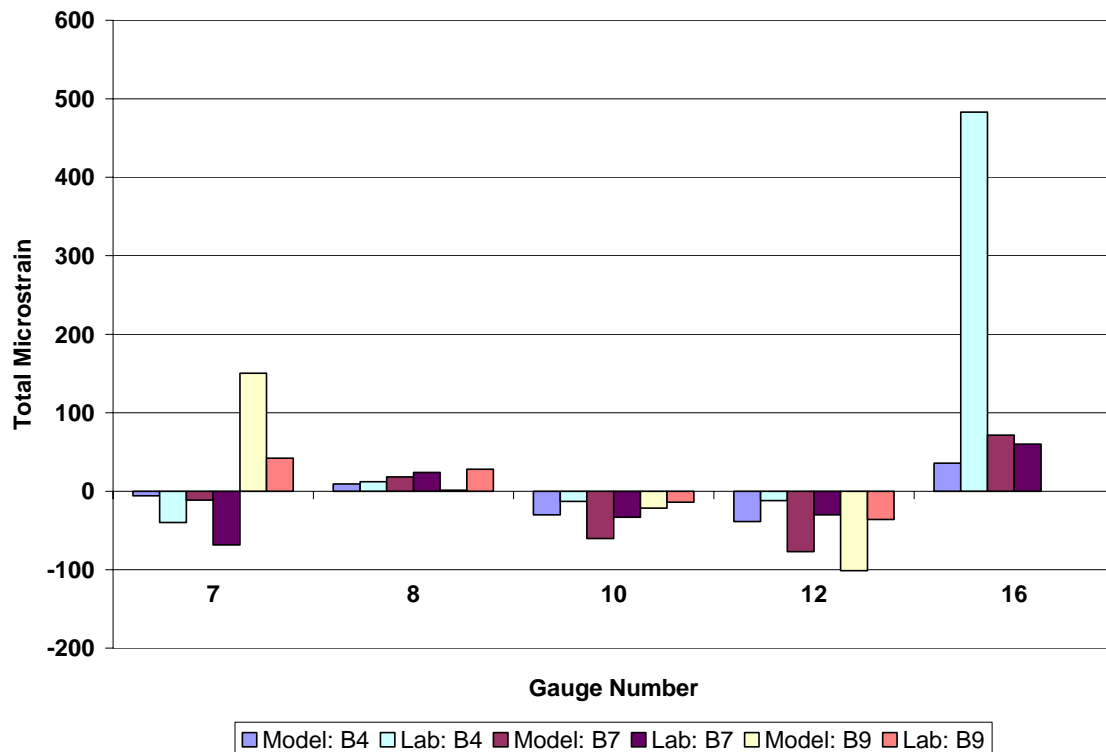


Figure 5.6: Lab Trial and Predicted Strains; Sleeve B, 1.6 mm Gap

It can be concluded from these comparisons that the FE model provides a reasonable prediction of the strains in the sleeve region in terms of the magnitudes of the strains and whether they would be tensile or compressive. In some instances, the lab results were considerably different from the FE predictions, but they seemed to be related possibly to instrumentation problems in isolated cases. The largest discrepancies were noted for the hoop strains on Gauge 5 at the center of the sleeve, and can not be explained at this time other than assigning it to experimental error.

The sleeve transfer functions can be calculated in a similar manner as was done for the field trials using the results predicted from the FE models. The results in Table 5.2 summarize the calculations for the gauges in the areas of the fillet weld toes on both sleeves.

The results can be discussed in terms of the similarities and differences between gauges in similar locations to examine the influence of the gap and pressure in the annulus between the sleeve and the pipe. The gauges at the weld toes, Gauge 15 and Gauge 18, show similar results so that the gap does not influence the strain behavior outside of the sleeve; this result was somewhat intuitive but was considered useful to emphasize. The other similarities in the transfer functions were noted for the B9 load case, 500 psi in the annulus between the sleeve and pipe, where the strains on the sleeve OD, Gauges 10 and 12 on Sleeve B and Gauges 9 and 11 on Sleeve A, are similar and show again that the higher compressive strains are observed on the outside edges of the sleeves. With these four gauges (9, 10, 11, and 12) there are differences when only the pipe is pressurized. At the sleeve ends we see higher strains when the sleeve is in contact with the pipe (Gauges 11 and 12), while at the locations of Gauges 9 and 10 the higher

strains are noted with a 1.6 mm gap between the sleeve and the pipe. The other gauge pair in similar locations, Gauges 13 and 16, shows that higher strains are observed with only the pipe pressurized, but the transfer functions are similar when the annulus is pressurized. The last gauge listed in Table 5.2 is Gauge 14 located on the pipe under Sleeve A, No Gap. When only the pipe is pressurized the transfer function is positive, whereas with the annulus and pipe pressurized the transfer function is negative.

Table 5.2: Pressure Transfer Functions from FE Models

	Sleeve B, 1.6 mm Gap				Sleeve A, No Gap				
	10	12	16	18	9	11	13	14	15
B7, 500 psi	-60	-80	80	120	-30	-105	100	30	190
$\Delta\epsilon / \Delta P$	-0.12	-0.16	0.16	0.24	-0.06	-0.21	0.20	0.06	0.38
B9, 500 psi	-20	-105	90	260	-20	-105	90	-40	240
$\Delta\epsilon / \Delta P$	-0.04	-0.21	0.18	0.52	-0.04	-0.21	0.18	-0.08	0.48

5.3 Circumferential Fillet Weld Root Details

The comparisons of the strains and the transfer functions provide some general trends and validation of the observed behaviors of full encirclement sleeves and indicate that the FE models provide a reasonable description of the sleeve behavior. To this point the comparisons have been made on a somewhat general basis and have discussed the strains at locations removed from the main areas of concern, i.e. the circumferential fillet weld root, as this region is the one most likely to contain cracks and possibly lead to failure, as shown in Figure 5.7.

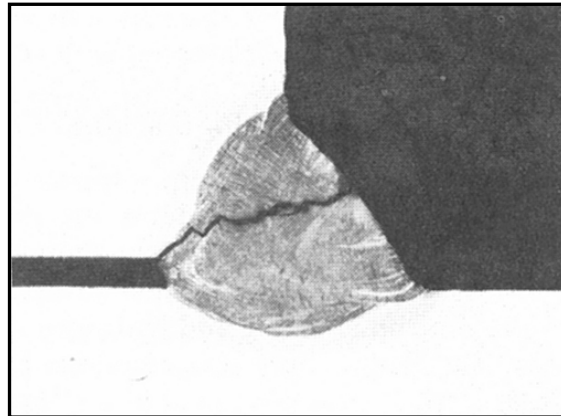


Figure 5.7: Example of Fillet Weld Root Crack

The details of the stress state at the weld root can be obtained from the FE models shown in Figures 4.9 and 4.10. The 500 psi load cases, B7 for only the pipe pressurized and B9 for both the pipe and sleeve pressurized, are shown at higher magnification in Figures 5.8 and 5.9 for Sleeve A, No Gap, and Sleeve B, 1.6 mm Gap, respectively.

In Figure 5.8 it is evident that the B7 case results in compressive strains on the pipe in the weld root region, and then the strains become more positive as the annulus is pressurized in the B9 example. Therefore the weld root is caused to open up as the annulus is pressurized. On the sleeve ID surface at the weld root one can see that the calculated strains are tensile and that there is a steep gradient at the weld root.

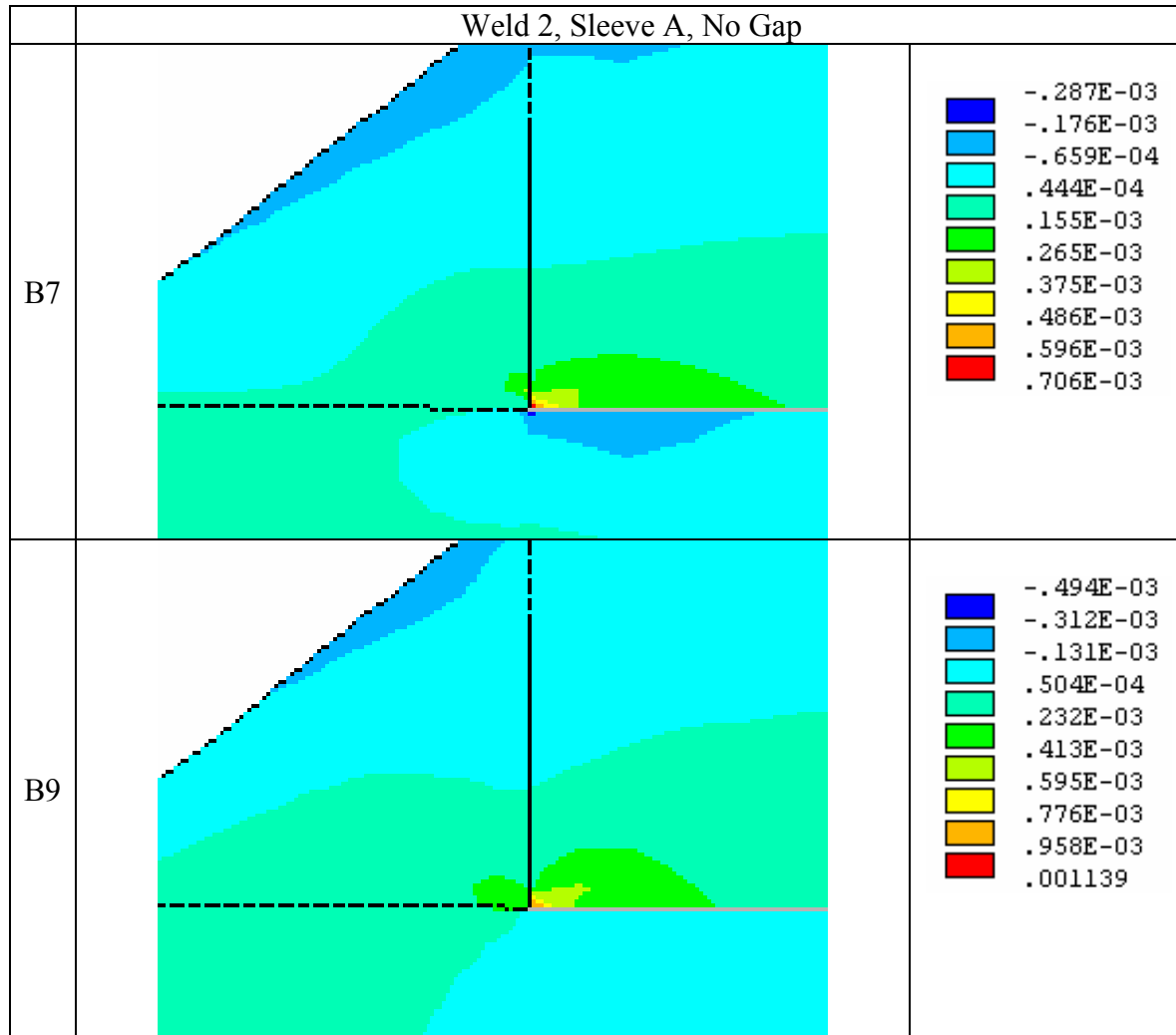


Figure 5.8: Axial Strain Results for Sleeve A, No Gap; B7: 500 psi to Pipe Only, and B9: 500 psi to Pipe and Annulus between Sleeve and Pipe

Looking at the results for Sleeve B with the 1.6 mm gap shows similar results by comparing the B7 and B9 cases. With only the pipe pressurized the strains are compressive at the weld root, but once the annulus is pressurized the strains become tensile and there is a tendency to open the weld root as a result of local bending. The results between Figures 5.8 and 5.9 show similar patterns of strain distribution and magnitudes at these maximum pressures. The measured strains did show some small differences, but these would not be evident in the scale that is shown in the ANSYS screen capture results.

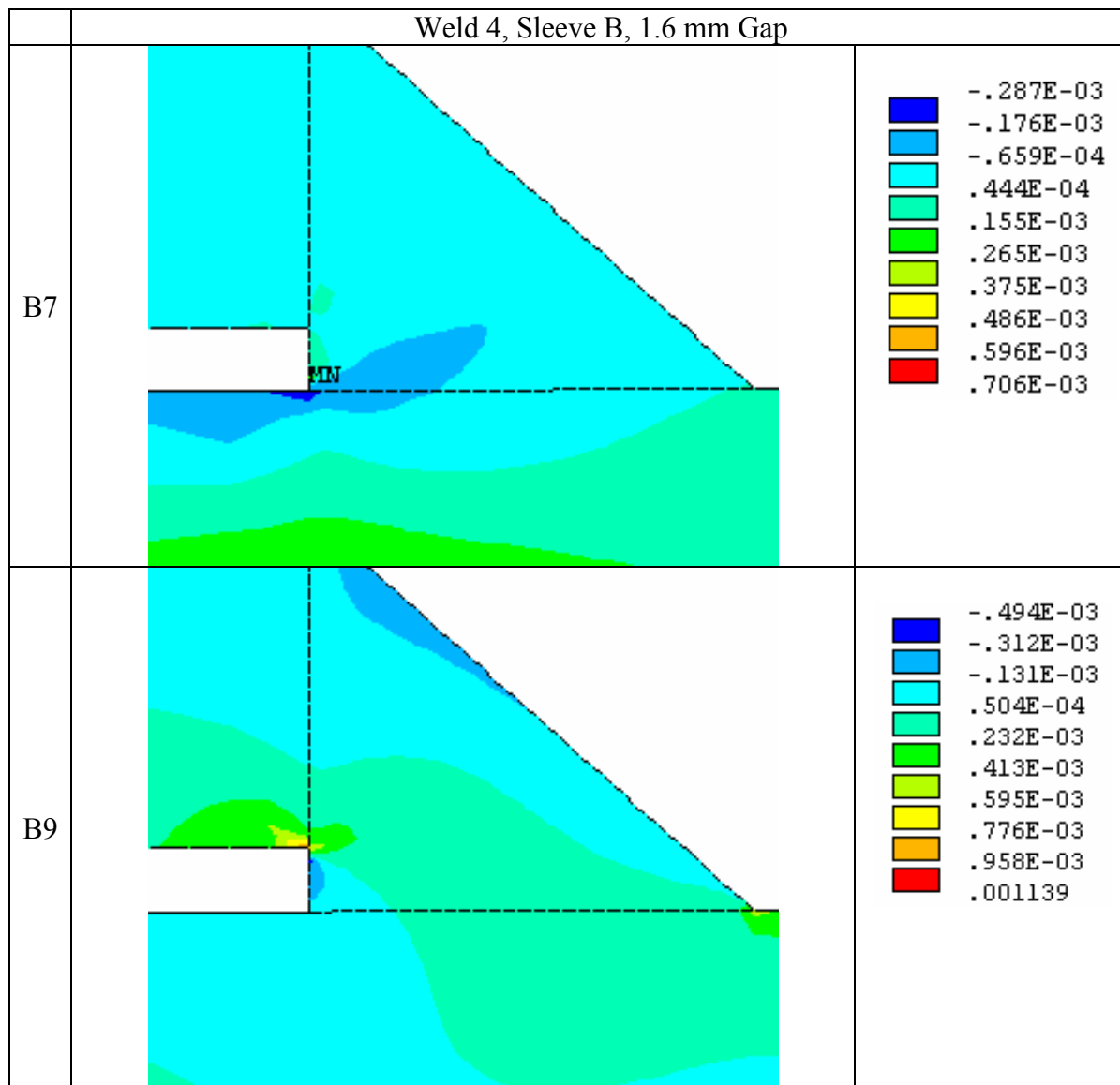


Figure 5.9: Axial Strain Results for Sleeve B, 1.6 mm Gap; B7: 500 psi to Pipe Only, and B9: 500 psi to Pipe and Annulus between Sleeve and Pipe

The shape of the pipe and sleeve after the pressure has been applied can be obtained from the ANSYS results and compared against the strain readings from both the field and lab trials (see Figures 5.10 to 5.15). These ‘deformed shape plots’ have the radial displacements exaggerated 1000 times for illustrative purposes. The scales on the right of each figure associate the displacements in mm with each color. It is noted that the magnification of the radial displacements for Sleeve B, 1.6 mm gap, shown in Figure 5.12 with only the pipe pressurized appears to cause the pipe to overlap the sleeve. This unrealistic result is due to the thousand fold exaggeration of the radial displacements in which the sleeve does not displace significantly and the pipe wall moves towards it to close the gap. Knowing that the predicted relative displacements between the pipe and sleeve are approximately 0.07mm, and that the gap is 1.6mm, the sleeve and pipe does not contact the sleeve.

The deformed shape with only the pipe pressurized with Sleeve A, no gap, in Figure 5.10 shows that the largest displacements occur in the thinner cross-section, i.e., pipe outside of the sleeve. The sleeve has a uniform radial displacement approximately one-third that observed for the pipe over most of its length. The fillet weld areas are contained in a zone with a definite curvature with the outer surface of the sleeve surface and pipe being curved inward. The shape of this transition region suggests that the outer surfaces would be in compression and the inner pipe surfaces would be in tension, and that this behavior is due to the difference in radial expansion under the sleeve compared to the pipe itself. This behavior is consistent with the measured laboratory trials. The radial displacements under the sleeve, 0.018 mm, and radial displacement of the pipe away from the sleeve, 0.058 mm, are approximately in the same relative proportions as the pipe and combined pipe sleeve thickness, 6.4 mm and 22.4 mm.

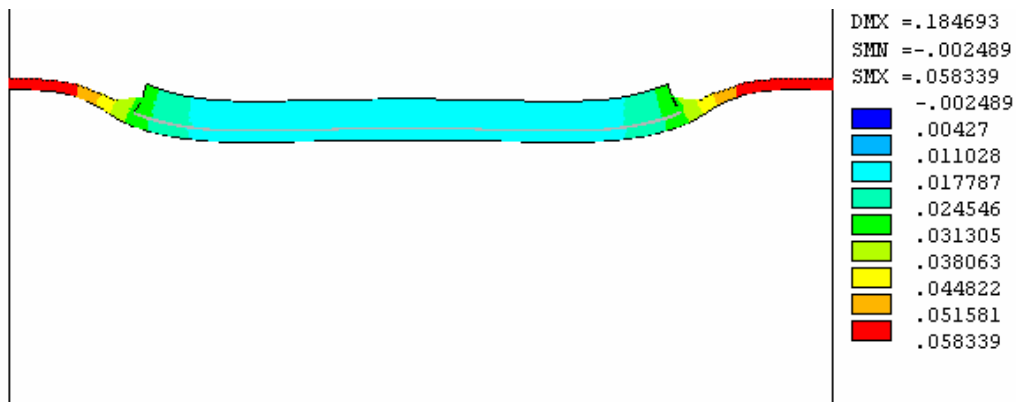


Figure 5.10: Sleeve A (Ungapped) Radial Displacement, Load Condition B7 (500 psi Pressurized Pipe Only)

The load case with pressure in both the pipe and the annulus of Sleeve A, no gap, shows that there is separation between the two surfaces and that the pipe in fact reduces its radius by 0.006 mm (Figure 5.11). Compared to the case with only the pipe pressurized, the sleeve and pipe both have slightly greater radial displacements with the annulus pressurized. This is due mainly to the sleeve not restraining the pressure as effectively as the sleeve and pipe combined thickness. The most notable difference with the application of pressure in the annulus is that there is a definite opening across the root of the weld.

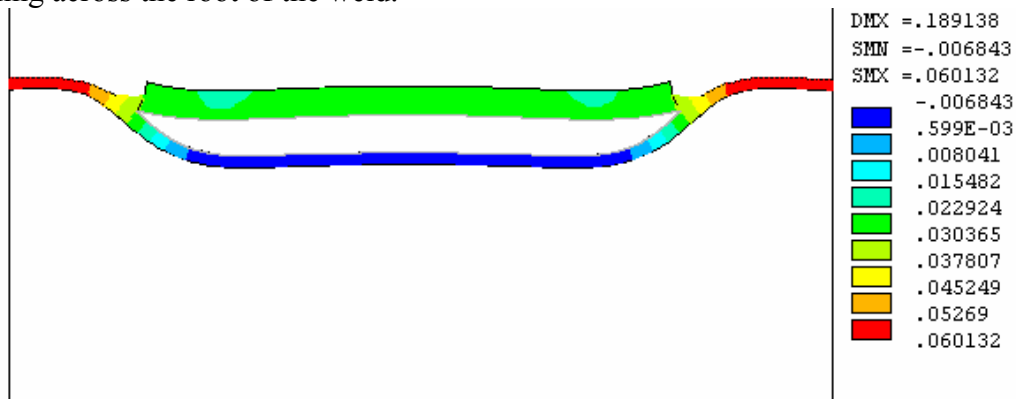


Figure 5.11: Sleeve A (Ungapped) Radial Displacement, Load Condition B9 (500 psi Pressurized Pipe and Sleeve Annuli)

The deformed shape for Sleeve B, 1.6 mm gap, shows the overlap of pipe and sleeve due to the exaggerated displacements, seen in Figure 5.12. In this model the pipe beneath the sleeve and the pipe outside of the sleeved area have the same displacements, and the 0.059 mm is the same displacement as was observed outside of the sleeved area with no gap between the sleeve and pipe, Sleeve A. With the 1.6 mm gap the sleeve reduces its radius slightly by 0.0025 mm and again the end of the sleeve OD and the pipe near the circumferential fillet weld go into compression with pressure applied only to the pipe. The sleeve end fillet weld restrains the pipe wall from expanding freely resulting in high local bending strains. These strains could be expected to be higher than those developed for the sleeve with no gap based upon the difference in pipe wall curvature when comparing Figures 5.12 and 5.10.

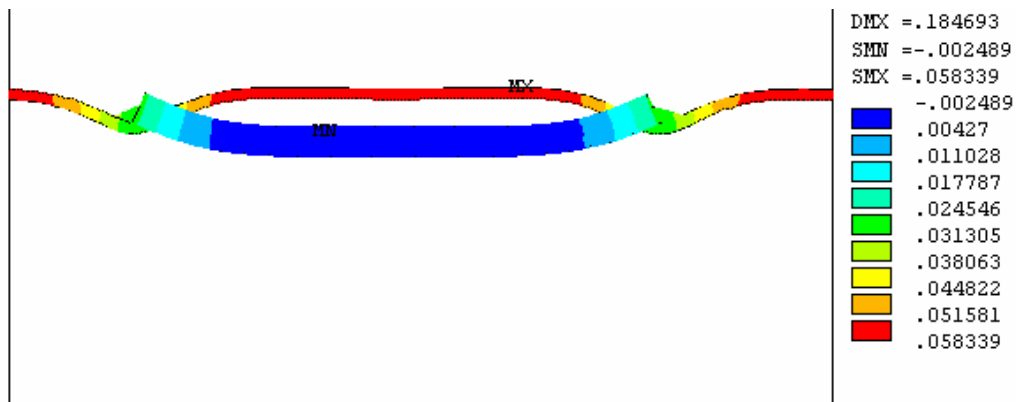


Figure 5.12: Sleeve B (Gapped) Radial Displacement, Load Condition B7 (500 psi Pressurized Pipe Only)

The load case with Sleeve B, 1.6 mm gap, and pressure applied to both the pipe and annulus (Figure 5.13) shows that the sleeve now has expanded, the pipe has a displacement 0.02 mm greater than the displacement observed without the annulus pressurized, and the pipe beneath the sleeve has a reduced radius from its original position. As was noted with the relative motion with Sleeve A, pressure applied to both the pipe and annulus has the effect of opening the root of the fillet welds on the ends of the sleeves.

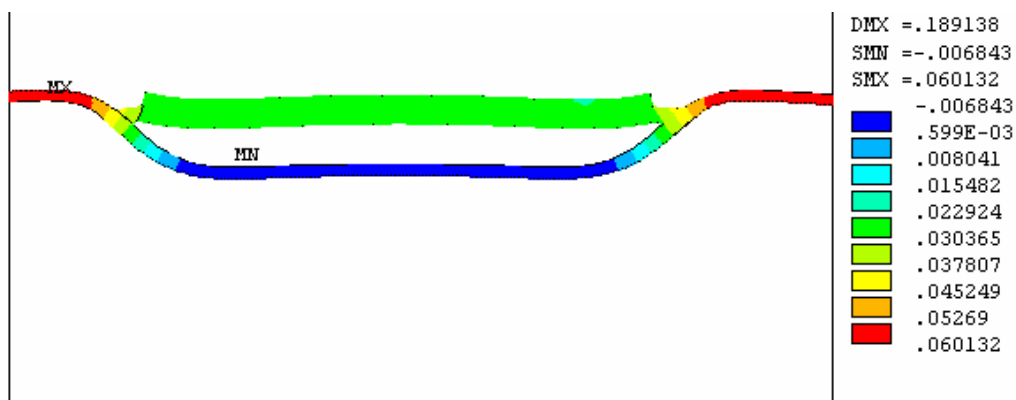


Figure 5.13: Sleeve B (Gapped) Radial Displacement, Load Condition B9 (500 psi Pressurized Pipe and Sleeve Annuli)

The similarities and differences amongst the FE load cases are evident when one compares the results as in the following Figures 5.14 and 5.15. While the overall deformed shapes and local strains will vary as a function of the pipe and sleeve geometry, some general statements regarding their deformations under pressure loads can be made as follows:

- ✗ the pipe wall under a loose fitting sleeve will expand towards the sleeve ID when only the pipe is pressurized;
- ✗ a tight fitting sleeve will provide support to the pipe wall it covers and restrain its radial expansion when only the pipe is pressurized;
- ✗ when the annulus between the pipe and the sleeve is pressurized, the radial deflection of the pipe wall will be reduced since there is equal pressure on both sides of the pipe wall; and
- ✗ when the annulus between the pipe and the sleeve is pressurized, the sleeve will separate from the pipe wall resulting in tensile stresses at the root of the sleeve fillet weld.

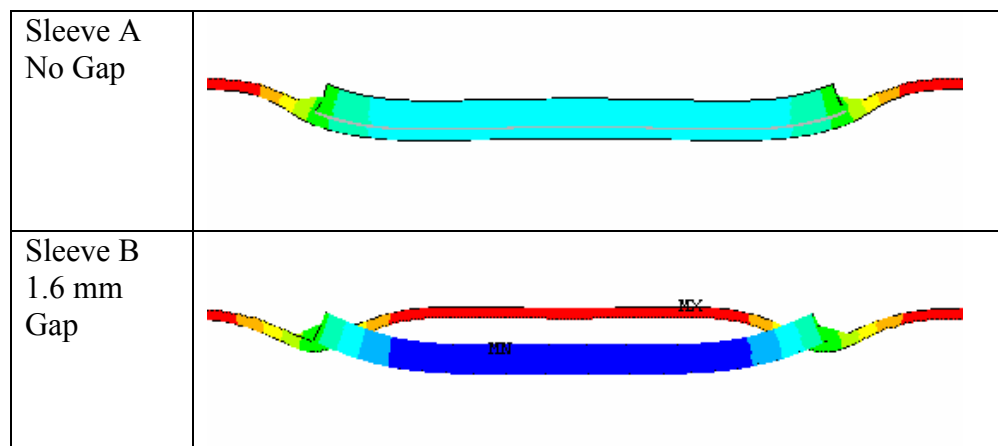


Figure 5.14: Comparison of Sleeves with 500 psi to Pipe

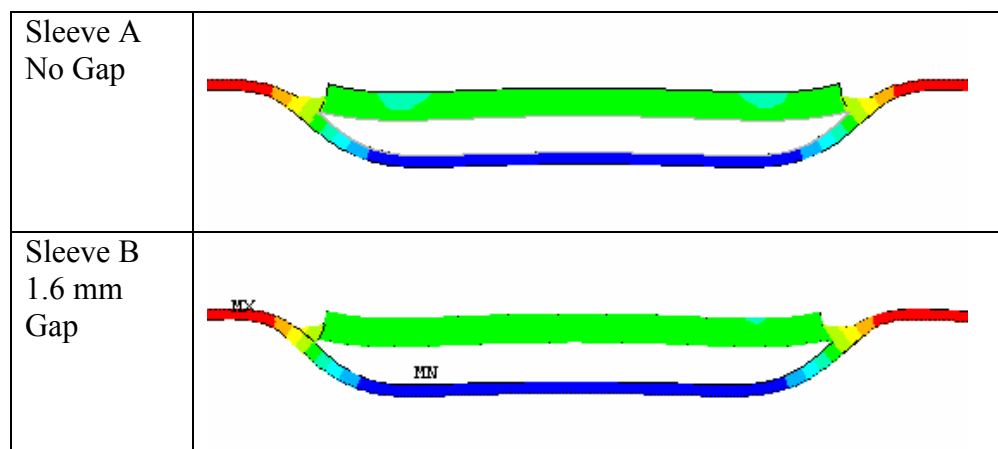


Figure 5.15: Comparison of Sleeves with 500 psi to Pipe and Annulus between Sleeve and Pipe

6. CONCLUDING REMARKS

6.1 Project Summary

The current project was assembled and completed to support the development of a better understanding of pressure retaining full encirclement repair sleeves often used as permanent repairs on pipelines to reinforce areas with defects, such as cracks or corrosion. The objective of this project was to support the development of tools for sleeve design and for conducting an engineering assessment to determine the tolerable dimensions of flaw indications at full encirclement repair sleeves. In particular, this project has been undertaken to validate the stresses estimated in the finite element analysis (FEA) models against actual in-service loading conditions experienced at reinforcing sleeves.

The work completed in this project has focused on the collection of full-scale experimental data describing pipe and sleeve strains. This data was collected in the field and laboratory as follows:

Condition	Field Data	Laboratory Data
Strains induced by sleeve welding	Collected	Collected
Strains induced by pressurization of the sleeved pipe	Collected	Collected
Strains induced by pressurization of the sleeved pipe and the annulus between the pipe and sleeve		Collected

Finite element models of the field and laboratory sleeved pipe segments were developed and subjected to the same applied loading conditions as the full-scale sleeved pipe segments. The results of the full-scale data collection (strains) were compared with those estimated based upon the finite element models to demonstrate the ability of the models to predict the behaviour of the sleeved pipe segments. Comparisons were made to illustrate:

- ✗ relative strain levels;
- ✗ the accuracy of the strain predictions;
- ✗ trends in the local strain transfer functions (i.e., strain response per unit change in pressure);
- ✗ deformation trends;
- ✗ the differences in behaviours of tight and loose fitting sleeves; and
- ✗ the effects of pressurizing the annulus between the pipe wall and sleeve.

6.2 Conclusions

While the scope of the full-scale experimentation was limited and the numerical modeling covered only the pipe and sleeve geometries involved in the full-scale trials, the results of this investigation are significant. Based upon comparisons of the physical trial data and the numerical modeling results developed in this project, it is possible to make the following conclusions with regards to the validity of the numerical model as a predictor of sleeved pipe behaviour:

- ✘ the finite element model results demonstrated behaviours that were consistent with expected behaviours;
- ✘ trends in the finite element model predictions of pipe and sleeve strains agreed with the full-scale data;
- ✘ with the exception of obvious experimental errors, the finite element model strains agreed well with measured strains; and
- ✘ the finite element model was able to describe the effects of pipe to sleeve gap and annulus pressurization that agreed with field experience and engineering judgment.

While the range of sleeve repair geometries investigated in this project was limited, some conclusions regarding the behaviour of these sleeve repairs can be made including:

- ✘ the deposition of sleeve end circumferential fillet welds will develop significant tensile strains across the root of the fillet weld when large sleeve to pipe gaps exist;
- ✘ tight fitting sleeves provide support to the contacted pipe wall and thus should be expected to reduce hoop strains while sleeves with larger gaps should not be expected to provide the same level of support;
- ✘ pressurization of the sleeve to pipe annulus will reduce the pipe wall radial deflection and thus limit pipe hoop strains beneath the sleeve;
- ✘ when the annulus between the pipe and the sleeve is pressurized, the sleeve will separate from the pipe wall resulting in tensile stresses at the root of the sleeve fillet weld; and
- ✘ the effect of the gap between the pipe and sleeve does not appear to have a significant impact on pipe or sleeve behavior when the annulus is pressurized. The primary difference in behavior being noted at the fillet weld root due to differences in weld geometry.

6.3 Recommendations

Based upon the experience developed in the completion of this project and the results that have been developed, a number of recommendations can be made to direct further research and the design of field repair sleeve applications. It is recommended, based upon the validation of the finite element modeling process in this project, that:

- ✘ a wider range of sleeve and pipe geometries (thickness, diameter, length) be modeled to develop more generalized statements regarding the observed behaviors and develop recommendations to support the selection of optimal sleeve to pipe geometries;
- ✘ further modeling of different pipe and sleeve geometries could be used to develop definitive recommendations regarding the conditions for which pressurizing the annular space between the pipe and sleeve is recommended;
- ✘ further work should be completed using the current results to define acceptable flaw limits for sleeve fillet welds and longitudinal seam welds;

- ✕ the numerical model could be extended to consider heated or mechanically tightened sleeves to demonstrate their impact on sleeve, pipe and weld behaviors; and
- ✕ similar trials and numerical modeling could be completed for various tee geometries to improve confidence or reduce conservatism inherent in their design in a similar fashion as recommend for sleeves.



APPENDIX A
LOCATIONS OF GAUGES, FIELD TRIALS

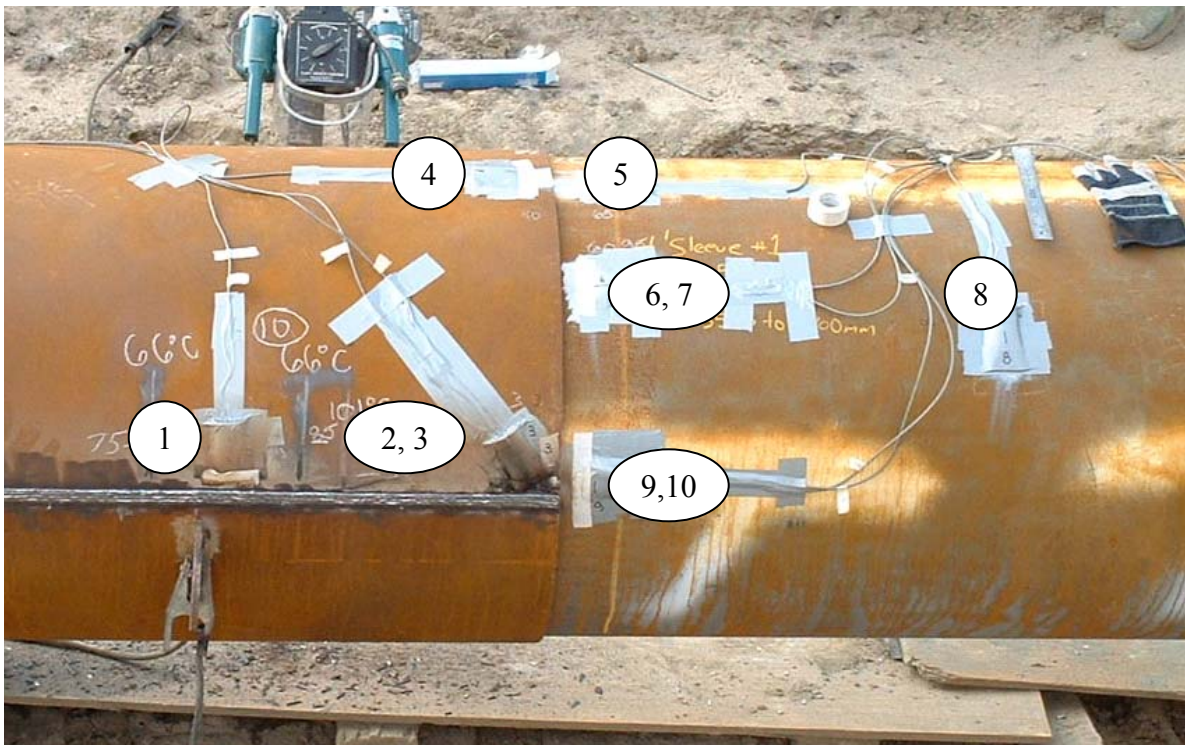


Figure A1: Sleeve 2 Gauge Locations. Similar numbering and placement were used for both sleeves; see below for gauge locations.

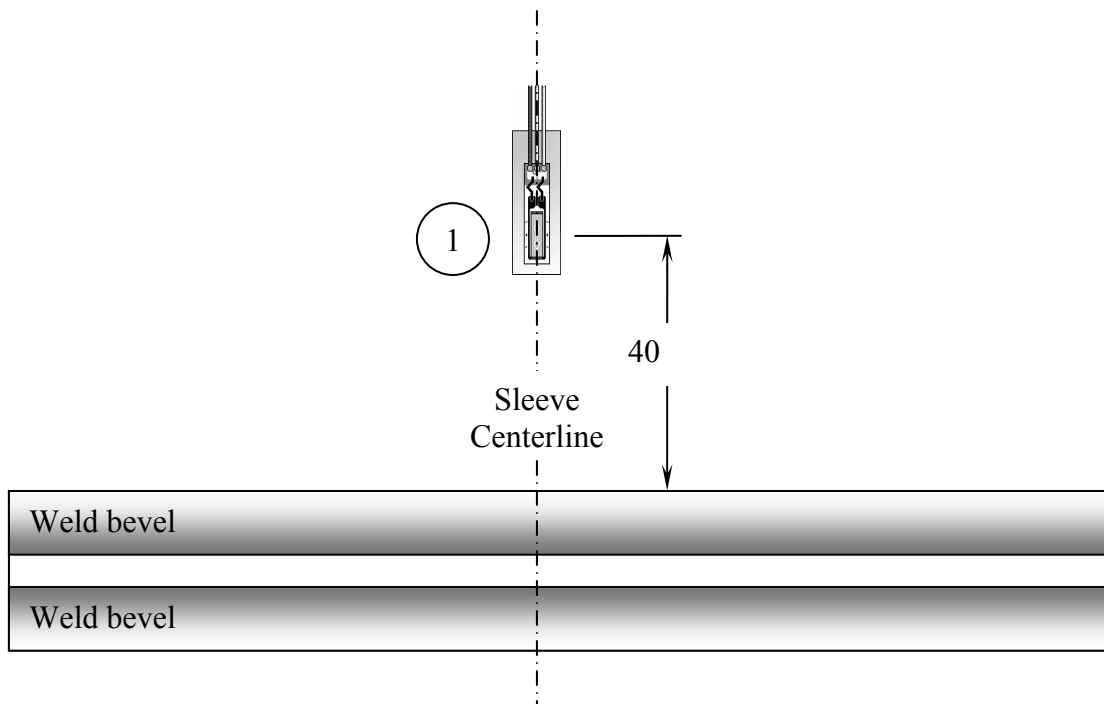


Figure A2: Sketch of Layout of Hoop Gauge 1 on the Sleeve

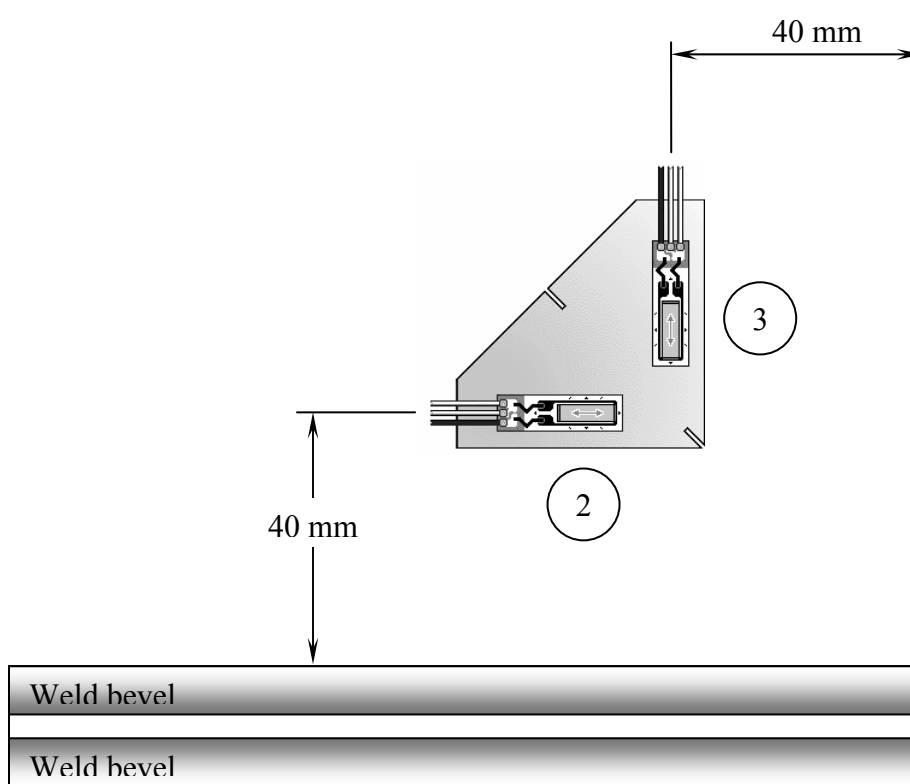


Figure A3: Sketch Showing Layout of Gauges 2 and 3 on the Sleeve

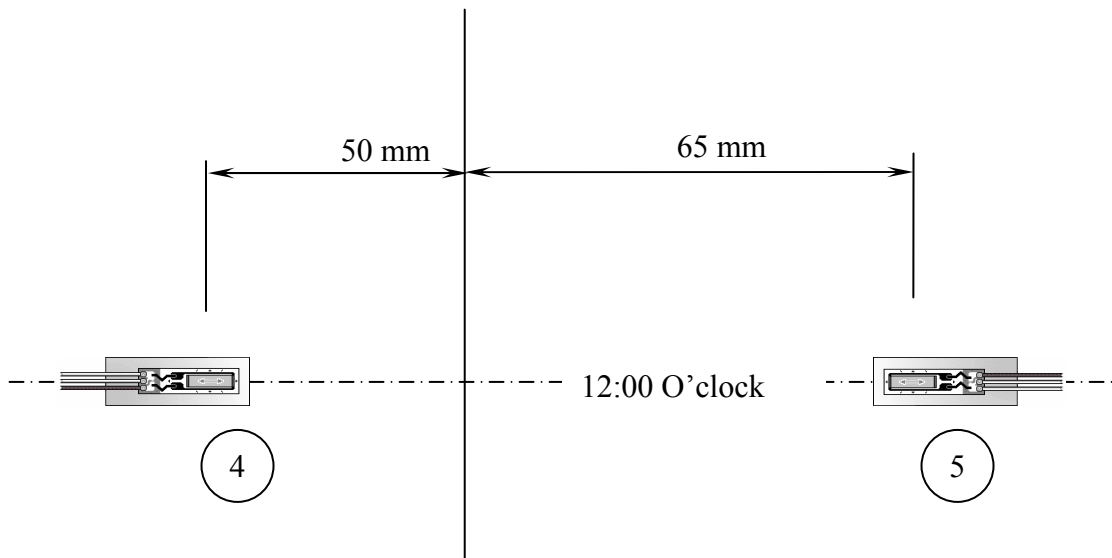


Figure A4: Sketch Showing Layout of Gauges 4 and 5 at the 12:00 O'clock Position

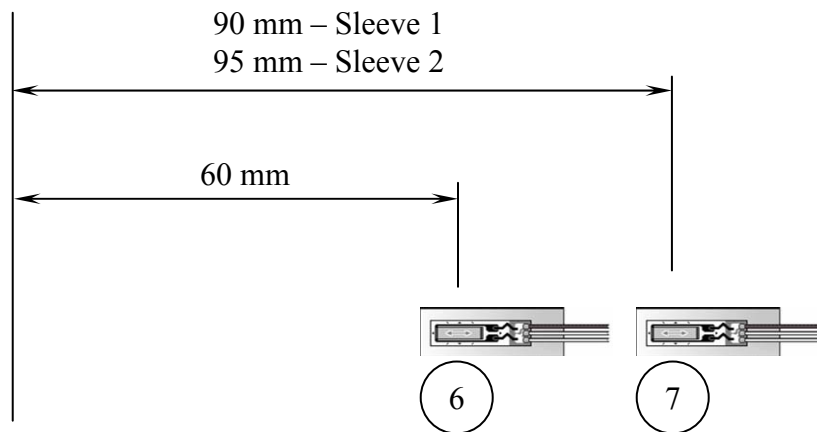


Figure A5: Sketch Showing the Layout of Gauges 6 and 7 on the Pipe at 10:30 O'clock Position

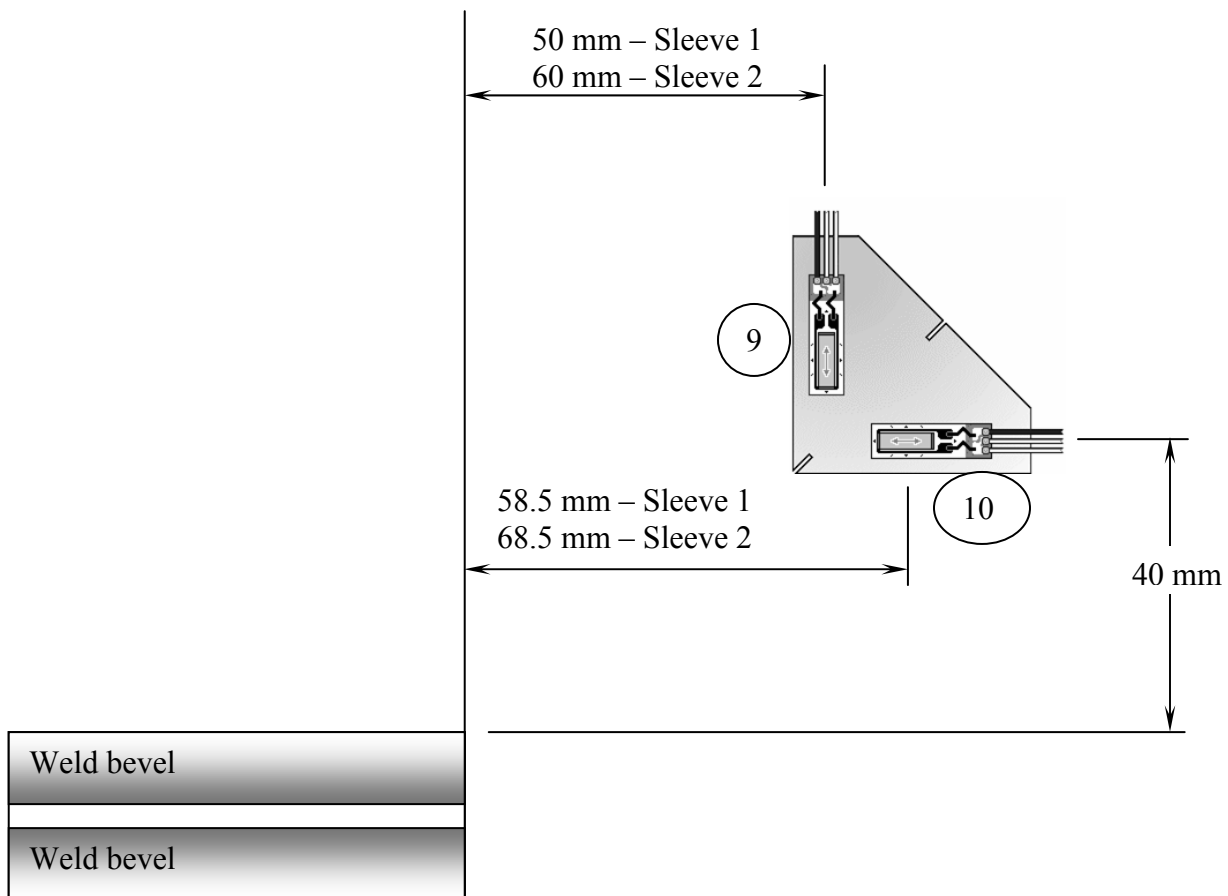


Figure A6: Sketch of Layout of Gauges 9 and 10 on the Pipe at the 9:30 O'clock Position



APPENDIX B

STRAIN GAUGE RESULTS, FIELD TRIALS

Table B1: Strain Gauge Readings for Sleeve 1 – KP 762.4199

	Time	1	2	3	4	5	6	7	8	9	10
28 September 1330 Start of Test	9/28/04 1:30 PM	0	0	0	0						
1st pass of each side completed	9/28/04 1:42 PM	97	247	-34	-13						
2nd pass completed	9/28/04 1:55 PM	123	180	28	-56						
3rd pass completed	9/28/04 2:03 PM	-121	5	119	-83						
4th pass completed	9/28/04 2:10 PM	108	27	253	-94						
5th pass completed	9/28/04 2:22 PM	319	-122	339	-110						
6th pass completed	9/28/04 2:30 PM	519	-127	465	-111						
7th pass completed	9/28/04 2:34 PM	640	-144	520	-116						
8th pass completed	9/28/04 2:42 PM	591	-261	521	-120						
9th pass completed	9/28/04 2:46 PM	639	-229	544	-123						
Cooled to pipe temperature	9/28/04 2:57 PM	317	-244	444	-128						
Connected remaining gauges	9/28/04 5:00 PM	287	-246	448	-128						
Arrived on site and connect gauges	9/29/04 8:35 AM	251	-233	393	-106	0	0	0	0	0	0
Completed east fillet weld	9/29/04 11:50 AM	310	-133	472	-74	-81	30	27	22	1	30
Start west fillet weld	9/29/04 12:15 PM										
1st pass completed and buffed	9/29/04 12:40 PM	323	563	-136	442	-222	364	133	27	58	165
2nd pass completed	9/29/04 1:00 PM	326	805	253	642	156	494	162	30	91	239
3rd pass completed	9/29/04 1:22 PM	310	1057	-669	872	68	550	106	31	74	279
4th pass completed	9/29/04 1:42 PM	299	1304	-750	1059	-206	545	48	37	169	352
	9/29/04 1:52 PM	305	1223	-826	976	107	472	18	10	128	331
5th pass completed	9/29/04 2:05 PM										
	9/29/04 2:10 PM	297	1310	-736	1022	-245	439	1	37	116	264
	9/29/04 2:22 PM	302	1266	-788	937	100	382	-36	27	93	258
	9/29/04 2:42 PM	302	1254	-789	914	-43	354	-55	26	90	254
	9/29/04 3:40 PM	285	1258	-816	896	-1	343	-64	10	81	236

Table B2: Strain Gauge Readings for Sleeve 2 – KP 767.6204

	Time	1	2	3	4	5	6	7	8	9	10
29 September Hoop Gauge On	9/29/04 4:18 PM								0		
	9/29/04 4:44 PM	0	0	0	0				136		0
	9/29/04 4:53 PM	-10	-14	-8	-13	0	0	0	132	0	0
	9/29/04 5:11 PM	-12	-12	-7	-16	6	4	6	118	-14	1
Started welding at 0850	9/30/04 8:30 AM	-36	-33	-26	-31	4	7	3	156	40	3
	3rd pass completed 9/30/04 9:04 AM	26	88	-252	-47	25	41	34	165	112	-90
	4th pass completed 9/30/04 9:10 AM	6	128	-39	-51	24	55	51	170	81	-200
	5th pass completed 9/30/04 9:24 AM	-472	-95	-123	-64	50	28	15	151	82	-22
	6th pass completed 9/30/04 9:37 AM	-241	187	280	-66	37	47	41	158	-49	-106
	7th pass completed 9/30/04 9:42 AM	36	-103	185	-67	56	46	34	129	-80	-18
	9/30/04 9:44 AM	-36	-104	167	-66	57	44	31	122	91	-17
	8th pass completed 9/30/04 9:47 AM	321	58	259	-43	49	66	74	-104	-397	-164
	9th pass completed 9/30/04 9:53 AM	369	-106	351	-56	71	71	60	76	-143	-55
	10th pass completed 9/30/04 10:00 AM	438	-85	400	-69	57	66	51	185	-75	-78
11th pass completed	9/30/04 10:09 AM	252	-159	323	-72	62	46	28	165	-112	40
	9/30/04 10:24 AM	97	-177	287	-70	51	26	8	143	-132	111
	9/30/04 10:30 AM										
	9/30/04 10:45 AM	90	-178	280	-71	58	23	5	134	-139	97
Started east fillet weld	9/30/04 11:19 AM	76	-176	289	-73	45	31	11	139	-139	131
	9/30/04 12:00 PM	86	-171	294	-64	54	39	19	147	-131	134
	Finished east fillet weld 9/30/04 12:30 PM	78	-170	300	-62	37	37	21	149	-126	145
	Started west fillet weld 9/30/04 1:20 PM	83	-163	306	-59	40	40	22	149	-117	155



	Time	1	2	3	4	5	6	7	8	9	10
1st pass completed	9/30/04 1:44 PM	84	364	-161	725	54	92	-49	156	-12	172
weld at 0730h	9/30/04 1:52 PM	92	322	-179	483	264	122	-34	149	-26	184
2nd pass completed	9/30/04 2:07 PM										
3rd pass started	9/30/04 2:08 PM										
	9/30/04 2:09 PM	82	561	-296	776	298	206	-62	142	7	290
weld at 0830	9/30/04 2:20 PM	92	524	-273	629	346	209	-56	144	22	349
3rd pass completed	9/30/04 2:30 PM	78	748	-556	839	-299	137	-137	142	134	245
4th pass started	9/30/04 2:36 PM										
	9/30/04 2:45 PM	89	716	-589	706	108	149	-112	148	155	302
	9/30/04 2:46 PM		710	-611						173	338
	9/30/04 2:47 PM		705	-618						208	309
	9/30/04 2:48 PM		102	645						343	125
in line with gauges	9/30/04 2:49 PM		602	90						803	-752
	9/30/04 2:50 PM		845	-						788	-592
				2223							
	9/30/04 2:51 PM		1025	-567						495	15
	9/30/04 2:52 PM		1068	-623						394	65
	9/30/04 2:53 PM		1042	-629						328	110
weld about 100 mm from 6	9/30/04 2:54 PM		999	-634			-30	-391		292	92
weld at 6	9/30/04 2:55 PM		952	-626			-836	-770		272	83
	9/30/04 2:56 PM						-211	-604			
	9/30/04 2:57 PM						-31	-327			
	9/30/04 2:58 PM						35	-238			
	9/30/04 2:59 PM						43	-201			
4th pass completed	9/30/04 3:00 PM	82	852	-605	723	-995	37	-194	149	251	103
5th pass started	9/30/04 3:05 PM										
	9/30/04 3:06 PM	85	821	-606	865	233	26	-218	144	251	106
weld at 0900h	9/30/04 3:11 PM	92	812	-667	828	-192	11	-227	159	728	-632
5th pass completed	9/30/04 3:20 PM	84	963	-567	1150	-473	-17	-224	154	274	92
	9/30/04 3:32 PM	87	935	-588	833	-305	-7	-221	154	266	108



APPENDIX C
STRAIN GAUGE DETAILS, LAB TRIALS

Table C1: Strain Gauge Summary

Gauge	Pipe	Sleeve	A	B	Hoop	Axial	Description	Gauge Type
1	●		●			●	4 mm from edge of sleeve on pipe ID	n-11-fa-5-120-11
2	●			●		●	4 mm from edge of sleeve on pipe ID	n-11-fa-5-120-11
3	●				●		10 mm from center of pipe	n-11-fa-5-120-11
4	●					●	10 mm from center of pipe	n-11-fa-5-120-11
5		●	●		●		10 mm from center of sleeve	n-11-fa-5-120-11
6		●	●			●	10 mm from center of sleeve	n-11-fa-5-120-11
7		●		●	●		10 mm from center of sleeve	n-11-fa-5-120-11
8		●		●		●	10 mm from center of sleeve	n-11-fa-5-120-11
9		●	●			●	50 mm from edge of sleeve	n-11-fa-5-120-11
10		●		●		●	50 mm from edge of sleeve	n-11-fa-5-120-11
11		●	●			●	10 mm from edge of sleeve	n-11-fa-5-120-11
12		●		●		●	10 mm from edge of sleeve	n-11-fa-5-120-11
13		●	●			●	ID sleeve, 20 mm from edge	LWK-06-W250B-350
14	●		●			●	OD pipe, 20 mm from edge	LWK-06-W250B-350
15	●		●			●	5 mm from weld toe	n-11-fa-2-120-11
16		●		●		●	ID sleeve, 20 mm from edge	LWK-06-W250B-350
17	●			●		●	OD pipe, 20 mm from edge	LWK-06-W250B-350
18	●			●		●	5 mm from weld toe	n-11-fa-2-120-11



APPENDIX D
STRAIN GAUGE RESULTS, LAB TRIALS

